PHYSICAL REVIEW D VOLUME 24, NUMBER 5 1 SEPTEMBER 1981

General theory of weak processes involving neutrinos. II. Pure leptonic decays

Robert E. Shrock
Institute for Theoretical Physics, State University of New York at Stony Brook, Stony Brook, New York 11794
(Received 23 January 1981)

We present a general theory of leptonic decays which consistently incorporates the possibility of nonzero neutrino masses and associated lepton mixing. We calculate the differential decay distribution $d^2\Gamma/dE_b d\cos\theta$ and the l_b polarization for "the" decay $l_a \to \nu_{l_a} l_b \bar{\nu}_{l_b}$, i.e., in general the incoherent sum of decays $l_a \to \nu_i l_b \bar{\nu}_j$ into all allowed mass eigenstates ν_i and $\bar{\nu}_j$. Expressions are also given for the average quantities $<\cos\theta>(E_b)$, $<\cos\theta>$ (integrated over E_b), $<E_b>(\theta)$, and $<E_b>$ for individual (i,j) decay modes and the observed sum. The total rate for massive-neutrino modes is calculated for the relevant experimental cases. These results are applied to analyze what the observable characteristics of massive neutrinos and lepton mixing would be in leptonic l_a decay. We show that $d\Gamma/dE_b$ would in general contain kinks at intermediate energies and carry out a search for these in existing μ and τ decay data. We further show that the conventional determination of the Lorentz structure of weak leptonic couplings via measurement of the spectral parameters ρ, η, ξ, and δ is not applicable in the presence of massive neutrinos and lepton mixing; a deviation of the observed parameters (with radiative corrections extracted) from their conventional $V-A$ values could be caused *either* by non-$(V-A)$ Lorentz structure *or* by massive-neutrino decay modes and lepton mixing. Thus, past measurements of the spectral parameters yield information only on the combined effects of the underlying Lorentz structure of the couplings and on possible neutrino masses and mixing, but not on either of these in isolation. The appropriate generalized formalism for the analysis of Lorentz structure in leptonic decays is given, and a quantitative study is performed of the effects of neutrino masses and mixing on the spectral parameters. We propose methods to distinguish between these effects and those due to possible non-$(V-A)$ Lorentz structure; these methods can be applied in a reanalysis of old μ and τ decay data, and can serve as part of a generalized framework for the analysis of forthcoming data. Within the context of the standard electroweak theory we apply our results to existing data to obtain new upper bounds on the possible contributions of massive neutrino modes. Finally, we determine the optimal ways in which, and the corresponding sensitivity with which, forthcoming experiments on μ and τ decay can search for massive neutrinos and lepton mixing.

I. INTRODUCTION

This is the second in a series of articles presenting a general theory of weak processes involving neutrinos, which incorporates consistently the possibility of nonzero neutrino masses and associated lepton mixing. The observations underlying this theory have been stated previously[1,2] and discussed at length in paper I of the series.[3] In this paper we shall construct a general theory of pure leptonic decays of the form $l_a \to \nu_{l_a} l_b \bar{\nu}_{l_b}$. As before, we shall work within the context of the standard $SU(2)_L \times U(1)$ electroweak gauge theory,[4] appropriately generalized to allow for neutrino masses and mixing,[5] and including n generations of fermions. The lepton and/or Higgs sectors of the theory are thus assumed to be expanded as necessary to allow for Dirac and/or Majorana neutrino masses as phenomenological possibilities. In the present analysis we shall consider massive Dirac neutrinos. Following the notation of Refs. 1–3, we label the charged leptons as $\{l_a\} \equiv \{l_1 \equiv e, l_2 \equiv \mu, l_3 \equiv \tau, \ldots, l_n\}$ and the corresponding weak-gauge-group eigenstates of the neutrinos as $\{\nu_{l_a}\}$. A far-reaching fact is that, in general,[6] in the case of massive (nondegenerate) neutrinos, the ν_{l_a} have no well-defined masses "$m(\nu_{l_a})$", but rather are linear combinations of the neutrino mass eigenstates ν_i, $i=1,\ldots,n$, as specified by the unitary transformation

$$\nu_{l_a} = \sum_{i=1}^{n} U_{ai} \nu_i , \tag{1.1}$$

where U is the lepton mixing matrix. For further background and for the classification of neutrinos according to whether they are in $\{\nu_{i_L}\}$ or $\{\nu_{i_H}\}$ and are dominantly or subdominantly coupled to a given charged lepton l_a, including the categories of "light dominantly coupled" (LDC), "light subdominantly coupled" (LSC), and similarly for heavy neutrinos (HDC and HSC), see Refs. 2 and 3.

The necessity of such a theory of weak processes is obvious, since experiments can only set upper bounds on neutrino masses but not show that any one of them is exactly zero. To set these upper limits, it is imperative to have a theory which takes account of the effects of the lepton mixing which is a general concomitant of these masses. Indeed, existing experiments do not even rule out a substantial mass $\lesssim 250$ MeV, for at least one neutrino, ν_3. Moreover, since the number of lepton generations, n, is not known and could be larger than 3. and since, regardless of the lower limits that may be established on the mass of a

fourth charged lepton, there are no such isolated bounds (i.e., bounds which are essentially free of mixing-angle dependence) on the mass of a ν_i, $i \geq 4$, there remains the very real possibility of several neutrinos with considerable masses which could occur, subdominantly coupled, in the decays of light leptons and hadrons. The importance of the general theory is obvious, since it shows[1-3] that past direct searches for neutrino masses, via nuclear and particle decays, were based on a tacit assumption that the neutrino weak eigenstates were also mass eigenstates in the massive as well as the massless case, which assumption is in general false. This assumption is evident in the standard conventional notation used in quoting neutrino-mass limits; "$m(\nu_e)$", "$m(\nu_\mu)$", and "$m(\nu_\tau)$" are stated to be less than their respective upper bounds, whereas in fact ν_e, ν_μ, and ν_τ have no well-defined masses at all. The necessary reinterpretation of these neutrino-mass limits was given in Ref. 1. Realizing the presence and falsity of the above tacit assumption, one sees that the standard kinematic tests for neutrino masses represent only a fraction of the most general set of tests and that they apply essentially only for the dominantly coupled mass eigenstates in a given decay. Thus, in Refs. 2 and 3 we proposed a new class of tests for neutrino masses and mixing and applied these to existing data to derive correlated bounds on these quantities. Two of the most promising tests relied upon the leptonic decays of pseudoscalar mesons and upon nuclear β decays. The former of these is especially sensitive and definitive, since massive-neutrino decay modes would yield monochromatic signals and could be enhanced kinematically by huge factors as large as 10^4–10^5. From an observation of such decay modes, one could determine individually the mass and weak coupling coefficient of each neutrino involved.

Here we shall analyze the leptonic decay $l_a \to \nu_{i_a} l_b \bar{\nu}_{i_b}$, which in general consists of an incoherent sum of the decays $l_a \to \nu_i l_b \bar{\nu}_j$ into all allowed mass eigenstates ν_i and $\bar{\nu}_j$. Several interesting questions arise in this analysis. What are the energy and angular distributions for an individual (i,j) mode? How, then, is the total observed differential distribution changed as a result of the presence of massive-neutrino decay modes and concomitant lepton mixing? Which kinematic quantities and which regions of phase space are most sensitive to these heavy neutrino decays? What is the comparative kinematic suppression of different kinds of massive-neutrino modes? In order to answer these questions, we shall calculate the differential decay distribution $d^2\Gamma/dE_b d\cos\theta$ for an individual (i,j) mode and for the resulting sum over all such allowed modes. Further, we shall give expressions for the average quantities describing the energy and angle of emission (relative to the polarization direction of the parent lepton l_a) of the l_b. Neutrino masses and mixing will be shown to have little effect on the l_b polarization.

Historically, the analysis of the differential distribution and related spectral parameters in μ and, later, τ decay played a very important role in establishing the $V-A$ nature of the respective weak couplings. However, we shall show that this conventional determination is not applicable in a general theory which admits neutrino masses and mixing. Even if the relevant weak couplings should be precisely $V-A$, the *observed* effective spectral parameters (after radiative corrections are divided out) would not have their conventional $V-A$ values, viz., $\rho=\frac{3}{4}$, $\eta=0$, $\xi=1$, and $\delta=\frac{3}{4}$. Thus a deviation of the observed spectral parameters from the conventional $V-A$ values could be caused *either* by non-$(V-A)$ Lorentz structure *or* by massive-neutrino decay modes and lepton mixing. Consequently, past measurements of the spectral parameters yield information only on the combined effects of the underlying Lorentz structure of the couplings and on possible neutrino masses and mixing, but not on either of these in isolation. Strictly speaking, the observed agreement of a given spectral parameter in μ or τ decay with the $V-A$ predictions (in the case of $\xi^{(\mu)}$, at the 2σ level) cannot be taken, by itself, to imply that the respective couplings are $V-A$ unless one has proved that the effects of possible massive-neutrino decays are negligible to the requisite degree of accuracy. We shall calculate precisely what these effects are for each spectral parameter, as a function of the relevant neutrino masses and mixing coefficients. Further questions which present themselves include the following. Given our constraints[2,3] on lepton mixing angles, how important are neutrino-mass and mixing effects for the four spectral parameters which have been measured in μ decay and for the one (ρ) which has been measured in τ decay? Are there any tests that one can apply to past and future data to distinguish between the effects on spectral parameters due to possible non-$(V-A)$ structure Lorentz structure and those due to possible neutrino masses and lepton mixing? (Yes; we shall propose such tests.) Can one analyze existing data on μ and τ decay to derive useful correlated bounds on the masses and coupling coefficients of heavy neutrinos? (Yes.) Finally, how might the forthcoming τ and very-high-precision μ-decay experiments best search for the manifestations of heavy neutrinos and, given their projected measurement accuracies, how large an effect might

they be able to detect? These questions will also be answered as part of our general analysis.

For the aid of the reader we give below an outline of the remainder of this paper.

II. General theory of the decay $l_a \to \nu_{l_a} l_b \bar{\nu}_{l_b}$.

A. Foundations.

B. General results on differential decay distributions.

C. Total rates.

D. Characteristics of differential decay distributions and average quantities.

E. Kinks in $d\Gamma/dE_b$.

F. Implications for effective spectral parameters and the determination of the Lorentz structure of weak couplings.

G. The l_b polarization.

II. GENERAL THEORY OF THE DECAY $l_a \to \nu_{l_a} l_b \bar{\nu}_{l_b}$

A. Foundations

As was pointed out in Refs. 2 and 3, and is indicated symbolically in Fig. 1, in a general theory which admits the possibility of nonzero neutrino masses and associated lepton mixing, a leptonic decay of the form $l_a \to \nu_{l_a} l_b \bar{\nu}_{l_b}$ really consists of the separate and incoherent decays $l_a \to \nu_i l_b \bar{\nu}_j$, where i and j each run from 1 to n, as allowed by phase space. The relative strength of each of these modes is determined by a coupling coefficient $|U^*_{ai} U_{bj}|^2$ and by a kinematic factor depending on the relevant particle masses. At present there are three known examples of this type of decay, namely $\mu \to \nu_\mu e \bar{\nu}_e$,[7] and $\tau \to \nu_\tau l_b \bar{\nu}_{l_b}$, $l_b = e, \mu$.[8] One may recall the nomenclature introduced in paper I, Sec. II, for the classification of these leptonic decays: for a given set of decays $l_a \to \nu_{l_a} l_b \bar{\nu}_{l_b}$, the specific decay $l_a \to \nu_i l_b \bar{\nu}_j$ will be labeled as the $(\nu_i, \bar{\nu}_j)$ or simply (i,j)th mode. Following a convention used before for a general weak decay of a fermion,[9] we shall denote the set of final-state masses in the decay $l_a \to \nu_i l_b \bar{\nu}_j$ as $(m_1, m_2, m_3) \equiv (m(\nu_i), m(\nu_j), m_b)$, where $m_b \equiv m_{l_b}$. We shall refer to a mode as HSC if ν_i or ν_j is an HSC neutrino (or if both are). More precisely, in μ decay the (i,j)th mode may be any of nine generic types, depending on whether ν_i is an LDC, LSC, or HSC neutrino in this decay, and similarly with $\bar{\nu}_j$.[10] These will be labeled as (LDC, LDC), (LDC, HSC), and so forth for the other six types. The defining conditions for these types are obvious generalizations of the ones which applied to M_{l2} decay, where M denotes a pseudoscalar meson. For the charge-conjugate decay $\bar{l}_a \to \bar{\nu}_{l_a} \bar{l}_b \nu_{l_b}$ we shall use the convention of labeling the $\bar{l}_a \to \bar{\nu}_i \bar{l}_b \nu_j$ decay as the $(\bar{\nu}_i, \nu_j)$ or (i,j)th mode. Given our definition of the sets $\{\nu_{i_L}\}$ and $\{\nu_{i_H}\}$, for leptonic τ decay there are actually 12 possible generic decay types: the 9 discussed before and, in addition, the types (HDC, LDC), (HDC, LSC), and (HDC, HSC).[10] One cannot experimentally distinguish the spectra of the modes involving only light (anti) neutrinos from the corresponding spectra involving massless neutrinos. (This was the reason for introducing the classification of the ν_i into $\{\nu_{i_L}\}$ and $\{\nu_{i_H}\}$ sets.) Consequently, the modes which are of primary interest as indicators of neutrino masses and mixing are of the types (LDC, HSC), (HSC, LDC), and, in the case of τ decay, also (HDC, LDC) and (HDC, HSC).

Muon decay has been well studied with very-high-precision, high-statistics experiments. A sizable amount of data has also been taken and analyzed on leptonic τ decay. Moreover, these decays have the merit that they are free of hadronic complications, and hence, for example, one can unambiguously calculate radiative corrections to the spectrum and rate. Given these advantageous features of $l_a \to \nu_{l_a} l_b \bar{\nu}_{l_b}$ decays, one is naturally led to investigate these decays to ascertain what information they could provide on possible neutrino masses and lepton mixing. Unfortunately, however, they do have several disadvantages in comparison with π_{l2} and K_{l2} decays. First, since the final state consists of three particles, the spectral distribution in the momentum and asymmetry angle of the l_b is continuous, and there is no monochromatic signal of the massive neutrinos. The observed distribution and rate are due to all of the modes (i,j) which are allowed by phase space to be present, and one cannot in general study any one of these modes in isolation, much less determine an individual $m(\nu_i)$ and $|U_{ai}|$ or $m(\nu_j)$ and $|U_{bj}|$. For instance, even if one observed a secondary incremental addition to the dominant light-neutrino spectrum which had an end-point energy (in units where $m_a \equiv 1$)

$$(E_b)_{\max}(m(\nu_i), m(\nu_j), m_b) = \tfrac{1}{2}\{1 + m_b^2 - [m(\nu_i) + m(\nu_j)]^2\}, \tag{2.1}$$

it is clear from Eq. (2.1) that, strictly speaking, this would not determine $m(\nu_i)$ or $m(\nu_j)$ separately. It is true that in μ decay, if the relative strength of the HSC mode were sufficiently large, one could argue indirectly that this mode must be

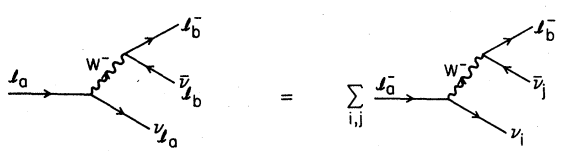

FIG. 1. General structure of "the" decay $l_a \to \nu_{l_a} l_b \bar{\nu}_{l_b}$.

of the type (LDC, HSC) or (HSC, LDC), so that a measurement of $(E_b)_{\max}(m(\nu_i), m(\nu_j), m_b)$ would effectively determine $m(\nu_{\rm HSC})$. However, this argument could only be applied over certain ranges of $m(\nu_{\rm HSC})$ where one has upper limits on the relevant mixing-matrix coefficients from the M_{l2} test and branching-ratio constraints, and it would be indirect. Furthermore, one would still not know whether the HSC (anti)neutrino was ν_i or $\bar{\nu}_j$ and hence whether the coupling coefficient was $|U^*_{a,\rm LDC\,i}U_{b,\rm HSC\,j}|^2 \simeq |U_{b,\rm HSC\,j}|^2$ or $|U^*_{a,\rm HSC\,i}U_{b,\rm LDC\,j}|^2 \simeq |U_{a,\rm HSC\,i}|^2$. The situation is more encouraging in τ decay since, given the present mass limit on ν_3 (see Refs. 1–3), the decay mode with the greatest strength could be (HDC, LDC), i.e., could already involve a neutrino of substantial mass. Indeed, it was precisely from an analysis of the electron momentum distribution in τ decay that this limit was derived. With more extensive τ decay data it will presumably be possible to reduce this upper limit on the mass of a hypothetical HDC ν_3. Because of this HDC possibility, however, it will be commensurately more complicated to try to search for any HSC contribution (due, for example, to a hypothetical ν_4, etc.) in leptonic τ decay. Moreover, one disadvantage of the $l_a \to \nu_{l_a} l_b \nu_{l_b}$ decays as a probe for massive neutrinos is that, as a consequence of the three-body nature of the final state, a mode involving neutrinos with masses $m(\nu_i \text{ or } \nu_j) \ll m_{l_a}$ is kinematically suppressed, independently of the concomitant mixing-angle suppression which is necessarily present in μ decay and also for HSC modes in τ decay. Thus, for example, whereas in M_{e2} decay an HSC ν_i mode might be enhanced by a relative kinematic rate factor $\bar{\rho}(\delta_e^M, \delta_i^M) \sim 10^4$–$10^5$, the opposite and more normal situation obtains in $l_a \to \nu_{l_a} l_b \nu_{l_b}$ decay. We shall make this statement more quantitative shortly.

Thus, if HSC neutrinos exist, a definitive proof, via particle decays, of this fact will probably rely upon the discovery of the resultant additional peak(s) in the l_a spectrum in $M_{l_a 2}$ decay. However, it is certainly worthwhile to analyze the characteristics of $l_a \to \nu_{l_a} l_b \bar{\nu}_{l_b}$ decay in the general context of massive neutrinos and lepton mixing, especially in view of its cleanliness and the existing high-precision data on μ decay (and prospects of even more precise measurements at the meson factories SIN, LAMPF, and TRIUMF). Moreover, although the primary emphasis of our work has been on tests for HSC neutrinos, it should be recalled that one can use leptonic l_a decay to search for, and set bounds on, the masses of the HDC (anti)neutrinos emitted. The methods for doing this are well known, and although they relied upon the incorrect identification of neutrino gauge-group and mass eigenstates, the effects of this are only slight for the decay modes in which both ν_i and $\bar{\nu}_j$ are dominantly coupled.[1-3] One might stress that, in contrast to the use of $M_{\mu 2}$ decays to set an upper bound on "$m(\nu_{l_b})$", the use of leptonic l_a decays to set upper limits on DC neutrino masses is always a two-step process. As the test has been applied in the past, the fact has been used (implicitly) that the existing upper limit on "$m(\nu_{l_b})$" was much lower than the upper limit that could be placed on "$m(\nu_{l_a})$". If this had not been true, then, for example, from the measurement of $(E_b)_{\max}$, one would only have obtained an upper limit on ["$m(\nu_{l_a})$" + "$m(\nu_{l_b})$"] but neither mass individually. Given this fact, experimentalists have then used a measurement of $(E_e)_{\max}$ in μ decay,[11] and the shape of the electron spectrum, with the Michel parameter ρ assumed to equal $\frac{3}{4}$ exactly in τ decay,[12,13] to set respective upper limits on "$m(\nu_\mu)$" and "$m(\nu_\tau)$".[14] As discussed in Refs. 1–3, these can be reinterpreted to yield, with only slight mixing-angle dependence, corresponding limits on $m(\nu_2)$ and $m(\nu_3)$, respectively. For μ decay this approach gave the upper bound[11] "$m(\nu_\mu)$" < 2.5 MeV (no confidence level cited), which is very good, although not as stringent as the best limit obtained from $\pi_{\mu 2}$ decay,[15] "$m(\nu_\mu)$" < 0.57 MeV (90% C.L.). The corresponding upper limit[13] "$m(\nu_\tau)$" < 250 MeV (90% CL) has recently been slightly improved by another upper bound derived from an analysis of $\tau \to \nu_\tau \pi$ decay, viz., "$m(\nu_\tau)$" < 245 MeV (2σ level).[14] Thus, there still remains the exciting possibility of observing in τ decay a full strength, dominantly coupled neutrino ν_3, with quite substantial mass. This would become an especially urgent task if an experiment which applies our M_{l2} test should discover an HSC ν_i peak in the spectra of one or more of the π_{l2} and K_{l2} decays corresponding to a mass $m(\nu_i)$ which is large enough for its kinematic effects to be observable in τ decay. If there are $n = 3$ generations of fermions, then such an HSC peak could only be due to the decay $M^\pm \to l_a^\pm(\bar{\nu}_3)$, so that one is guaranteed to be able to see its effects unsuppressed by small mixing angles in the decays $\tau \to \nu_3 e \bar{\nu}_1$ and $\tau \to \nu_3 \mu \bar{\nu}_2$. If $n > 3$, then the hypothetical HSC ν_i peak discovered in M_{l2} decay might be due to ν_3 or to $\nu_{i>3}$; in the latter case it would again be an HSC neutrino in τ decay. However, the HSC coupling coefficient which modulates the strength of the decays $\tau \to \nu_i l_b \nu_{j \neq b}$, $|U^*_{3i}U_{bb}|^2 \simeq |U_{3i}|^2$ might not be overly small for some $i > 3$, such as $i = 4$.

Because of the primary role of M_{l2} decay in the search for HSC neutrinos, we treated the Lorentz structure of the relevant amplitude in complete generality in paper I. However, it seems premature to carry out the analogous calculations for

$l_a \to \nu_{l_a} l_b \bar{\nu}_{l_b}$ decay, and consequently, we shall assume here that the charged-current couplings are $V-A$. After analyzing the theoretical aspects of leptonic decays, we shall briefly discuss the application of our results to existing data to derive correlated bounds on neutrino masses and mixing.

B. General results on differential decay distributions

We proceed to state our results for l_a leptonic decays in the general context of nonzero neutrino masses and lepton mixing. Only very massive and/or slowly moving outgoing (anti)neutrinos would be likely to decay within the experimental detector. Hence, with this exception, to be discussed later, the experimentally measurable quantities are generically the same as in the conventional l_a leptonic decay, although now the final-state quantities have independent values for each of the (i,j) modes. These quantities are the parent lepton polarization $\vec{P}_{l_a^\pm} \equiv \langle \vec{\sigma}_{l_a^\pm} \rangle$, the momentum of the outgoing charged lepton $\vec{p}_b \equiv \vec{p}_{l_b}$, and hence also the angle of emission of the l_b relative to parent-lepton-polarization direction $\hat{P}_{l_a}$,

$$\theta \equiv \cos^{-1}(\hat{p}_b \cdot \hat{P}_{l_a}), \tag{2.2}$$

and finally, the l_b polarization $\vec{P}_{l_b}$. More specifically, in μ decay, especially with the advent of meson factories at SIN, LAMPF, and TRIUMF, one can produce a beam of highly polarized muons and can measure all of the final-state quantities mentioned above with great precision and statistical accuracy. In the case of the τ, the situation is more difficult. Since it is produced via the reaction $e^+e^- \to \tau^+\tau^-$, at center-of-mass energies $\sqrt{s}$ not $\gg 2m_\tau$, at least for the existing data from which τ decay properties were inferred, and since the τ lifetime is quite short, $\sim 10^{-13}$ sec, it has not so far been possible to observe the τ track directly. Owing to the fact that in the leptonic decay under consideration here one thus only observes the outgoing e or μ, it is not possible, on an event-by-event basis, to reconstruct $\vec{p}_\tau$ and hence the kinematics of the decay. If, as is true of a substantial amount of τ decay data, $(\sqrt{s} - 2m_\tau)/(2m_\tau) \lesssim 1$, so that the τ is relatively slowly moving, then the severity of this reconstruction problem is reduced somewhat. Concerning the initial τ polarization, because of the time-dependent buildup of transverse e^+ and e^- beam polarizations (relative to the plane of the storage ring), the $\tau^\pm$ may have a longitudinal polarization without any violation of parity in its production. Given a knowledge of the beam polarization, one could predict $\vec{P}_{\tau^\pm}$ as a function of $\sqrt{s}$ and $\hat{p}_\tau$. It is true that one can still perform a search for HSC, and, more excitingly, HDC modes in τ decay data using appropriate Monte Carlo simulation methods. But clearly it is not possible at the present time to achieve the same degree of control over the parent lepton polarization or to reconstruct the decay kinematics as accurately in τ, as in μ, decay.

The general expression for P_{l_b} will be given below; assuming that one does not measure the l_b polarization, the differential decay distributions for the decay $l_a \to \nu_i l_b \bar{\nu}_j$ and its charge conjugate can be written as

$$\frac{d^2\Gamma}{dE_b d\cos\theta}(l_a^- \to \nu_i l_b^- \bar{\nu}_j;\ l_a^+ \to \bar{\nu}_i l_b^+ \nu_j) = \Gamma_0(m_a)\left|U^*_{ai}U_{bj}\right|^2 \frac{d^2\overline{\Gamma}^{(\pm)}}{dE_b d\cos\theta}\left(E_b, \cos\theta; \frac{m(\nu_i)}{m_a}, \frac{m(\nu_j)}{m_a}, \frac{m_b}{m_a}\right). \tag{2.3}$$

Here

$$\Gamma_0(m_a) \equiv \frac{G_0^2 m_a^5}{192\pi^3} \tag{2.4}$$

with

$$\frac{G_0}{\sqrt{2}} \equiv \frac{g^2}{8m_W^2}, \tag{2.5}$$

where g is the gauge coupling of the $SU(2)_L$ factor group in the electroweak $SU(2)_L \times U(1)$ gauge group, as in Eq. (4.4) of paper I. Γ_0 represents the total rate to lowest order, in the case where $m_b = 0$ and $m(\nu_i) = m(\nu_j) = 0\ \forall\, i,j$. As was noted in paper I, G_0 is *not* the "usual" muon decay constant, $G_\mu = G_0^{(\text{apparent})}$ and the difference is not just the standard kinematic correction factor for the nonzero electron mass. This matter will be dealt with more fully later. The reduced differential decay distribution $d^2\overline{\Gamma}/dE_b d\cos\theta$ is normalized such that, when integrated to yield a rate, it gives unity if all of the masses of the final-state particles vanish. By the usual application of the theorems on homogeneous functions, it follows that $d^2\overline{\Gamma}^{(\pm)}/dE_b d\cos\theta$ depends only on the ratios of each of the masses of the final-state particles to the parent lepton mass. Accordingly, in our analysis of this function, we shall use units in which $m_a \equiv 1$. The reduced differential distribution can conveniently be written in terms of the momentum transfer Q^2 to the

neutrino-antineutrino pair, where

$$Q^2 = 1 - 2E_b + m_b{}^2 , \tag{2.6}$$

$$\frac{d^2\overline{\Gamma}^{(\mp)}}{dE_b d\cos\theta}(E_b,\cos\theta;\, m(\nu_i), m(\nu_j), m_b) = f_1(E_b;\, m(\nu_i), m(\nu_j), m_b) + \zeta\,|\vec{P}_{l_a}|\cos\theta f_s(E_b;\, m(\nu_i), m(\nu_j), m_b) , \tag{2.7}$$

where

$$\zeta = \pm 1 \quad \text{for } l_a^{\mp} , \tag{2.8}$$

$$f_1(E_b;\, m(\nu_i), m(\nu_j), m_b) = \lambda^{1/2}(1, Q^2, m_b{}^2)\{2Q^2(1 + m_b{}^2 - Q^2)A_{ij} + [(1 - m_b{}^2)^2 - Q^4]B_{ij}\} , \tag{2.9}$$

$$f_s(E_b;\, m(\nu_i), m(\nu_j), m_b) = \lambda(1, Q^2, m_b{}^2)[2Q^2 A_{ij} - (1 - m_b{}^2 - Q^2)B_{ij}] , \tag{2.10}$$

and

$$A_{ij} = \lambda^{3/2}\left(1, \frac{m(\nu_i)^2}{Q^2}, \frac{m(\nu_j)^2}{Q^2}\right), \tag{2.11}$$

$$B_{ij} = 2\lambda^{1/2}\left(1, \frac{m(\nu_i)^2}{Q^2}, \frac{m(\nu_j)^2}{Q^2}\right)\left[1 + \frac{m(\nu_i)^2 + m(\nu_j)^2}{Q^2} - 2\left(\frac{m(\nu_i)^2 - m(\nu_j)^2}{Q^2}\right)^2\right]. \tag{2.12}$$

In these formulas we use the standard kinematic function

$$\lambda(x,y,z) \equiv x^2 + y^2 + z^2 - 2(xy + yz + zx) . \tag{2.13}$$

The functions f_1 and f_s, and hence the full reduced differential decay distribution, $d^2\overline{\Gamma}^{(\mp)}/dE_b d\cos\theta$, have the symmetry property

$$f_{1,s}(E_b;\, m_1, m_2, m_b) = f_{1,s}(E_b;\, m_2, m_1, m_b) , \tag{2.14}$$

$$\frac{d^2\overline{\Gamma}^{(\mp)}}{dE_b d\cos\theta}(E_b,\cos\theta;\, m_1, m_2, m_b) = \frac{d^2\overline{\Gamma}^{(\mp)}}{dE_b d\cos\theta}(E_b,\cos\theta;\, m_2, m_1, m_b) . \tag{2.15}$$

Although in the $V-A$ case considered here the decay amplitude is symmetric under the interchange $l_b \leftrightarrow \nu_i$ by a Fierz identity, this symmetry is not present in $d^2\overline{\Gamma}^{(\mp)}/dE_b d\cos\theta$, because one has picked out the energy and angle of the l_b while integrating over the analogous quantities for ν_i. However, when one finally integrates over $\cos\theta$ and E_b to obtain the total reduced rate for the (i,j) mode, this symmetry is restored. Combining this result with Eq. (2.14), it follows that the total reduced rate $\overline{\Gamma}(m(\nu_i),\, m(\nu_j),\, m_b)$ is a completely symmetric function of its three arguments:

$$\overline{\Gamma}(m_1, m_2, m_3) = \overline{\Gamma}(m_{\pi(1)}, m_{\pi(2)}, m_{\pi(3)}) , \tag{2.16}$$

where π is an automorphism of Z_3.

Thus, the LDC (and any LSC) modes, with $m(\nu_{i_L}) \ll 1$ and also, given our definition of the sets $\{\nu_{i_L}\}$ and $\{\nu_{i_H}\}$, $m(\nu_{i_L})^2 \ll m_b{}^2$, are described to a very good approximation by the functions

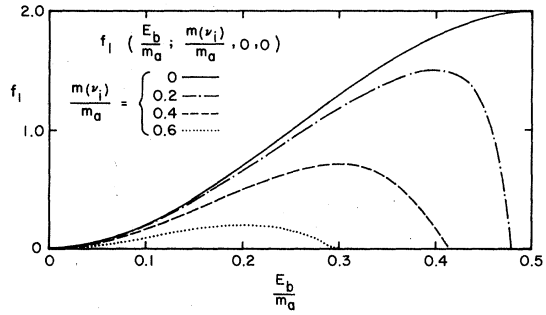

FIG. 2. The function $f_1(E_b/m_a;\, m(\nu_i)/m_a,\, m(\nu_j)/m_a,\, m_b/m_a)$ for the case where $m(\nu_j) = m_b = 0$ (or $\ll m_a$), but $m(\nu_i)$ is substantial. This function and all other quantities shown in these figures are symmetric under the interchange $m(\nu_i) \leftrightarrow m(\nu_j)$. In this figure and Fig. 3 the m_a dependence is rendered explicit, but thereafter the units are chosen such that $m_a \equiv 1$.

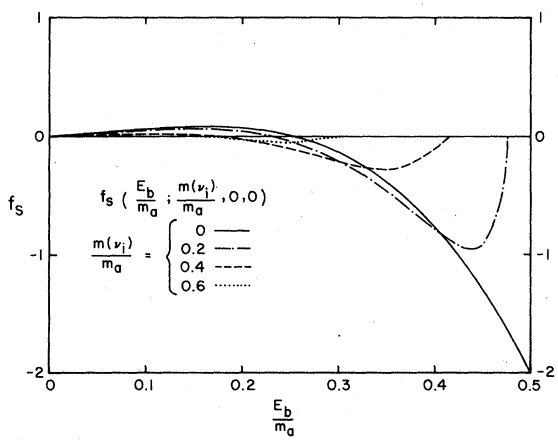

FIG. 3. Same as Fig. 2 but for the function f_s.

$$f_1(E_b;0,0,m_b)=8(E_b^2-b)^{1/2}[-4E_b^2+3(1+b)E_b-2b] \tag{2.17}$$

and

$$f_s(E_b;0,0,m_b)=8(E_b^2-b)(1-4E_b+3b)\,, \tag{2.18}$$

where

$$b\equiv m_b^2\,. \tag{2.19}$$

These functions are plotted as the curves labeled (a) in Figs. 2 and 3, respectively, for the realistic case in which $m_b^2\ll 1$, a condition which obtains in both μ decay and the two leptonic τ decays. It is useful to recall some characteristics of the behavior of these functions as a background for analyzing the effects of neutrinos of non-negligible mass. Although all of these characteristics are easily derived from the well-known formulas (2.17) and (2.18), we record them here because they will be useful for our later discussion. As E_b increases from m_b to $(1+b)/2$, f_1 increases from 0 to

$$f_{1\max}(0,0,m_b)=2(1-b)^3\,. \tag{2.20}$$

The function f_s increases from 0 to a maximum at

$$\begin{aligned}(E_b)_{f_{s\max}}(0,0,m_b)&=\tfrac{1}{12}[1+3b+(1+54b+9b^2)^{1/2}]\\&\simeq \tfrac{1}{6}+\tfrac{5}{2}b \quad \text{for } b\ll 1\,,\end{aligned} \tag{2.21}$$

where it is equal to

$$\begin{aligned}f_{s\max}(0,0,m_b)&=\tfrac{1}{27}[(1+3b)(1-138b+9b^2)\\&\quad+(1+54b+9b^2)^{3/2}]\\&\simeq \tfrac{2}{27}-2b \quad \text{for } b\ll 1\,.\end{aligned} \tag{2.22}$$

It then decreases, passing through 0 at

$$(E_b)_{f_s=0}(0,0,m_b)=\frac{1+3b}{4} \tag{2.23}$$

and reaching the end-point value

$$\begin{aligned}f_s((E_b)_{\max};0,0,m_b)&=f_{s\min}(0,0,m_b)\\&=-2(1-b)^3\\&=-f_1((E_b)_{\max};0,0,m_b)\,.\end{aligned} \tag{2.24}$$

The equality in Eq. (2.24) relating f_1 and f_s is, of course, no accident; its implications for the search for the effects of massive-neutrino decay modes will be explored further below. In μ decay, for which one has the greatest amount of high-precision data, $b\equiv m_e^2/m_\mu^2=2.3\times 10^{-5}$, so that the $O(b)$ corrections are extremely small.

In order to display the effects of massive (anti) neutrinos on the double-differential distribution, we show in curves (b)–(d) of Figs. 2 and 3 the functions f_1 and f_s in the case of primary interest, where either ν_i or $\bar{\nu}_j$ has a substantial mass, the other is light, and, independently, $m_b^2\ll 1$. This case is described to high accuracy by the functions $f_{1,s}(E_b;m,0,0)=f_{1,s}(E_b;0,m,0)$. In terms of the convenient variable

$$a\equiv m^2\,, \tag{2.25}$$

we have

$$\begin{aligned}f_1(E_b;m,0,0)&=8E_b^2(1-2E_b)^{-3}(1-2E_b-a)^2\\&\quad\times[8E_b^2-2(5+a)E_b+3(1+a)]\end{aligned} \tag{2.26}$$

and

$$\begin{aligned}f_s(E_b;m,0,0)&=8E_b^2(1-2E_b)^{-3}(1-2E_b-a)^2\\&\quad\times[8E_b^2-2(3+a)E_b+1-a]\,.\end{aligned} \tag{2.27}$$

One can observe first that as $m=\{m(\nu_i)$ or $m(\nu_j)\}$ increases, the physical region is commensurately reduced in accordance with Eq. (2.1). As is evident in Fig. 2, for $m(\nu_{i\ \text{or}\ j})\neq 0$, f_1 reaches a maximum at an intermediate value of the l_b energy

$$(E_b)_{f_{1\max}}(m,0,0)=\left(\frac{1-m}{2}\right). \tag{2.28}$$

Although special values $(E_b)_s(m(\nu_i),m(\nu_j),0)$ such as this necessarily approach zero as $m\equiv m(\nu_i)+m(\nu_j)\to 1$, it is useful to define the ratios

$$(\bar{E}_b)_s(m(\nu_i),m(\nu_j),0)\equiv\frac{(E_b)_s(m(\nu_i),m(\nu_j),0)}{(E_b)_{\max}(m(\nu_i),m(\nu_j),0)}\,, \tag{2.29}$$

where s denotes a generic special value, and the denominator is given by Eq. (2.1); these usually have nonzero limits as $m\to 1$. In the case at hand

$$(\bar{E}_b)_{f_{1\max}}(m,0,0)=\frac{1}{1+m}\,. \tag{2.30}$$

At the value of E_b given in Eq. (2.28)

$$f_{1\max}(m,0,0)=2(1-m)^4(1+4m+m^2)\,. \tag{2.31}$$

Note that for $m\ll 1$, the reduction in $f_{1\max}$ is actually second order in m. For f_s, as m increases from zero, the position of the maximum and zero shift downward, and there appears a minimum at a value of $E_b<(E_b)_{\max}$. The position of the zero becomes

$$(E_b)_{f_s=0}(m,0,0)=\tfrac{1}{8}[3+a-(1+14a+a^2)^{1/2}] \tag{2.32}$$

The analytic expressions for the positions of the maximum and minimum are rather complicated. Let us define the auxiliary functions

$$w_1 \equiv \left\{\left(\frac{a^2}{288}\right)\left[1+\left(\tfrac{338}{81}\right)a+a^2 - (1-a)\left(1+\tfrac{838}{81}\,a+a^2\right)^{1/2}\right]\right\}^{1/3}, \tag{2.33a}$$

$$w_2 \equiv \left[w_1+\tfrac{1}{36}+\tfrac{1}{9}\,a+\left(\tfrac{25}{324}\right)a^2 w_1^{-1}\right]^{1/2}, \tag{2.33b}$$

$$w_3 \equiv -w_1+\tfrac{1}{18}+\tfrac{2}{9}a-\left(\tfrac{25}{324}\right)a^2 w_1^{-1}, \tag{2.33c}$$

and

$$w_4 \equiv \tfrac{1}{2}\left[w_3+\tfrac{1}{108}\left(1+6a+18a^2\right)w_2^{-1}\right]^{1/2}. \tag{2.33d}$$

Then

$$(E_b)_{f_S\,\max}(m,0,0) = -w_4-\tfrac{1}{2}w_2+\tfrac{5}{12} \tag{2.33e}$$

and

$$(E_b)_{f_S\,\min}(m,0,0) = w_4-\tfrac{1}{2}w_2+\tfrac{5}{12}. \tag{2.33f}$$

The total differential decay distribution for "the" decay $l_a \to \nu_{l_a} l_b \bar{\nu}_{l_b}$, i.e., the set of (i,j) decays $l_a \to \nu_i l_b \bar{\nu}_j$, is then

$$\frac{d^2\Gamma}{dE_b\, d\cos\theta}(E_b,\cos\theta; l_a \to \nu_{l_a} l_b \bar{\nu}_{l_b}) = \Gamma_0(m_a)\sum_{i,j}|U_{ai}^* U_{ij}|^2 \frac{d^2\overline{\Gamma}}{dE_b\, d\cos\theta}(E_b,\cos\theta; l_a \to \nu_i l_b \bar{\nu}_j), \tag{2.34}$$

where the sum runs over all (i,j) modes allowed by phase space (henceforth, this will be implicit), and similarly for the charge-conjugate decay. Hence,

$$\Gamma(l_a \to \nu_{l_a} l_b \bar{\nu}_{l_b}) = \Gamma_0(m_a)\sum_{i,j}|U_{ai}^* U_{bj}|^2 \overline{\Gamma}\left(\frac{m(\nu_i)}{m_a}, \frac{m(\nu_j)}{m_a}, \frac{m_b}{m_a}\right). \tag{2.35}$$

Stated in words, given that one detects only the l_b, the differential distribution and total rate represent a sum of all the specific (i,j) modes allowed by phase space. The sum is, of course, incoherent, since the actual final states are different, although the observed particle is the same. Equations (2.34) and (2.35) also apply in the case where a heavy ν_i and/or $\bar{\nu}_j$ decay(s), if one integrates over the additional observables describing the (anti)neutrino decay products. This has profound implications for the meaning of the observed μ decay constant G_μ and the predicted value of the W-boson mass m_W which is calculated using this constant as an input. These will be discussed later.

Apart from the possible HDC decay $\tau \to \nu_3 l_b \bar{\nu}_{j=b}$ (and, strictly speaking, also $\mu \to \nu_2 e \bar{\nu}_1$),[10] together with similar decays of hypothetical l_a, $a \geq 4$, the massive-neutrino decay modes are constrained to be HSC and hence yield small additions to the LDC channels(s). Thus, in determining the effects of the HSC modes, as part of the general theory of weak decays involving neutrinos and as a framework for a generalized analysis of the relevant data, it is necessary to take into account the order-α corrections to the DC mode(s), since these may be comparable to the lowest-order rates for the HSC decays. These corrections can be divided into two types: (1) pure electromagnetic, including virtual and real photons, and (2) electroweak, excluding (1). The pure electromagnetic corrections to the spectrum and rate for μ decay were calculated long ago in the local $V-A$ theory, assuming that $m(\nu_\mu) = m(\nu_e) = 0$ (Ref. 16); to leading order in m_μ^2/m_W^2, with the same assumption concerning neutrino masses, these apply again in the present electroweak gauge theory. One-loop electroweak corrections to the total μ decay rate have been analyzed by a number of authors.[17,19] An important simplification is that, to leading order in m_μ^2/m_W^2, the full amplitude has the same Dirac form as the tree-level amplitude; i.e., the correction just amounts to an overall multiplicative factor in the amplitude.[20] This means that it changes the rate, but not the normalized differential distribution, in contrast to the pure electromagnetic correction, which changes both. With the same assumptions and obvious changes in masses, the calculations of Refs. 17–19 also apply to leptonic τ decays. Hence, in our discussion of the differential distributions, it is only necessary to include the pure electromagnetic corrections to the DC modes. Moreover, concerning the order-α corrections, in μ decays, terms of order $(\alpha/\pi)(m_e^2/m_\mu^2)$ and $(\alpha/\pi)m(\nu_{\mathrm{LDC}\ i\ \mathrm{or}\ j})^2/m_\mu^2$ are negligible relative to those of order (α/π). The analog is also true, albeit to a lesser extent, in leptonic τ decay. Thus, to a good approximation, especially in μ decay, one can use the order-α correction, evaluated dropping m_b^2/m_a^2, and, we note, also $m(\nu_{\mathrm{LDC}\ i\ \mathrm{or}\ j})^2/m_\mu^2$ terms, except, in the former case, for $\ln(m_b/m_a)$ terms where this would lead to infrared divergences. Analytically,

$$f_{1,s}^{(c)} = f_{1,s}^{(0)} + \left(\frac{\alpha}{2\pi}\right) f_{1,s}^{(2)} + O\left(\left(\frac{\alpha}{\pi}\right)^2\right), \tag{2.36}$$

where the superscript (c) denotes "corrected", and $f_{1,s}^{(0)} \equiv f_{1,s}$ can be read off from Eqs. (2.6)–(2.13).

In the only case where these order-α corrections must be included, viz., that in which ν_i and $\bar{\nu}_j$ are LDC (anti)neutrinos, Eq. (2.19) can be approximated as

$$f_{1,s}^{(c)}(E_b; m(\nu_i), m(\nu_j), m_b) = f_{1,s}^{(0)}(E_b; m(\nu_i), m(\nu_j), m_b) + \left(\frac{\alpha}{2\pi}\right) f_{1,s}^{(2)}(E_b; 0, 0, m_b \ll 1), \tag{2.37}$$

where the function $f_1^{(2)}(E_b; 0, 0, m_b)$ and, for $m_b/m_a \ll 1$, the function $f_s^{(2)}(E_b; 0, 0, m_b/m_a \ll 1)$, were calculated in Ref. 16. Qualitatively, $f_1^{(2)}(E_b; 0, 0, m_b \ll 1)$ is positive for $E_b \lesssim 0.335$ and negative for larger values of E_b, so that $(E_b)_{f_1^{(c)}\max}(0, 0, m_b \ll 1)$ is slightly smaller than $(E_b)_{\max}(0, 0, m_b \ll 1)$. Moreover, $f_{1\max}^{(c)}(0, 0, m_b \ll 1) \lesssim f_{1\max}(0, 0, m_b \ll 1)$. The correction $f_s^{(2)}(E_b; 0, 0, m_b \ll 1)$ is negative for $E_b \lesssim 0.405$ and positive for larger E_b, so that $(E_b)_{f_s^{(c)}\max}(0, 0, m_b \ll 1)$, $f_{s\max}^{(c)}(0, 0, m_b \ll 1)$, and $(E_b)_{f_s^{(c)}=0}(0, 0, m_b \ll 1)$ are all slightly smaller than their lowest-order counterparts, which can be read off from Eqs. (2.21)–(2.23). These facts will be useful for our later analysis of the effects of HSC decay modes. Note that there is an apparent infrared divergence in both $f_1^{(2)}$ and $f_s^{(2)}$ at $E_b = (E_b)_{\max}$. This would be important for the differential distribution, were it not for the fact that when one properly sums multiple soft-photon emission to all orders in α, the apparently divergent term actually exponentiates into a form which vanishes as $E_b \to (E_b)_{\max}$.[21] The full order-α pure electromagnetic corrections $f_{1,s}^{(2)}(E_b; m(\nu_i), m(\nu_j), m_b)$ have not, to our knowledge, been calculated; however, they are not of immediate interest, because (1) as explained before, for all known l_a decays, in the case of (L or H)DC modes these functions are very well approximated by $f_{1,s}^{(2)}(E_b; 0, 0, m_b \ll 1)$; and (2) for HSC decay modes, where $m(\nu_{i \text{ or } j})^2/m_a^2$ might not be $\ll 1$, the order-α corrections to the tree-level decay rates are second order in small quantities (α and $|U_{ai}^* U_{bj}^*|^2$, HSC i or j) and hence are negligible to this level of accuracy. Thus, with radiative corrections of type (1) included where necessary, Eq. (2.34) can be written as

$$\frac{d^2\Gamma}{dE_b d\cos\theta}(l_a^- \to \nu_{l_a} l_b^- \bar{\nu}_{l_b}; l_a^+ \to \bar{\nu}_{l_a} l_b^+ \nu_{l_b}) \propto \Gamma_0(m_a)\Big[\sum_{\text{DC } i,j} |U_{ai}^* U_{bj}|^2 (f_1^{(c)} + \zeta |\vec{P}_{l_a}| \cos\theta f_s^{(c)}) + \sum_{\text{SC } i,j} |U_{ai}^* U_{bj}|^2 (f_1 + \zeta |\vec{P}_{l_a}| \cos\theta f_s)\Big], \tag{2.38}$$

where the DC sum must include, but is not necessarily limited to, the term $i = a$, $b = j$; the arguments of the functions $f_{1,s}$ are left implicit; and the proportionality rather than equality relation applies because, for the reason given above, we have not included corrections of type (2). These will be incorporated in our later discussion of G_μ, m_W, and m_Z.

C. Total rates

Let us next present expressions for the reduced rates for the decays of interest and subsequently analyze the features of the differential decay distributions. As will be obvious, unless otherwise noted, the expressions are accurate to lowest order in α. For analytical purposes it is again useful to deal with these quantities individually for given (i,j) decay modes in order to describe the effects of massive (anti)neutrinos. We will later use the results in the treatment of the actual observed distribution and rate which, as was stressed above, are sums of *all* of the allowed modes [except for any modes where one detects the decay(s) of one or both of the final-state (anti)neutrinos]. If all of the final-state-lepton masses are nonzero, the reduced rate $\bar{\Gamma}(m(\nu_i), m(\nu_j), m_b)$ can be expressed in terms of elliptic integrals. However, the analytic result is not particularly enlightening, and for the purpose of numerical evaluation it is simpler to use the integral representation directly. Moreover, since we are primarily interested here in the characteristics of l_a decays involving (anti) neutrinos with masses $m(\nu_i)$ or $m(\nu_j)$ not $\ll m_a$, and since $m_b^2 \ll m_a^2$ for μ and both leptonic τ decays,[22] it follows that for most of our discussion we shall only need expressions for $\bar{\Gamma}$ where one of the final-state masses is negligibly small. It is obvious that, other things (such as the degree of U suppression) being comparable, the decays with $m(\nu_{i \text{ or } j}) \not\ll m_a$ are of greatest interest, because the effects of massive neutrinos would be essentially undetectable if $m(\nu_{i,j}) \ll m_a$. Accordingly, although most of our results, such as Eqs. (2.7)–(2.12) and the consequent total rate, are completely general, we shall concentrate on this case here. If one of the final-state masses is zero or much smaller than the other two, then the rate takes a reasonably simple form. Because of the symmetry property (2.16) we can, with no loss of generality, choose $m_3 = 0$. The same property also implies that $\bar{\Gamma}(m_1, m_2, 0)$ can be expressed as a function of

the variables (m_1+m_2) and $|m_1-m_2|$. Since most terms in the reduced rate depend only on the squares of these masses, it is convenient to introduce the variables

$$a_i \equiv m_i^2, \quad i=1,2. \tag{2.39}$$

Further, we define the equivalent variables

$$s \equiv a_1 + a_2 \tag{2.40}$$

and

$$D \equiv (a_1 - a_2)^2 \tag{2.41}$$

and the functions

$$r(u,s,D) \equiv (u^2 - 2us + D)^{1/2}, \tag{2.42a}$$

$$t(s,D) \equiv \tfrac{1}{2}(s^2 - D)^{1/2} = m_1 m_2, \tag{2.42b}$$

$$L_1(u,s,D) \equiv \ln\left(\frac{u - s + r(u,s,D)}{2t(s,D)}\right), \tag{2.43a}$$

and

$$L_2(u,s,D) \equiv \ln\left(\frac{su - D - D^{1/2} r(u,s,D)}{2ut(s,D)}\right). \tag{2.43b}$$

(In the present case, $u=1$: the functional dependence on u will be used in its full generality later.)

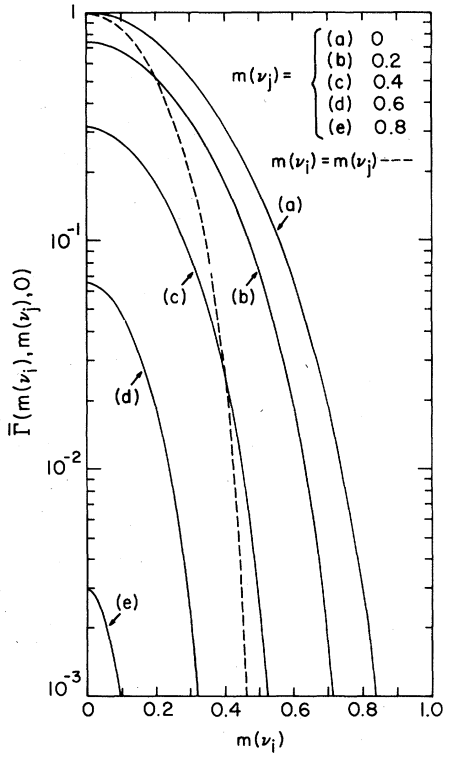

FIG. 4. The reduced rate $\overline{\Gamma}(m(\nu_i), m(\nu_j), 0)$ for leptonic l_a decay as a function of $m(\nu_i)$ for various values of $m(\nu_j)$. This function is applicable to the case $m_b^2 \ll 1$ which obtains in the known l_a decays.

Then

$$\overline{\Gamma}(m_1,m_2,0) = \tfrac{1}{2}[2 - 3s^3 - s^2 + (5D-14)s - 13D] \times r(1,s,D) - \tfrac{3}{2}[s^4 - 2(D+2)s^2 + D^2 - 4D] \times L_1(1,s,D) + 12sD^{1/2} L_2(1,s,D). \tag{2.44}$$

Alternatively, the reduced rate can, of course, be expressed directly in terms of the variables a_1 and a_2. This does not significantly shorten the results as a whole; however, the coefficient of the first ln term takes the simpler form $12(a_1^2 + a_2^2 - 2a_1^2 a_2^2)$. The function $\overline{\Gamma}(m_1,m_2,0)$ decreases rapidly from 1 to 0 as the quantity (m_1+m_2) increases from 0 to 1. We plot this function in Fig. 4 for the case of primary interest here, where $m_b^2 \ll 1$, and m_1 and m_2 represent the masses of the heavy (anti)neutrinos emitted in l_a decay; i.e., we plot $\overline{\Gamma}(m(\nu_i), m(\nu_j), 0)$. This graph shows that leptonic l_a decays involving one or two neutrinos with masses $m(\nu_{i,j}) \not\ll 1$ are severely suppressed kinematically. This is, of course, the normal situation; the fact that massive-neutrino modes were essentially unsuppressed until $m(\nu_i)$ approached $m(\nu_i)_{\max}$ in $\pi_{\mu 2}$ decay and were enhanced significantly in $K_{\mu 2}$ decay and drastically in M_{e2} decays relied upon the very special dynamical suppression of the corresponding decays into light or massless neutrinos. In using the curves of Fig. 4, one should again recall that in all cases except[10] the interesting (HDC, LDC) one in τ decay, the complete rate for the decay into massive (anti)neutrino(s) is further suppressed by small HSC coupling coefficient(s) via the factor $|U_{ai}^* U_{bj}|^2$ which multiplies the reduced rate.

There are two special cases of Eq. (2.44) which are of interest. The first is the case where there is only one final-state particle with nonzero (or, for approximations, non-negligible) mass. Let us denote this mass by m and use the variable $a \equiv m^2$ as in Eq. (2.25). Then Eq. (2.44) reduces to the well-known result

$$\overline{\Gamma}(m,0,0) = (1 - 8a + a^2)(1-a^2) + 12a^2 \ln\left(\frac{1}{a}\right). \tag{2.45}$$

This case describes $l_a \to \nu_i l_b \bar{\nu}_j$ decays (and their charge conjugates) in which ν_i or $\bar{\nu}_j$ has a mass $m(\nu_{i \text{ or } j}) \not\ll 1$ while the other two masses are negligibly small, $m(\nu_{j \text{ or } i})^2 \ll 1$, $m_b^2 \ll 1$. Accordingly, the rate (2.45) is plotted in Fig. 2 as curve (a), with the identification $m(\nu_i) = m$, $m(\nu_j)^2 \ll 1$, $m_b^2 \ll 1$; of course, the same curve applies for the other identification $m(\nu_j) = m$, $m(\nu_i)^2 \ll 1$, $m_b^2 \ll 1$. Another special case occurs when two of the final-state masses are equal, say $m_1 = m_2$, and the third is zero or negligibly small. This situation would

have appeared to be too artificial to have any physical interest if one were incorrectly to consider ν_{l_a} and ν_{l_b} to be mass eigenstates, since for example in μ decay, there would have been no reason for any masses in the set $\{"m(\nu_\mu)", "m(\bar{\nu}_e)", m_e\}$ to be equal, except, for the former two, in the trivial case of zero mass. However, given the basic observation in Refs. 1–3, this situation *is* seen to be physically relevant, as it describes the diagonal subset of the l_a decays in which $i=j$, i.e., the set $\{l_a \to \nu_i l_b \bar{\nu}_i\}$, $i=1,\ldots,k \leq n$, as allowed by phase space. With the notation $m_1 = m_2 \equiv m$ and (2.29), Eq. (2.44) becomes

$$\bar{\Gamma}(m,m,0) = (1-14a-2a^2-12a^3)(1-4a)^{1/2} + 24a^2(1-a^2)\ln\left(\frac{1+(1-4a)^{1/2}}{1-(1-4a)^{1/2}}\right). \tag{2.46}$$

This function is plotted as the dashed curve in Fig. 4.

An interesting question is the following: for a given total mass in the final state, $m_{\rm tot} = \sum_{i=1}^{3} m_i$, what is the optimal division of this mass among the three particles to maximize the reduced rate. In the case where all of the masses are nonzero, the answer is the symmetric choice $m_i = m_{\rm tot}/3$, $i=1,2,3$. Similarly, for the case in which one of the m_i, say m_3, is zero or negligible, the reduced rate is maximized for $m_1 = m_2 = m_{\rm tot}/2$. Figure 5 shows how the reduced rate varies for this case as a function of the variable $m_>/m_< \equiv \max(m_1,m_2)/\min(m_1,m_2)$. As is evident from this graph, the maximum at $m_1 = m_2$ is a rather gentle one. This behavior is relevant in the comparison of the reduced rates for (HSC, HSC) modes versus (HSC, LDC) or (LDC, HSC) modes, and, in the case of τ decay, also (HDC, HSC) type decays versus (HDC, LDC) decays.[10] In order to maximize the reduced rate for a given $m_{\rm tot}$, it would actually be slightly preferable, from the point of view of the kinematics alone, to have an (HSC i, HSC j) or (HDC i, HSC j) mode with $m(\nu_i) \simeq m(\nu_j) \simeq m_{\rm tot}/2$ rather than one of the three modes listed above involving only a single heavy neutrino, if such existed, with $m(\nu_r) = m_{\rm tot}$. But this slight effect is in general completely overwhelmed by the double U suppression of the (HSC i, HSC j) mode relative to the (HSC r, LDC s) or (LDC s, HSC r) modes, and, in τ decay, by the single U suppression of the (HDC i, LDC j) mode relative to the U-allowed (HDC r, LDC s) mode (if an HDC ν_3, exists).

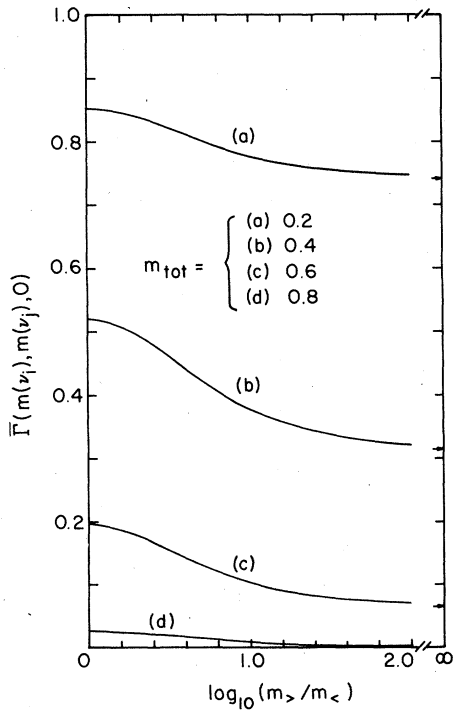

FIG. 5. The reduced rate $\bar{\Gamma}(m(\nu_i), m(\nu_j), 0)$ as a function of the ratio $(m_>/m_<)$ for various values of $m_{\rm tot} = m_> + m_<$, where $m_> \equiv \max\{m(\nu_i), m(\nu_j)\}$ and $m_< \equiv \min\{m(\nu_i), m(\nu_j)\}$.

D. Characteristics of differential decay distributions and average quantities

We next proceed to describe the double-differential decay distribution, especially with a view toward determining in which regions of the variables E_b and θ an HSC or HDC contribution might have the largest rate, relative to the sum of the dominant light-neutrino modes. It is thus necessary first to recall the behavior of the differential distribution for these light-neutrino modes. The special case of Eqs. (2.6)–(2.13) for $m(\nu_i) \ll m_b^2$ and $m(\nu_j) \ll m_b^2$ corresponds formally to the conventional distribution calculated assuming that $"m(\nu_{l_a})" = "m(\nu_{l_a})" = 0$. For comparison with the massive-neutrino modes, it will be useful to have a plot of the distribution, which is given for l_a^- decay, with $|\vec{P}_{l_a}| = 1$ in Fig. 6. In this and all other figures, the differential distribution for l_a^+ decay is related to that for the l_a^- decay shown by the replacement $\theta \to \pi - \theta$. Henceforth, to avoid awkward notation, we shall speak only of l_a^- decay; all of our comments will apply to l_a^+ decay with this transformation rule. As will be clear from the context, we shall generally consider the LDC distribution to lowest order, but will point out the effects of electromagnetic corrections where they are important. For

$$0 \simeq m_b < E_b < (E_b)_{\rm iso}(m(\nu_i) \ll 1, m(\nu_j) \ll 1, m_b \ll 1) = \tfrac{1}{4},$$

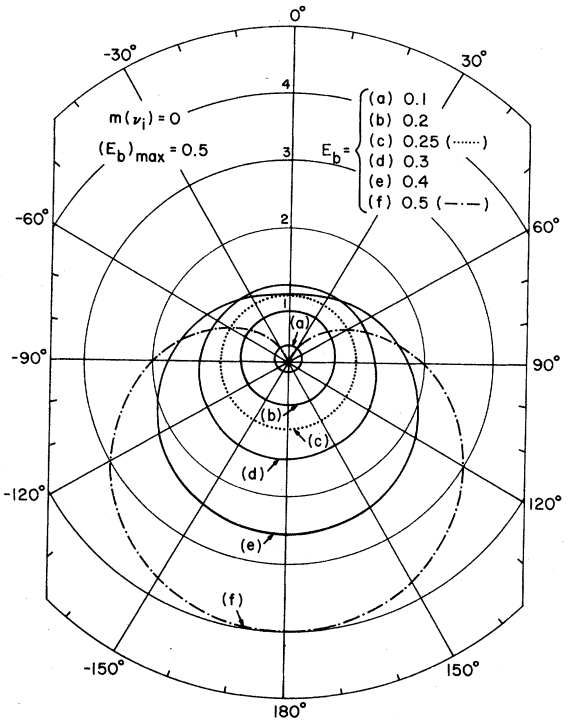

FIG. 6. The reduced double-differential distribution $d^2\overline{\Gamma}^{(-)}/dE_b d\cos\theta(E_b, \theta; m(\nu_i)=0,\ m(\nu_j)=0,\ m_b=0$ (or $\ll 1$)) for leptonic l_a decay as a function of θ, for various values of E_b. The dotted curve represents the value $E_b = (E_b)_{iso}$, where $f_s = 0$; the dot-dashed curve represents $E_b = (E_b)_{180°\ max}$. This distribution and all of the other quantities shown in these figures apply for l_a^- decay; the corresponding quantities for l_a^+ decay are obtained by the replacement $\cos\theta \to -\cos\theta$.

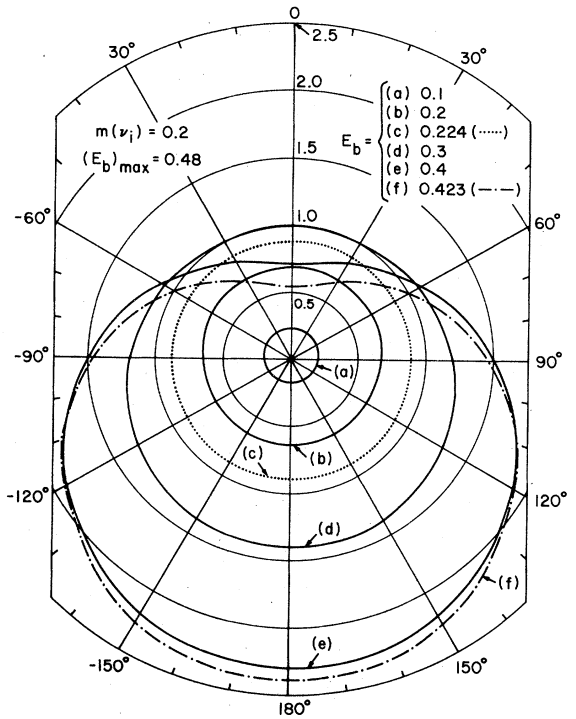

FIG. 7. Same as Fig. 6 but for $m(\nu_i)=0.2$. Note the successive expansions of the radial scale in Figs. 7–9.

the l_b^- is emitted preferentially into the hemisphere parallel to the parent lepton spin. Here $(E_b)_{iso}(m(\nu_i), m(\nu_j), m_b)$ is defined as the value of E_b at which the angular distribution is isotropic, i.e., at which f_s vanishes; at this value of E_b, $d^2\overline{\Gamma}^{(\mp)}/dE_b d\cos\theta = 1$. For

$$(E_b)_{iso}(0,0,0) < E_b < (E_b)_{max}(0,0,0) = \tfrac{1}{2},$$

the l_a^- is emitted preferentially into the hemisphere opposite to $\hat{P}_{l_a^-}$. As E_b increases through this range, the angular distribution for $|\theta| > 90°$ increases monotonically as a function of E_b. (This is true for arbitrary $m_b < 1$.) However, for $|\theta| < 90°$ (and arbitrary $m_b < 1$) a helicity effect operates to retard the increase of the distribution. For $m_b \ll 1$, the angular distribution reaches a maximum at

$$(E_b)_{\theta\ max}(\theta; m(\nu_i)=0, m(\nu_j)=0, m_b=0) = \frac{1}{6}\left(\frac{3+\cos\theta}{1+\cos\theta}\right) \tag{2.47}$$

for which energy

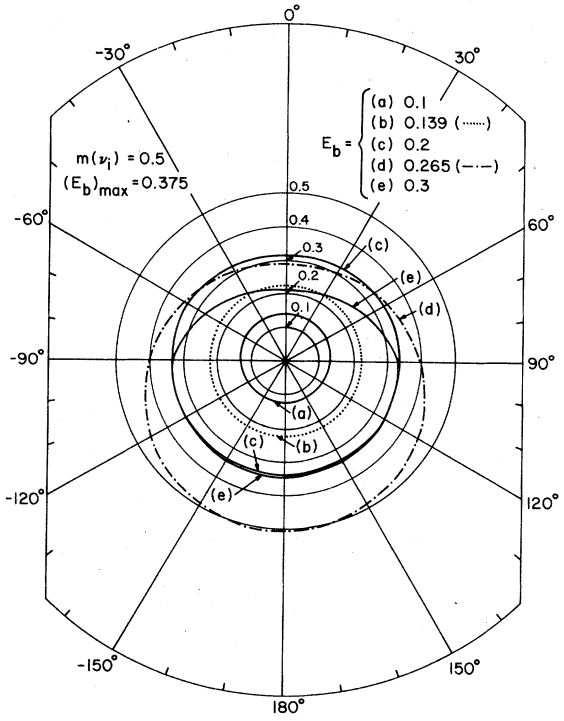

FIG. 8. Same as Fig. 6 but for $m(\nu_i)=0.5$.

$$\frac{d^2\overline{\Gamma}^{(-)}}{dE_b d\cos\theta}((E_b)_{\theta\max},\theta;0,0,0)=\frac{2(1+\frac{1}{3}\cos\theta)^3}{(1+\cos\theta)}. \quad (2.48)$$

For $|\theta|<90°$ and $E_b>(E_b)_{\theta\max}(\theta;0,0,0)$, $d^2\overline{\Gamma}^{(-)}/dE_b d\cos\theta$ decreases. Retaining m_b now, as $E_b\to(E_b)_{\max}(0,0,m_b)=(1+m_b^2)/2$,

$$\frac{d^2\overline{\Gamma}^{(-)}}{dE_b d\cos\theta}(E_b,\theta=0°,m(\nu_i)=0,m(\nu_j)=0,m_b)\to 0\,.$$

That is, in this limit, the l_b^- is forbidden from being emitted in the direction of the l_a^- spin. This is a consequence of the $V-A$ nature of the couplings and the constraint of angular momentum conservation. Although it is not stressed in the literature, this vanishing occurs for arbitrary $m_b<1$, as is clear from Eq. (2.24), and in no way represents an approximation of $m_b\ll 1$. The order-α radiative corrections do not alter this statement, as can be verified by inspection of the results of Ref. 16, taking proper account of the exponentiation of the apparent logarithmic divergence at $E_b=(E_b)_{\max}$. The vanishing does, however, require that $m(\nu_i)$ and $m(\nu_j)$ be strictly equal to zero. An immediate corollary is that a potentially promising place to search for HSC (anti)neutrino contributions might be at large l_b energies, near $\theta=0°$ for l_b^- and $180°$ for l_b^+. (Unfortunately, to anticipate our results below, even in these regions it would still be quite difficult to observe any possible HSC contribution modes.)

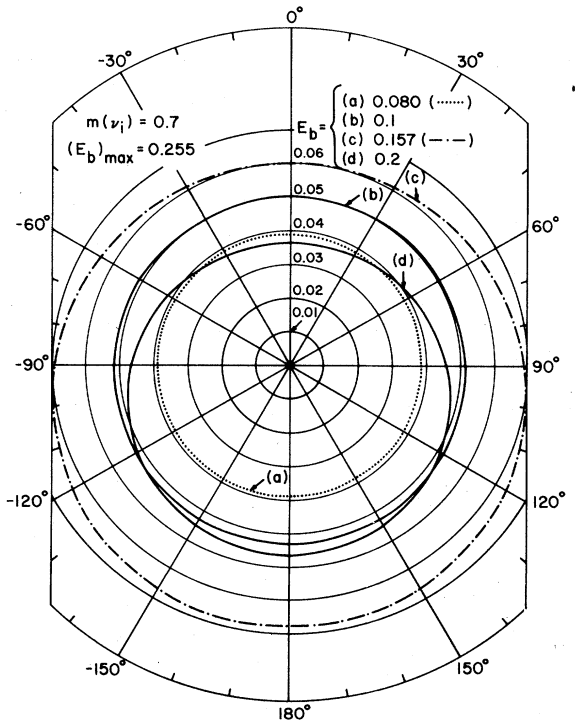

FIG. 9. Same as Fig. 6 but for $m(\nu_i)=0.7$.

If heavy-neutrino modes are present at all, the types that are most likely to be observed in l_a decay are (HSC, LDC), (LDC, HSC), and for $l_a=l_3\equiv\tau$ also possibly (HDC, LDC). We shall therefore concentrate on these types of decay modes. For the reduced rate we may without loss of generality take $m(\nu_i)$ to be the non-negligible mass, with $m(\nu_j)^2\ll 1$ and $m_b^2\ll 1$. The double-differential distribution for this case is formed from the functions $f_1(E_b;m,0,0)$ and $f_s(E_b;m,0,0)$ given in Eqs. (2.26) and (2.27); it is plotted for $|\vec{P}_{l_a}|=1$ and the representative values $m(\nu_i)=0.2$, 0.5, and 0.7 in Figs. 7, 8, and 9, respectively. Note the successive expansions of the radial scale. As in the figures, we shall assume here that $|\vec{P}_{l_a}|=1$; it is straightforward to extend our comments to the case of a parent lepton which is not completely polarized. The value of E_b at which the distribution is isotropic is $(E_b)_{\rm iso}(m(\nu_i),0,0)=(E_b)_{f_s=0}(m(\nu_i),0,0)$, as given in Eq. (2.32). In contrast to the behavior for $m(\nu_i)=m(\nu_j)=0$ with arbitrary $m_b<1$, not only in the range $|\theta|<90°$, but rather for any θ, there exists a value of E_b, namely $E_b=(E_b)_{\theta\max}(\theta;m(\nu_i),0,0)$ such that at this point

$$\frac{d}{dE_b}\left(\frac{d^2\overline{\Gamma}^{(-)}}{dE_b d\cos\theta}\right)=0$$

and

$$\frac{d^2}{dE_b^2}\left(\frac{d^2\overline{\Gamma}^{(-)}}{dE_b d\cos\theta}\right)<0\,,$$

i.e., the angular distribution reaches a maximum. In general, $(E_b)_{\theta\max}(\theta;m(\nu_i),0,0)$ is the solution to a cubic equation and the analytic result is somewhat cumbersome. For a given $m(\nu_i)$, the minimum value of $(E_b)_{\theta\max}(\theta;m(\nu_i),0,0)$ occurs at $\theta=0°$:

$$(E_b)_{\theta\max}(\theta=0°;m(\nu_i),0,0)$$
$$=r_2+\tfrac{4}{9}+\left(\frac{9a+1}{324}\right)r_2^{-1}, \quad (2.49)$$

where

$$r_2\equiv\tfrac{1}{6}\{\tfrac{1}{2}[ar_1-(\tfrac{2}{27}+a+9a^3)]\}^{1/3} \quad (2.50)$$

and

$$r_1\equiv(1+14a+81a^2)^{1/2}. \quad (2.51)$$

Again, for fixed $m(\nu_i)$, the maximum value of $(E_b)_{\theta\max}(\theta;m(\nu_i),0,0)$ occurs at $\theta=180°$:

$$(E_b)_{\theta\max}(\theta;m(\nu_i),0,0)=r_3+\tfrac{1}{6}a+\tfrac{1}{2}-\tfrac{1}{18}a^2r_3^{-1}, \quad (2.52)$$

where

$$r_3\equiv\tfrac{1}{2}\{\tfrac{1}{6}a^2[r_1-(\tfrac{7}{9}a+9)]\}^{1/3}. \quad (2.53)$$

The expression for $(E_b)_{\theta\,\max}$ is particularly simple at $\theta = 90°$, where it is equal to $(E_b)_{f_1\max}(m(\nu_i), 0, 0)$, as given in Eq. (2.28). Since some of our results for special values of E_b are rather complicated, it is appropriate to provide graphical representations of $(E_b)_{\rm iso}$ and, for special values of θ, $(E_b)_{\theta\,\max}$, as functions of $m(\nu_i)$. Inasmuch as $(E_b)_{\theta\,\max}$ is a monotonically increasing function of θ in the physical range $0° \leq |\theta| \leq 180°$, it suffices to plot this quantity for $\theta = 0°$, 90°, and 180°. These curves are plotted together with the maximum allowed energy $(E_b)_{\theta\,\max}(m(\nu_i), 0, 0)$ in Fig. 10(a). One can see in this graph how as $m(\nu_i) \to 0$, $(E_b)_{\rm iso}$ approaches $\frac{1}{4}$ and $(E_b)_{0°\,\max} \to \frac{1}{3}$, while the other curves approach $\frac{1}{2}$. Furthermore, one may note that

$$(E_b)_{\rm iso}(m(\nu_i), 0, 0) < (E_b)_{\theta\,\max}(m(\nu_i), 0, 0) \quad \forall\theta \text{ and } \forall m(\nu_i) < 1 . \quad (2.54)$$

Figure 10(b) shows the corresponding ratios, as

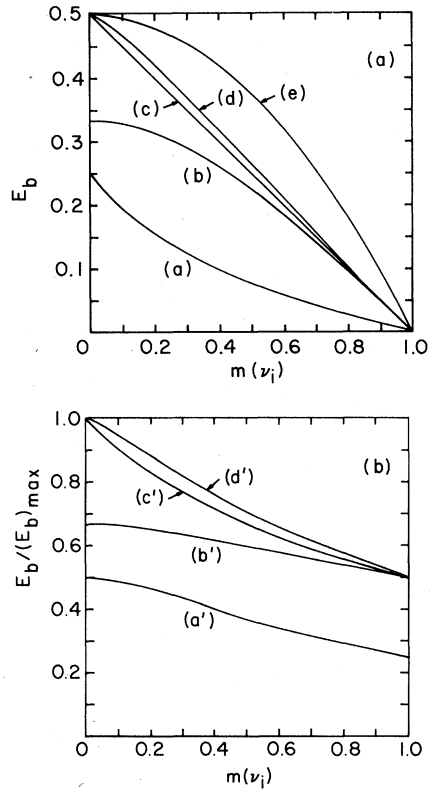

FIG. 10. (a) Special values of E_b for leptonic l_a^- decay for the case involving one (anti)neutrino of non-negligible mass, taken here to be ν_i. The curves represent (a) $(E_b)_{iso}$, (b) $(E_b)_{0°\,\max}$, (c) $(E_b)_{90°\,\max}$, (d) $(E_b)_{180°\,\max}$, and (e) $(E_b)_{\max}$. The same curves apply to l_a^+ decay with the replacement $\theta \to \pi - \theta$. (b) Special values of the reduced energy $\bar{E}_b \equiv E_b/(E_b)_{\max}$ for l_a^- decay, for the case in Fig. (a). The curves represent (a) $(\bar{E}_b)_{iso}$, (b) $(\bar{E}_b)_{0°\,\max}$, (c) $(\bar{E}_b)_{90°\,\max}$, and (d) $(\bar{E}_b)_{180°\,\max}$.

defined in Eq. (2.29). As $m(\nu_i) \to 1$, $(\bar{E}_b)_{\rm iso} \to \frac{1}{4}$, while $(\bar{E}_b)_{\theta\,\max} \to \frac{1}{2}$ for all θ.

Let us next examine the feasibility of trying to search for massive-neutrino modes at large E_b, near $\theta = 0°$, where, for perfect initial polarization, i.e., $|\vec{P}_{l_a}| = 1$, the light-neutrino modes are highly suppressed. In fact, even in the case where one has the greatest control over the l_a polarization, namely μ decay, it is not precisely unity. For example, in the experiment of Plano,[23] in which the asymmetry parameter ξ was measured, $|\vec{P}_\mu| = 0.87$. Moreover, one must take careful account of the processes responsible for the depolarization of μ^+'s in absorbers.[24] In the case of τ decay, $\vec{P}_\tau$ depends on the details of the machine physics of the e^+e^- storage ring through its dependence on the $e^\pm$ polarization transverse to the plane of the ring. It also depends on the center-of-mass energy $\sqrt{s}$ and the direction in which the τ was produced. However, we will show that, even in the ideal case of $|\vec{P}_{l_a}| = 1$, it would be a demanding task to detect the presence of massive-neutrino modes by this method. We will concentrate on HSC rather than HDC modes here because, owing to the better control that one has over the parent lepton polarization in μ, as opposed to τ decay, the test to be evaluated here is presumably more feasible in the former decay.[10] The problem with the method of searching for HSC decays in this region of phase space is that in order to avoid the helicity suppression, $\max\{m(\nu_i), m(\nu_j)\}$ cannot be small compared with unity. But precisely because of this, $(E_b)_{\max}(m(\nu_i), m(\nu_j), 0)$ is significantly smaller than the maximum of $\frac{1}{2}$ for the light-neutrino modes. (Again, the corrections to these formulas due to finite m_b are negligible for μ decay and small for τ decay in the case where the neutrino masses are sufficiently large that one has a reasonable chance of observing their effects.) Thus, one is forced to search for an (i,j) HSC mode in the range $E_b < (E_b)_{\max}(m(\nu_i), m(\nu_j), 0)$ and indeed cannot approach too close to this maximum without suffering a prohibitive reduction in the decay rate for the (i,j) mode. It is then a quantitative question whether or not the differential decay distribution for the light-neutrino modes rises rapidly enough to remain larger than that for a massive-neutrino mode as E_b decreases from $\frac{1}{2}$ to the range where the latter decay can occur. From our analysis we find, unfortunately, that for all $m(\nu_{i\ \text{or}\ j})$ this light-neutrino dominance does obtain. Two typical comparisons are shown in Fig. 11. In the first set one considers selecting l_b's with $E_b = 0.49$.[25] Then it is only possible to search for HSC modes with $m(\nu_i) + m(\nu_j) \leq 0.141$. Neglecting double HSC modes because of their double U suppression, we con-

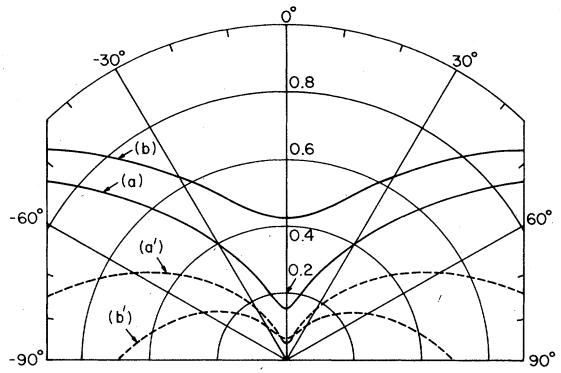

FIG. 11. Comparison of the reduced double-differential decay distributions for leptonic l_a^- decay involving light or massless (anti)neutrinos with that for the decay involving one (anti)neutrino of non-negligible mass, taken here to be ν_i. The curves represent (a) $d^2\overline{\Gamma}^{(-)}/dE_b d\cos\theta(E_b=0.49,\ \theta;\ m(\nu_i)=0,\ m(\nu_j)=0,\ m_b=0$ (or $\ll 1$)), (a′) same as (a) but for $m(\nu_i)=0.1$, (b) same as (a) but for $E_b=0.47$, (b′) same as (b) but for $m(\nu_i)=0.2$.

sider a decay with $m(\nu_i)=0.1$ and $m(\nu_j)\ll 1$, $m_b \ll 1$, for which $(E_b)_{\max}=0.495$. The reduced double-differential decay distribution

$$\frac{d^2\overline{\Gamma}^{(-)}}{dE_b d\cos\theta}(E_b=0.49,\theta;m(\nu_i)=0.1,m(\nu_j)=0,m_b=0)$$

for this mode is plotted as the dashed curved labeled (a′) in Fig. 11. The corresponding light-neutrino reduced differential decay distribution $d^2\overline{\Gamma}^{(-)}/dE_b d\cos\theta(0.49,\theta;0,0,0)$ is represented by the solid curved labeled (a). As is clear from the figure, even for θ near 0°, and, *a fortiori*, for neighboring values of θ, the light-neutrino distribution is much larger than that for the massive-neutrino mode. Moreover, the full differential distribution for the HSC decay mode will be further suppressed by the small coupling coefficient $|U_{ai}^* U_{bj}|^2$, HSC i or j, relative to the full LDC differential distribution. The curves labeled (b) and (b′) present a similar comparison for $E_b=0.47$. Here $\{m(\nu_i)+m(\nu_j)\}_{\max}=0.245$, and accordingly we choose $m(\nu_i)=0.2$, $m(\nu_j)\ll 1$, and $m_b\ll 1$, for which case $(E_b)_{\max}=0.48$. Again, the dashed curve represents the HSC reduced differential decay distribution $d^2\overline{\Gamma}^{(-)}/dE_b d\cos\theta(0.47,\theta;0.2,0,0)$ while the solid curve represents $d^2\overline{\Gamma}^{(-)}/dE_d\cos\theta(0.47,\theta;0,0,0)$. The same conclusion follows from this comparison as from the one above.

The properties of the differential distribution are described in a compact way by certain average quantities. These include, first, the average l_b emission angle, relative to the l_a spin, $\langle\theta\rangle$, or equivalently, $\langle\cos\theta\rangle$, as a function of energy. This is given, for $l_a^-\to\nu_{l_a}l_a^-\bar{\nu}_{l_b}$ and $l_a^+\to\bar{\nu}_{l_a}l_b^+\nu_{l_b}$ decays ($\zeta=\pm 1$), respectively, by

$$\langle\cos\theta\rangle^{(\mp)}(E_b)=\frac{\frac{1}{3}\zeta|\vec{\mathbf{P}}_{l_a}|\sum_{i,j}|U_{ai}^*U_{bj}|^2 f_s(E_b;m(\nu_i),m(\nu_j),m_b)_{[c]}\Theta((E_b)_{\max}(m(\nu_i),m(\nu_j),m_b)-E_b)}{\sum_{r,s}|U_{ar}^*U_{bs}|^2 f_1(E_b;m(\nu_r),m(\nu_s),m_b)_{[c]}\Theta((E_b)_{\max}(m(\nu_r),m(\nu_s),m_b)-E_b)}\ , \tag{2.55}$$

where the subscript $[c]$ indicates that for DC modes the function is understood to contain the order-α electroweak correction [of which only the pure electromagnetic part or type (1) part survives in ratios such as Eq. (2.55), as explained before], while for SC modes the function represents the lowest-order result. The E_b-dependent phase-space restrictions are rendered explicit in Eq. (2.55) by the appropriate Θ-function factors, where $\Theta(x)=1$ if $x>0$ and 0 if $x<0$. As before, we shall concentrate on l_a^- decay and accordingly make the convention that if the superscript $(\mp)$ is omitted from a given quantity, that quantity is understood to refer to l_a^- decay. An average quantity equivalent to $\langle\cos\theta\rangle$ is the asymmetry

$$a^{(\mp)}(E_b)\equiv\frac{(d^2\Gamma^{(\mp)}/dE_b d\cos\theta)(E_b,\theta)-(d^2\Gamma^{(\mp)}/dE_b d\cos\theta)(E_b,\pi-\theta)}{(d^2\Gamma^{(\mp)}/dE_b d\cos\theta)(E_b,\theta)+(d^2\Gamma^{(\mp)}/dE_b d\cos\theta)(E_b,\pi-\theta)}=3\langle\cos\theta\rangle^{(\mp)}(E_b)\ . \tag{2.56}$$

The value of $\langle\cos\theta\rangle$ or the asymmetry averaged over all l_b energies is also of interest:

$$\langle\cos\theta\rangle^{(\mp)}=\tfrac{1}{3}\langle a\rangle^{(\mp)}=\frac{\frac{1}{3}\zeta|\vec{\mathbf{P}}_{l_a}|\sum_{i,j}|U_{ai}^*U_{bj}|^2 F_{s;0}(m(\nu_i),m(\nu_j),m_b)_{[c]}}{\sum_{r,s}|U_{ar}^*U_{bs}|^2 F_{1;0}(m(\nu_r),m(\nu_s),m_b)_{[c]}} \tag{2.57}$$

where

$$F_{z;n}(m(\nu_i),m(\nu_j),m_b)\equiv\int_{m_b}^{(E_b)_{\max}(m(\nu_i),m(\nu_j),m_b)}dE_b E_b^n f_z(E_b;m(\nu_i),m(\nu_j),m_b)\ ,\quad z=1\text{ or }s\ . \tag{2.58}$$

Thus, in particular,

$$F_{1;0}(m_1,m_2,m_3)=\tfrac{1}{2}\overline{\Gamma}(m_1,m_2,m_3)\ . \tag{2.59}$$

From the symmetry property (2.14), it follows that

$$F_{z;n}(m_1, m_2, m_b) = F_{z;n}(m_2, m_1, m_b) . \tag{2.60}$$

The higher symmetry of $F_{1;0}(m_1, m_2, m_b)$ was stated in Eq. (2.16).

One can also measure the mean l_b energy as a function of emission angle; this quantity is given by

$$\langle E_b \rangle^{(\mp)}(\cos\theta) = \frac{\sum_{i,j} |U_{ai}^* U_{bj}|^2 [F_{1;1}(m(\nu_i), m(\nu_j), m_b) + \zeta |\vec{P}_{l_a}| \cos\theta F_{s;1}(m(\nu_i), m(\nu_j), m_b)]_{[c]}}{\sum_{r,s} |U_{ar}^* U_{bs}|^2 [F_{1;0}(m(\nu_r), m(\nu_s), m_b) + \zeta |\vec{P}_{l_a}| \cos\theta F_{s;0}(m(\nu_r), m(\nu_s), m_b)]_{[c]}} . \tag{2.61}$$

The mean value of E_b, averaged over all θ, is then

$$\langle E_b \rangle^{(-)} = \langle E_b \rangle^{(+)} \equiv \langle E_b \rangle = \frac{\sum_{i,j} |U_{ai}^* U_{bj}|^2 F_{1;1}(m(\nu_i), m(\nu_j), m_b)_{[c]}}{\sum_{r,s} |U_{ar}^* U_{bs}|^2 F_{1;0}(m(\nu_r), m(\nu_s), m_b)_{[c]}} . \tag{2.62}$$

Equation (2.14) implies, *a fortiori*, that a generic average quantity, denoted as $\mathcal{A}^{(\mp)}(\{\omega\}; m(\nu_i), m(\nu_j), m_b)$ (where $\{\omega\}$ represents a set of one or zero additional kinematic variables) satisfies the symmetry property

$$\mathcal{A}^{(\mp)}(\{\omega\}; m_1, m_2, m_b) = \mathcal{A}^{(\mp)}(\{\omega\}; m_2, m_1, m_b) . \tag{2.63}$$

We proceed to state our results for the integral functions appearing in Eqs. (2.57)–(2.61). In contrast to $F_{1;0}(m(\nu_i), m(\nu_j), m_b)$, which involves elliptic integrals if all of its arguments are nonzero, $F_{s;0}(m(\nu_i), m(\nu_j), m_b)$ can be expressed in terms of elementary functions. The expression is most simply written in terms of the variables s and D defined in Eqs. (2.40) and (2.41) and

$$u \equiv (1 - m_b)^2 . \tag{2.64}$$

[The latter variable enters as the upper limit of the integration over $Q^2 = (1 + m_b^2 - 2E_b)$; it was this integration variable that was actually used for the calculations, as before in Eqs. (4.40)–(4.45) of Ref. 9.] We find

$$\begin{aligned} F_{s;0}(m_1 \equiv m(\nu_i), m_2 \equiv m(\nu_j), m_b) = {} & (\tfrac{1}{2}u^3 - 4u^{5/2} - \tfrac{7}{2}su^2 + \tfrac{22}{3}u^2 + 20su^{3/2} - 4u^{3/2} - \tfrac{1}{4}s^2u - \tfrac{104}{3}su - \tfrac{13}{4}Du \\ & + 20su^{1/2} + 8Du^{1/2} + 8Du^{-1/2} - \tfrac{3}{4}s^3 + 2s^2 + \tfrac{5}{4}Ds - \tfrac{20}{3}D)r(u, s, D) \\ & + 3[(s^2 + D)(u^2 - 4u^{3/2} + 6u - 4u^{1/2}) - \tfrac{1}{4}s^4 + \tfrac{2}{3}s^3 + \tfrac{1}{2}Ds^2 - 2Ds - \tfrac{1}{4}D^2]L_1(u, s, D) \\ & + 6D^{1/2}(su^2 - 4su^{3/2} + 6su - 4su^{1/2} - \tfrac{2}{3}D)L_2(u, s, D) . \end{aligned} \tag{2.65}$$

For the $F_{z;1}$ integrals we will concentrate on the case of primary interest, where $m(\nu_i)$ and/or $m(\nu_j) \ll 1$. We obtain

$$\begin{aligned} F_{1;1}(m(\nu_i), m(\nu_j), 0) = {} & \tfrac{1}{80}[45s^4 - 30s^3 - (75D + 69)s^2 + (54D - 136)s + 24D^2 - 307D + 14]r(1, s, D) \\ & + \tfrac{9}{16}[s^5 - s^4 - 2(D + \tfrac{2}{3})s^3 + 2(D + 2)s^2 + D(D + 4)s + D(4 - D)]L_1(1, s, D) \\ & + \tfrac{9}{2}D^{1/2}[s + \tfrac{1}{3}D]L_2(1, s, D) \end{aligned} \tag{2.66}$$

and

$$\begin{aligned} F_{s;1}(m(\nu_i), m(\nu_j), 0) = {} & \tfrac{1}{80}[45s^4 - 120s^3 + (141 - 75D)s^2 + (204D + 84)s + 24D^2 + 423D - 6]r(1, s, D) \\ & + \tfrac{9}{16}[s^5 - 3s^4 + (4 - 2D)s^3 + (6D - 4)s^2 + D(D - 12)s - 3D^2 - 4D]L_1(1, s, D) \\ & - \tfrac{9}{2}D^{1/2}[s + D]L_2(1, s, D) . \end{aligned} \tag{2.67}$$

As before, in studying the effects of massive-neutrino modes on these average quantities, the first step is to describe their behavior for the (LDC, LDC) mode(s). For analytical purposes, let us pretend that $U = 1$ exactly, in order to isolate such mode(s). The form that $\langle \cos\theta \rangle^{(\mp)}(E_b) = \frac{1}{3}\alpha^{(\mp)}(E_b)$ would then take is obvious from Eqs. (2.55), (2.17), and (2.18). The function $\langle \cos\theta \rangle^{(-)}(T_b; 0, 0, m_b)$ where $T_b \equiv E_b - m_b$, is plotted as curve (a) in Fig. 12 for the realistic case in which $b \ll 1$. Following our practice in the graphs dealing with $d^2\overline{\Gamma}^{(-)}/dE_b d\cos\theta$, we shall again take $|\vec{P}_{l_a}| = 1$ for the figures pertaining to the average quantities; it is straightforward to modify these for the case $|\vec{P}_{l_a}| < 1$. Curves (b)–(e) are included to show the effects of $m_b \ll 1$, and for these the variable T_b is a more convenient one to use than E_b. As T_b decreases from $(1 - m_b)^2/2$, $\langle \cos\theta \rangle^{(-)}(T_b; 0, 0, m_b)$ increases

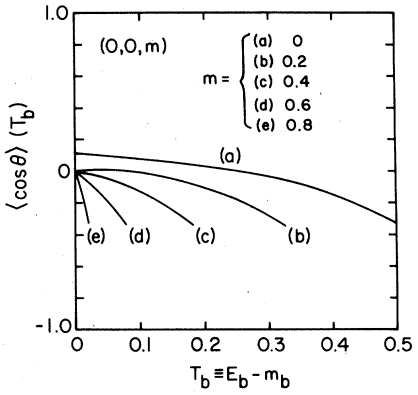

FIG. 12. The average value $\langle\cos\theta\rangle^{(-)}(T_b)$ in the decay $l_a^- \to \nu_i l_b^- \bar{\nu}_j$ for the case $(m(\nu_i), m(\nu_j), m_b) = (0,0,m)$. In this and all of the other figures, the curves obviously also apply for the cases where any of the (mass) = 0 entries are replaced by (mass) $\ll 1$. For brevity the superscript (–) is omitted in Figs. 12–14 and 16–19.

from a minimum of $-\frac{1}{3} - O(\alpha/\pi)$. As is evident from the graph, the tree-level value of $-\frac{1}{3}$ is true for arbitrary $m_b < 1$. The average value $\langle\cos\theta\rangle^{(-)}(T_b)$ passes through zero at $T_b = (T_b)_{\rm iso}(0,0,m_b) = (1-m_b)(1-3m_b)/4$ and, for $m_b \ll 1$, approaches $\frac{1}{9}$ as T_b decreases further. However, as $T_b \to 0$, $\langle\cos\theta\rangle^{(-)}(T_b; 0,0,m_b \ll 1)$ finally drops sharply to zero. The resulting overall average is

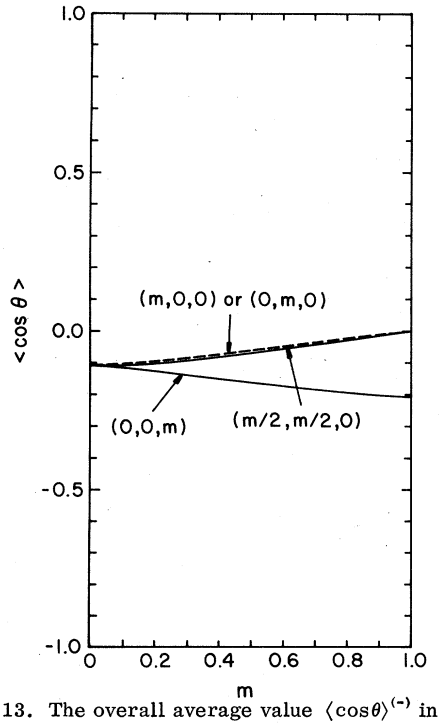

FIG. 13. The overall average value $\langle\cos\theta\rangle^{(-)}$ in the decay $l_a^- \to \nu_i l_b^- \bar{\nu}_j$ for the cases $(m(\nu_i), m(\nu_j), m_b) = (0,0,m)$, $(m,0,0)$, or $(0,m,0)$, and $(m/2, m/2, 0)$.

$$\langle\cos\theta\rangle^{(\mp)}(0,0,m_b) = \tfrac{1}{3}a^{(\mp)}(0,0,m_b) = \frac{\pm\frac{1}{3}|\vec{P}_{l_a}| F_{s;0}(0,0,m_b)}{F_{1;0}(0,0,m_b)}, \quad (2.68)$$

where $F_{s;0}(0,0,m_b)$ can be extracted from Eq. (2.65):

$$F_{s;0}(0,0,m_b) = -\tfrac{1}{6}[1 - 32b^{3/2}(1+3b) + 90b^2 + 40b^3 - 3b^4]. \quad (2.69)$$

The quantity $\langle\cos\theta\rangle^{(-)}(0,0,m_b)$ is plotted as the $(0,0,m)$ curve in Fig. 13, together with certain other curves to be discussed later. In passing, we note that the precise value of the end point of this curve is $\langle\cos\theta\rangle^{(-)}(0,0,1) = -\frac{5}{24}$. For μ decay, the kinematically exact tree-level result is $\langle\cos\theta\rangle^{(\mp)}(0,0,m_e/m_\mu) = \mp\frac{1}{9}(1.000\,183\,5)$; the radiative correction, computed[16] assuming that the maximum E_b observed in $0.99(m_\mu/2)$, changes this result by the factor 1.0003.

For the energy averages in the (LDC, LDC) mode(s) Eq. (2.60) reduces to

$$\langle E_b\rangle^{(\mp)}(\theta;0,0,m_b) = \frac{F_{1;1}(0,0,m_b) \pm |\vec{P}_{l_a}| \cos\theta F_{s;1}(0,0,m_b)}{F_{1;0}(0,0,m_b) \pm |\vec{P}_{l_a}| \cos\theta F_{s;0}(0,0,m_b)}, \quad (2.70)$$

where

$$F_{1;0}(0,0,m_b) = \tfrac{1}{40}(1-b)(7 - 18b + 142b^2 - 18b^3 + 7b^4) - \tfrac{3}{2}b^2(1+b)\ln\left(\frac{1}{b}\right) \quad (2.71)$$

and

$$F_{s;1}(0,0,m_b) = \tfrac{1}{120}(-9 + 25b + 150b^2 - 512b^{5/2} + 450b^3 - 125b^4 + 21b^5). \quad (2.72)$$

Thus

$$\langle E_b\rangle^{(\mp)}(\theta;0,0,m_b \ll 1) = \frac{7}{20}\left[\frac{1 \mp \frac{3}{7}|\vec{P}_{l_a}|\cos\theta}{1 \mp \frac{1}{3}|\vec{P}_{l_a}|\cos\theta}\right] + O\left(b; \frac{\alpha}{\pi}\right). \quad (2.73)$$

The quantity $\langle E_b\rangle^{(-)}(\theta;0,0,m_b)$ is plotted for the full range of m_b (and $|\vec{P}_{l_a}| = 1$) in Fig. 14. The mean energy averaged over all θ is

$$\langle E_b\rangle(0,0,m_b) = \frac{F_{1;1}(0,0,m_b)}{F_{1;0}(0,0,m_b)}, \quad (2.74)$$

which is manifestly the same for l_a^- and l_a^+ decays and independent of $|P_{l_a}|$. The averages $\langle E_b\rangle$, $\langle T_b\rangle$, and the corresponding ratios $\langle\bar{E}_b\rangle$ and $\langle\bar{T}_b\rangle$ are shown in Figs. 15(a) and 15(b) for the $(0,0,m_b)$ case. The only nonobvious end-point value is $\bar{T}_b(0,0,1) = \frac{4}{7}$. For μ decay the kinematically ex-

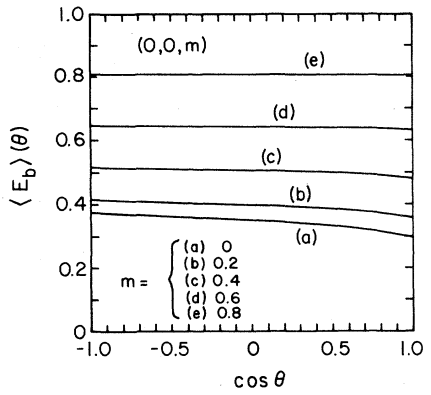

FIG. 14. The average energy $\langle E_b\rangle^{(-)}(\theta)$ in the decay $l_a^- \to \nu_i l_b \bar{\nu}_j$ for the case $(0,0,m)$.

act tree-level average is $\langle E_b\rangle(0,0,m_e/m_\mu) = \frac{7}{20}(1.000\,104)$.

To determine the effects of the modes involving (anti)neutrinos of non-negligible masses, we consider the values of the average quantities for individual (i,j) decay modes. It is true that unless one could identify a specific mode $l_a \to \nu_i l_b \bar{\nu}_j$, e.g., by observing the decays of both the ν_i and $\bar{\nu}_j$, such averages for individual modes are not directly measureable. However, they yield valuable insights into the changes in the observed averages due to all allowed modes, (2.25)–(2.57) and (2.61) and (2.62), and therefore merit careful analysis. We shall concentrate on the single H(D or S)C case $m(\nu_{i \text{ or } j}) \ll 1$, $m(\nu_{j \text{ or } i}) \ll 1$, $m_b \ll 1$, which can be well approximated by the sets $(m,0,0)$ or $(0,m,0)$. We shall also comment on the diagonal case $i=j$, which at best could be (HDC, HSC) and would otherwise by (HSC, HSC). The analogs of Eqs. (2.55)–(2.57) and (2.61) and (2.62) for individual decay modes are obvious and will not be written out. For the reader's convenience we list the special cases of the relevant integral functions below [recall also Eq. (2.59) together with the results (2.45) and (2.46)]:

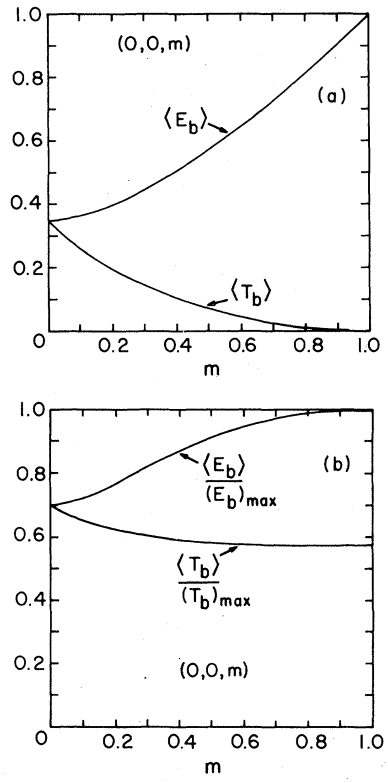

FIG. 15. (a) The overall average energies $\langle E_b\rangle$ and $\langle T_b\rangle$ in leptonic $l_a^\pm$ decay for the case $(0,0,m)$. (b) Same as Fig. (a), but for the reduced overall average energies $\langle \bar{E}_b\rangle \equiv \langle E_b\rangle/(E_b)_{\max}$ and $\langle \bar{T}_b\rangle \equiv \langle T_b\rangle/(T_b)_{\max}$.

$$F_{s;0}(m,0,0) = -\tfrac{1}{6}(1-a)(1-11a-47a^2-3a^3) - 2a^2(3+2a)\ln\left(\frac{1}{a}\right), \tag{2.75}$$

$$F_{1;1}(m,0,0) = \tfrac{1}{40}(1-a)(7-68a-188a^2+12a^3-3a^4) + \tfrac{3}{2}a^2(3+a)\ln\left(\frac{1}{a}\right), \tag{2.76}$$

$$F_{s;1}(m,0,0) = -\tfrac{3}{40}(1-a)(1-14a-94a^2-14a^3+a^4) - \tfrac{9}{2}a^2(1+a)\ln\left(\frac{1}{a}\right), \tag{2.77}$$

$$F_{s;0}(m,m,0) = -\tfrac{1}{6}(1-22a-42a^2+36a^3)(1-4a)^{1/2} - 4a^2(3-4a+3a^2)\ln\left(\frac{1+(1-4a)^{1/2}}{1-(1-4a)^{1/2}}\right), \tag{2.78}$$

$$F_{1;1}(m,m,0) = \tfrac{1}{40}(7-136a-138a^2-120a^3+360a^4)(1-4a)^{1/2} + 3a^2(3-2a-3a^2+6a^3)\ln\left(\frac{1+(1-4a)^{1/2}}{1-(1-4a)^{1/2}}\right), \tag{2.79}$$

$$F_{s;1}(m,m,0) = -\tfrac{3}{40}(1-28a-94a^2+160a^3-120a^4)(1-4a)^{1/2} - 9a^2(1-a)(1-a+2a^2)\ln\left(\frac{1+(1-4a)^{1/2}}{1-(1-4a)^{1/2}}\right). \tag{2.80}$$

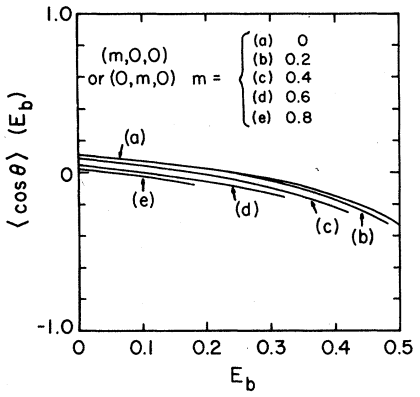

FIG. 16. The average value $\langle\cos\theta\rangle^{(-)}(E_b)$ in the decay $l_a^- \to \nu_i l_b^- \bar{\nu}_j$ for the cases $(m,0,0)$ or $(0,m,0)$.

We plot $\langle\cos\theta\rangle^{(-)}(E_b; m, 0, 0)$ in Fig. 16 for various values of m. As one can see from the graph, for a fixed E_b, $\langle\cos\theta\rangle^{(-)}(E_b; m, 0, 0)$ decreases monotonically as a function of m. However, the physical region moves to progressively lower E_b values as m increases, and the rate at which this happens is sufficiently rapid that

$$\langle\cos\theta\rangle^{(-)}(E_b; m, 0, 0)_{\min} = \langle\cos\theta\rangle^{(-)}((E_b)_{\max}; m, 0, 0)$$

actually increases monotonically as a function of m. For fixed m, $\langle\cos\theta\rangle^{(-)}(E_b; m, 0, 0)$ decreases from

$$\langle\cos\theta\rangle^{(-)}(E_b; m, 0, 0)_{\max} = \langle\cos\theta\rangle^{(-)}(E_b = 0; m, 0, 0) = \tfrac{1}{9}\left(\frac{1-a}{1+a}\right) \tag{2.81}$$

to

$$\langle\cos\theta\rangle^{(-)}(E_b; m, 0, 0)_{\min} = \langle\cos\theta\rangle^{(-)}(E_b = (1-a)/2; m, 0, 0) = -\tfrac{1}{3}\left(\frac{1-a}{1+a}\right). \tag{2.82}$$

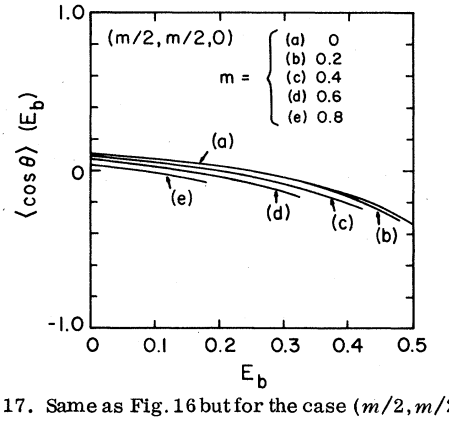

FIG. 17. Same as Fig. 16 but for the case $(m/2, m/2, 0)$.

The quantity $\langle\cos\theta\rangle^{(-)}(E_b; m/2, m/2, 0)$ is plotted in Fig. 17. The same qualitative features are evident; however,

$$\langle\cos\theta\rangle^{(-)}\left(E_b; \frac{m}{2}, \frac{m}{2}, 0\right)_{\max} = \langle\cos\theta\rangle^{(-)}\left(E_b = 0; \frac{m}{2}, \frac{m}{2}, 0\right) = \tfrac{1}{9}(1-a), \tag{2.83}$$

while

$$\langle\cos\theta\rangle^{(-)}\left(E_b; \frac{m}{2}, \frac{m}{2}, 0\right)_{\min} = \langle\cos\theta\rangle^{(-)}\left(E_b = \frac{1-a}{2}; \frac{m}{2}, \frac{m}{2}, 0\right) = -\tfrac{1}{3}\left(\frac{1-a}{1+a}\right). \tag{2.84}$$

One easily proves that for fixed m, for all physical E_b,

$$\langle\cos\theta\rangle^{(-)}\left(E_b; \frac{m}{2}, \frac{m}{2}, 0\right) \geq \langle\cos\theta\rangle^{(-)}(E_b; m, 0, 0), \tag{2.85}$$

where the inequality is satisfied as an equality only if $m = 0$, or, for $m \neq 0$, if $E_b = (E_b)_{\max} = (1-a)/2$.

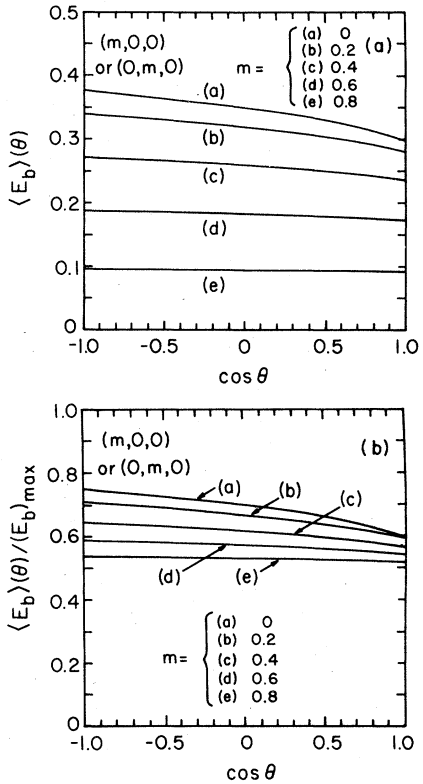

FIG. 18. (a) The average energy $\langle E_b\rangle^{(-)}(\theta)$ in the decay $l_a^- \to \nu_i l_b^- \bar{\nu}_j$ for the cases $(m,0,0)$ or $(0,m,0)$. (b) Same as Fig. (a) but for the reduced average energy $\langle \bar{E}_b\rangle^{(-)}(\theta)$.

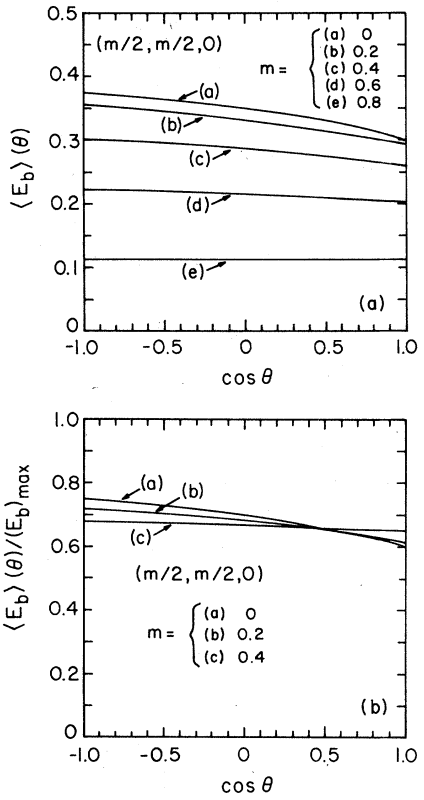

FIG. 19. (a) The average energy $\langle E_b\rangle^{(-)}(\theta)$ in the decay $l_a^- \to \nu_i l_b \bar{\nu}_j$ for the case $(m/2, m/2, 0)$. (b) Same as in Fig. (a) but for the reduced average energy $\langle \bar{E}_b\rangle^{(-)}(\theta)$.

The overall averages $\langle\cos\theta\rangle^{(-)}(m(\nu_i), m(\nu_j), m_b)$ are shown together in Fig. 13 for the $(m, 0, 0)$ or $(0, m, 0)$ and $(m/2, m/2, 0)$ cases. For both of these $\langle\cos\theta\rangle^{(-)}$ increases monotonically from $-\frac{1}{9}$ i.e., $\theta = 96.4^\circ$) to 0 as m increases from 0 to 1. We interpret this physically as a result of the decreased helicity suppression of $d^2\overline{\Gamma}^{(-)}/dE_b d\cos\theta (E_b \lesssim (E_b)_{\max}, \theta \sim 0^\circ)$ as one or both (anti) neutrino masses increase(s) from zero. It is interesting that an increase in m_b has the opposite effect on $\langle\cos\theta\rangle^{(-)}$. From the analytic expressions which we have given, it is straightforward to prove that

$$\langle\cos\theta\rangle^{(-)}(m, 0, 0) \geq \langle\cos\theta\rangle^{(-)}\left(\frac{m}{2}, \frac{m}{2}, 0\right) \geq \langle\cos\theta\rangle^{(-)}(0, 0, m), \qquad (2.86)$$

where the first part of the inequality is realized as an equality only at the points $m = 0$ and $m = 1$, and the second part only at $m = 0$. The two inequalities are apparent in Fig. 13.

Next, in Figs. 18(a) and 18(b) we plot the average energy as a function of θ, $\langle E_b\rangle^{(-)}(\theta; m, 0, 0) = \langle E_b\rangle^{(-)}(\theta; 0, m, 0)$ and the corresponding ratio $\langle \bar{E}_b\rangle^{(-)}(\theta; m, 0, 0)$. Figures 19(a) and 19(b) show the analogous quantities for the diagonal $(m/2, m/2, 0)$ modes. For both of the $(m, 0, 0)$ or $(0, m, 0)$ and $(m/2, m/2, 0)$ cases, at a fixed value of m, $\langle E_b\rangle^{(-)}(\theta)$ decreases monotonically with increasing $\cos\theta$; we interpret this behavior as a consequence of the helicity suppression of the $\theta \sim 0^\circ$, $E_b \lesssim (E_b)_{\max}$ part of the decay distribution $d^2\overline{\Gamma}^{(-)}/dE_b d\cos\theta$, which preferentially weights lower values of E_b as $\cos\theta$ increases from -1 to $+1$. This also aids in understanding the fact that as m increases, the curves become flatter, since with increasing m, there is commensurately less helicity suppression of $d^2\overline{\Gamma}^{(-)}/dE_b d\cos\theta$ for $\theta \lesssim 0^\circ$, relative to other values of θ, for fixed E_b. Analytically, one can show that

$$\lim_{m\to 1}\frac{F_{s;0}}{F_{1;0}}(m, 0, 0) = \lim_{m\to 1}\frac{F_{s;0}}{F_{1;0}}\left(\frac{m}{2}, \frac{m}{2}, 0\right) = 0 \quad (2.87)$$

and

$$\lim_{m\to 1}\frac{F_{s;1}}{F_{1;1}}(m, 0, 0) = \lim_{m\to 1}\frac{F_{s;1}}{F_{1;1}}\left(\frac{m}{2}, \frac{m}{2}, 0\right) = 0 \quad (2.88)$$

from which it follows that

$$\lim_{m\to 1}\frac{\partial}{\partial\cos\theta}\langle E_b\rangle^{(\mp)}(\theta; m(\nu_i), m(\nu_j), 0) = 0 \qquad (2.89)$$

for both of the two cases $(m, 0, 0)$ and $(m/2, m/2, 0)$. It is interesting that also

$$\lim_{m\to 1}\frac{\partial}{\partial\cos\theta}\langle E_b\rangle^{(\mp)}(\theta; 0, 0, m_b) = 0, \qquad (2.90)$$

as was evident in Fig. 14, but the reason is different than in the massive-neutrino cases. In the latter, as a consequence of Eqs. (2.87) and (2.88), both the numerator and denominator of $\langle E_b\rangle^{(\mp)} \times (\theta; m(\nu_i), m(\nu_j), 0)$ become independent of $\cos\theta$ as $m \to 1$. In contrast, in the $(0, 0, m)$ case

$$\lim_{m\to 1}\frac{F_{s;0}(0, 0, m)}{F_{1;0}(0, 0, m)} = \lim_{m\to 1}\frac{F_{s;1}(0, 0, m)}{F_{1;1}(0, 0, m)} = -\frac{5}{8} \qquad (2.91)$$

[recall that for the first ratio this yielded the endpoint value $\langle\cos\theta\rangle^{(\mp)}(0, 0, m) = \mp\frac{5}{24}$ in Fig. 13]. Hence, rather than losing their dependence on $\cos\theta$ as $m \to 1$, the numerator and denominator of $\langle\cos\theta\rangle^{(\mp)}(\theta; 0, 0, m)$ approach the same function of $\cos\theta$, viz., $[1 \mp (\frac{5}{8})|\vec{P}_{l_a}|\cos\theta]$, multiplied by $F_{1;1}(0, 0, m)$ and $F_{1;0}(0, 0, m)$, respectively. This then implies the result (2.91). The flat lines which are approached in the limit $m \to 1$ are $\langle E_b\rangle^{(\mp)}(\theta; 0, 0, 1) = 1$, $\langle E_b\rangle^{(\mp)}(\theta; 1, 0, 0) = \frac{1}{2}$, and $\langle E_b\rangle^{(\mp)}(\theta; \frac{1}{2}, \frac{1}{2}, 0) = \frac{2}{3}$.

Finally, in Figs. 20(a) and 20(b) we show the overall average energies $\langle E_b\rangle$ and $\langle \bar{E}_b\rangle$ for the $(m, 0, 0)$ or $(0, m, 0)$ and $(m/2, m/2, 0)$ modes. As with the angular averages, one can prove inequalities relating the energy averages for the various modes. These apply for the θ-dependent average

energies and, *a fortiori*, for the overall averages. We shall denote this fact by the use of the symbol $\{\theta\}$ in the respective argument lists. Then

$$\langle E_b\rangle^{(\mp)}(\{\theta\};m,0,0) \leq \langle E_b\rangle^{(\mp)}\left(\{\theta\};\frac{m}{2},\frac{m}{2},0\right) \leq \langle E_b\rangle^{(\mp)}(\{\theta\},0,0,m), \quad (2.92)$$

where in the first case the equality holds only at $m=0$ and 1, and in the second case only at $m=0$. Further,

$$\langle \bar{E}_b\rangle^{(\mp)}(\{\theta\};m,0,0) \leq \langle \bar{E}_b\rangle^{(\mp)}\left(\{\theta\};\frac{m}{2},\frac{m}{2},0\right) \leq \langle \bar{E}_b\rangle^{(\mp)}(\{\theta\};0,0,m) \quad (2.93)$$

and here the equalities hold only at $m=0$.

E. Kinks in $d\Gamma/dE_b$

We next proceed to analyze further observable effects of massive-neutrino modes in leptonic l_a decay and to apply our results to existing data on μ and τ decay. Let us begin with the isotropic part of the l_b momentum or energy spectrum. In the conventional view of neutrino-mass effects in lepton decays, which neglected the important role of lepton mixing, implicitly considered ν_e, ν_μ, etc. to be mass eigenstates and thus considered a decay such as $\mu \to \nu_\mu e\bar{\nu}_e$ to remain a single decay in this massive-neutrino case, it was thought that the only observable effect on $d\Gamma/dE_b$ would be, as in the Kurie plot in β decay, an early falloff of the spectrum before the end point. As we have shown previously,[2,3] however, contrary to this past view, the general l_b spectrum $d^2\Gamma/dE_b d\cos\theta$ consists of an incoherent sum of the spectra due to the subset of the n^2 modes $l_a \to \nu_i l_b \bar{\nu}_j$; $i,j=1,\ldots,n$, which is allowed by phase space. Hence, in particular, $d\Gamma/dE_b$ will show kinklike behavior at each of the various end points $E_b=(E_b)_{\max}(m(\nu_i),m(\nu_j),m_b)$ of the respective (i,j) modes. If a dominantly coupled (anti)neutrino had a non-negligible mass, then there would be an observable early end-point falloff in $d\Gamma/dE_b$, but this is not a necessary characteristic of the l_b spectrum, even in the presence of neutrinos of substantial mass. For example, if the DC (anti)neutrinos are sufficiently light, but there is a heavy (anti)neutrino occurring in one of the decay modes, then the l_b spectrum would show no early end-point falloff but would have a kink at an intermediate value of E_b given by the appropriate special case of Eq. (2.1) for the heavy (anti)-neutrino decay mode. In Fig. 21 we present a schematic illustration of the general E_e spectrum in μ decay, for the case $\nu_i=\nu_{[i]}$ (see Ref. 2 for notation), $|U_{i,j\neq i}|^2 \ll |U_{i,j=i}|^2$, $n=3$, $m_\mu > m_e + m(\nu_i)+m(\nu_j)\,\forall\, i,j=1,2,3$, and one heavy neutrino, i.e., $\{i_L\}=\{1,2\}$ and $\{i_H\}=\{3\}$. The different

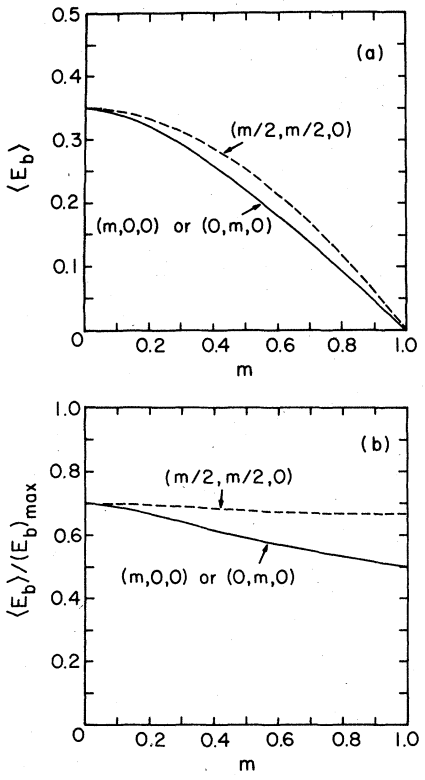

FIG. 20. (a) The overall average energy $\langle E_b\rangle$ in the leptonic $l_a^\pm$ decay, for the cases $(m,0,0)$ or $(0,m,0)$ and $(m/2,m/2,0)$. (b) Same as in Fig. (a) but for the reduced average energy $\langle \bar{E}_b\rangle$.

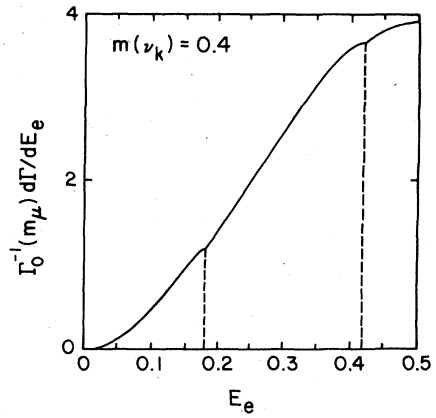

FIG. 21. Schematic illustration of the isotropic spectrum $\Gamma_0^{-1}(m_\mu)d\Gamma/dE_e$ in μ decay, for the case $n=3$, $\nu_i=\nu_{[i]}$, $\{i_L\}=\{1,2\}$, and $\{i_H\}=\{3\}$, with $m(\nu_3)=0.4$, in units of m_μ. The end-point energy of the set of decay modes $\mu\to\nu_3 e\bar{\nu}_{1\text{ or }2}$ and $\mu\to\nu_{1\text{ or }2}e\bar{\nu}_3$ occurs at $E_e=0.42$, while that of the mode $\mu\to\nu_3 e\bar{\nu}_3$ occurs at $E_e=0.18$, as indicated on the graph. The contributions of both the single HSC and the double HSC modes are exaggerated for visual clarity. See Table I for a classification of the decay modes involved in this example.

types of decay modes are listed in approximate order of decreasing strength, due to phase space and/or mixing-angle suppression.

We have carried out a search for such kinks in existing data on $d\Gamma/dE_b$ in μ and leptonic τ decay. The e^+ momentum spectrum in μ^+ decay has been measured in a number of studies, including the Columbia-Nevis experiments of Plano[23] and Peoples[26] and the Chicago experiments of Sherwood,[27] Fryberger,[28] and Derenzo.[29] The experiment of Ref. 28 measured the whole spectrum, while those of Refs. 26–28 measured the high-energy part from ~20–25 MeV to ~53 MeV (since this part is most sensitive to the ρ parameter which they sought to determine). The experiment of Derenzo[29] concentrated on a high-precision study of the low-energy part but also included a measurement of the whole spectrum. (The low-energy part had been found to be important not just for the determination of the spectral parameter η but also, indirectly, for the parameter ρ.) To set a definitive limit on possible kinks it would be necessary to carry out χ^2 fits to the data from each of these experiments, with the parameters of the fitting curve being the values of the (anti)neutrino masses and coupling coefficients $|U^*_{2i}U_{1j}|^2$ for the set of (i,j) modes included. A first approach would be to determine the χ^2 for the hypothesis of one mode involving a $(\overline{\nu})$ of non-negligible mass, together with the usual set of (LDC, LDC), (LDC, LSC), and (LSC, LDC) modes, which latter set would yield the same momentum dependence for the e^+ spectrum. This fit would require folding in the (different) spectrometer acceptance, momentum resolution, and e^+ energy loss functions for each of the experiments considered. The importance of these factors is obvious from the observed e^+ momentum spectra, which all have early end-point falloffs that one would incorrectly attribute to a nonzero $m(\nu_2)$ if one failed to incorporate the effects of e^+ energy loss and imperfect momentum resolution. Accordingly, such a detailed χ^2 fit to μ decay data seems to be more appropriately the task of the experimentalists. However, from our own analysis of the momentum spectra presented in Refs. 23 and 26–29 we find no compelling evidence for such a kink and can set a rough upper limit of order 1% on the incremental addition that a heavy (anti)neutrino mode could contribute to these spectra. As has been discussed before,[2,3] leptonic l_a decay does not have the sensitivity to heavy subdominantly coupled neutrinos that leptonic pseudoscalar-meson decay does. Thus, if one establishes the upper limit ϵ on the contribution of an HSC (i,j) mode, the resultant upper limit on the coupling coefficient for this mode is $|U^*_{ai}U_{bj}|^2 < \epsilon/\overline{\Gamma}(m(\nu_i)/m_a, m(\nu_j)/m_a, m_b/m_a)$. Now, the reduced rate in the denominator is always less than unity and, as was evident in Fig. 4, falls rapidly with increasing $[m(\nu_i)+m(\nu_j)]$. Consequently, the upper bound on $|U^*_{ai}U_{bj}|^2$ is never as good as that on the relative rate and is usually substantially worse. This is, of course, the opposite of the situation in $M^+(=\pi^+, K^+) \to l^+_a \nu_i$ decay, where the analogous reduced kinematic rate function $\overline{\rho}(\delta^M_{l_a} \equiv (m_{l_a}/m_M)^2, \delta^M_{\nu_i} \equiv [m(\nu_i)/m_M]^2)$ either remained near unity for $m(\nu_i)$ nearly up to the phase-space limit or increased significantly, in $K^+ \to \mu^+\nu_i$ decay, and drastically in $(\pi,K)^+ \to e^+\nu_i$ decay, so that, for example, a modest upper bound of ~25% on the relative rate for an HSC mode in K_{e2} decay over the mass range $m(\nu_i) \in$ (82 MeV, 163 MeV) actually yielded the extremely stringent upper limits 10^{-5}–10^{-6} on $|U_{1i}|^2$ [see Ref. 2 or Eq. (2.28) in Ref. 3]. Recall, moreover, that for fixed relative rate, this and similar bounds on $|U_{ai}|^2$ from $(\pi,K)_{l2}$ decay improved with increasing $m(\nu_i)$ since over most of the physical region $\overline{\rho}(\delta^M_{l_a}, \delta^M_{\nu_i})$ was an increasing function of $m(\nu_i)$. In the present case the rough upper limit of ~1% on the contribution of an HSC (i,j) mode in μ decay yields the bound $|U^*_{2i}U_{1j}|^2 \lesssim 0.01/\overline{\Gamma}(m(\nu_i)/m_\mu, m(\nu_j)/m_\mu, m_e/m_\mu)$ which deteriorates rapidly with increasing neutrino masses and, for example, in the case of a single HSC mode, ceases to be a nontrivial bound for $m(\nu_{i \text{ or } j}) \gtrsim 78$ MeV [with $m(\nu_{j \text{ or } i}) \simeq 0$]. Unfortunately, the region of large $|\vec{p}_e|$ where one might search for kinks representing the end points of massive-neutrino modes which involve (anti)neu-

TABLE I. Muon decay modes for the case $n=3$, $\nu_i = \nu_{[i]}$, $\{i_L\}=\{1,2\}$, and $\{i_H\}=\{3\}$ schematically illustrated in Fig. 21. For a given (i,j) mode, $m_{\text{tot}} \equiv m_e + m(\nu_i) + m(\nu_j)$. See text for further comments.

	$m_{\text{tot}} \simeq m_e$	
U favored	$\mu \to \nu_2 e \overline{\nu}_1$	(LDC, LDC)
singly U suppressed	$\mu \to \nu_2 e \overline{\nu}_2$	(LDC, LSC)
	$\mu \to \nu_1 e \overline{\nu}_1$	(LSC, LDC)
doubly U suppressed	$\mu \to \nu_1 e \overline{\nu}_2$	(LSC, LSC)
	$m_{\text{tot}} \simeq m_e + m(\nu_3)$	
singly U suppressed	$\mu \to \nu_3 e \overline{\nu}_1$	(HSC, LDC)
	$\mu \to \nu_2 e \overline{\nu}_3$	(LDC, HSC)
doubly U suppressed	$\mu \to \nu_3 e \overline{\nu}_2$	(HSC, LSC)
	$\mu \to \nu_1 e \overline{\nu}_3$	(LSC, HSC)
	$m_{\text{tot}} \simeq m_e + 2m(\nu_3)$	
(doubly U suppressed)	$\mu \to \nu_3 e \overline{\nu}_3$	(HSC, HSC)

trinos of small mass and hence suffer little kinematic suppression, is also a region where the observed e^+ momentum spectrum deviates considerably from the theoretical one because of the experimental factors noted above. The bound obtained from our kink search in μ decay is clearly not as stringent as similar ones which we have derived from our study of $(\pi,K)_{l2}$ decays. We have included it here to show what kind of a limit can be extracted from existing data on this decay. Furthermore, in view of future experiments on μ decay at LAMPF (Ref. 30) and TRIUMF,[31-33] and on τ decay at SPEAR,[34] which will improve on the accuracy of previous work, we feel that it is worthwhile to present the correct general method of studying the e^+ momentum spectrum in order that it might be adopted in future data analyses.

A search for kinks can also be carried out with τ decay data. It may be recalled that data on the decays[12,13] $\tau \to \nu_\tau l_a \bar{\nu}_{i_a}$, $l_a = e, \mu$ and[14] $\tau \to \nu_\tau \pi$ has been analyzed to set upper limits on "$m(\nu_\tau)$" [in particular, $m(\nu_3)$]. The ability to set these limits relied upon the fact that ν_3 is a dominantly coupled mass eigenstate in τ decay whereas, if allowed by phase space, it is subdominantly coupled in β, μ, π, and K decays. However, as was the case with μ decay, no search for kinks in leptonic decay data has been reported. τ decay might have an important advantage in the search for heavy, subdominantly coupled neutrinos: if lepton mixing is hierarchical, as quark mixing is, at least for the first three generations,[35] then a τ decay mode involving an HSC $(\bar{\nu})_i$, $i \geq 4$, such as $\tau \to \nu_i l_a \bar{\nu}_{j=a}$, $a = 1, 2$, might suffer substantially less mixing-angle suppression than the analogous decay $\mu \to \nu_i e \bar{\nu}_1$. Of course, independently of this, there would be less kinematic phase-space suppression of the heavy-ν_i mode in τ decay than in μ decay. The analysis of $l = e$ or μ spectra in leptonic τ decay is complicated by the fact that the τ's do not decay at rest, and the observed momenta involve Lorentz boosts depending on the angle of emission of the l relative to the direction of motion of the τ. Moreover, certain experiments did not have high detection efficiency for low-energy electrons. We have analyzed the actual or reduced e or μ momentum distributions reported by the pioneering SLAC-LBL experiments of Perl *et al.*[36,37] and the DASP (Ref. 38) and DELCO (Ref. 13) collaborations. It should be noted that such an analysis depends on the Lorentz structure taken for the $\tau\nu_\tau$ vertex. The SLAC-LBL experiment[36] showed that a $V-A$ form for this vertex was favored over a $V+A$ form, and, more recently, the DELCO experiment[13] has established that, assuming "$m(\nu_\tau)$" = 0 (and extracting radiative corrections), and ρ parameter in $\tau \to \nu_\tau e \bar{\nu}_e$ decay is equal to 0.72 ± 0.15, consistent with $V-A$ but not with $V+A$ or pure V or A. The latter experiment then assumed an exact $V-A$ $\tau\nu_\tau$ coupling in deriving its limit "$m(\nu_\tau)$" < 250 MeV (90% C.L.). We have made the same assumption in our search for kinks. However, even if one were to use the weighted mean of the measured values of ρ, the conclusions of our kink search would not be significantly altered. Since the spectra presently available do not extend to very low $E_i \sim m_i$, experiments have not directly determined the parameter η for τ decay and, for the same reason, the value of η assumed has no significant effect on the conclusions of our kink search. Dips such as might result from kinks in the τ rest-frame spectra can be observed in these distributions, e.g., at $r \simeq 0.3$ in Figs. 2(b) and 2(c) of Ref. 37, at $z \simeq 0.62$ in Fig. 3 of Ref. 13, and at $|\vec{p}_e| \simeq 1.1$ GeV in Fig. 3 of Ref. 38. However, as is obvious from the values just given, the dips do not in general occur at the same positions in the spectra from different experiments. Furthermore, it is difficult to assess the significance of these dips in view of the sizable statistical fluctuations expected in such small data samples. A full analysis would entail a χ^2 likelihood test of the hypothesis of one or more HSC neutrino modes in addition to the dominantly coupled mode(s). We believe that this would be a very worthwhile task for the respective experimental groups to perform on existing and forthcoming leptonic τ decay data.[39]

F. Implications for effective spectral parameters and the determination of the Lorentz structure of weak couplings

Our generalized theory of weak decays involving neutrinos has very important implications for the meaning of the spectral parameters[40] measured in μ and leptonic τ decays. As a corollary of the basic point[2] that the observed decay distribution is an (incoherent) sum of all of the individual modes allowed by phase space, it follows that, just as with the averages $\langle\cos\theta\rangle^{(\mp)}(E_b)$, $\langle\cos\theta\rangle^{(\mp)}$, $\langle E_b(\theta)\rangle^{(\mp)}$, and $\langle E_b\rangle$ discussed above, the measured spectral parameters ρ, η, ξ, and δ represent effective quantities due to all of these modes that are present. Thus, since the presence and strength of the massive-neutrino modes are E_b dependent, in contrast to the conventional view, in the general theory the measurement of leptonic l_a decay yields a *family* of different values for each spectral parameter, depending on the ranges of E_b used in the determination of these parameters. We shall now analyze the effects of neutrino masses and mixing on the experimentally measured spectral parameters. Our analysis has three applications. First, it is a necessary, and hitherto missing, foundation for the determination of the Lorentz structure of

the relevant weak leptonic weak couplings from the spectral parameters in μ and τ decay. Second, it can be used to obtain correlated bounds on neutrino masses and mixing angles analogous to those given in Refs. 2 and 3. Third, given the expected sensitivity of forthcoming experiments on μ and τ decay,[30-34] our analysis shows to what extent, and how best they can search for the signatures of neutrino masses and mixing via their measurements of the spectral parameters. We shall suggest concrete new methods for extracting these parameters from the raw data which are designed to optimize the sensitivity of the above search.

Let us elaborate on the first application. Contrary to the conventional view, the measurement of the spectral parameters (with radiative corrections taken into account to the requisite level of accuracy) does *not* test the Lorentz structure of the relevant weak couplings in isolation. Rather, these parameters depend not just on the Lorentz structure of these couplings, but also on the masses and mixing angles of the (anti)neutrinos that occur in the various decay modes. The measurement of ρ, η, ξ, and δ would provide a direct test of the Lorentz structure of the weak couplings only if $m(\nu_i)=0$ for all i, so that $U\equiv 1$. Operationally, of course, one can never verify this condition exactly, so that, in practice, in order to use the measured values of these spectral parameters to determine the Lorentz structure of the relevant weak couplings to a given degree of precision, one must prove that the effects of possible neutrino masses and mixing are negligible to this order of accuracy. No such proof has previously been given, and indeed, at present, deviations of the spectral parameters from their $V-A$ values (after radiative corrections have been divided out) cannot be attributed alone to a difference in the Lorentz structure from $V-A$, but must be regarded as possibly being due in part to massive neutrinos and lepton mixing. Thus, specifically, *even* if the relevant weak couplings should be exactly of the $V-A$ type (in charge-changing order, and hence also, for this special case, in charge-retention form), the observed values of the spectral parameters, after radiative corrections are extracted, would *not* in general have their conventional $V-A$ values, $\rho=\frac{3}{4}$, $\eta=0$, $\xi=1$, and $\delta=\frac{3}{4}$. This result is similar to our earlier demonstration in paper I that even if the $l_a\nu_{l_a}$ coupling should be precisely $V-A$, the measured value of $R_M\equiv B(M^+\to e^+\text{“}\nu_e\text{”})/B(M^+\to\mu^+\text{“}\nu_\mu\text{”})$,[41] where $M=\pi$ or K, would not in general be equal to the value predicted by the $V-A$ theory with radiative corrections incorporated (as well as they can be), again because of the effects of neutrino masses and mixing. Furthermore, in the conventional view, although one optimally would use different ranges of E_b to determine different spectral parameters (e.g., mainly high E_b for ρ and low E_b for η, notwithstanding the correlation between them), this was only for the purpose of maximizing the sensitivity of the determination. Thus, for example, if (with a given input for η) one μ-decay experiment used the e^+ energy range from 30 to $\lesssim 53$ MeV to measure ρ, while another with equal statistics used the range from 20 to $\lesssim 53$ MeV, then although the former might have somewhat greater sensitivity, if the experimental acceptances and resolution and radiative corrections were taken into account properly, both experiments would yield the same value of ρ, to within their errors. However, this is *not* true in the general theory of leptonic μ or τ decay, because the admixture of massive-neutrino modes is E_b dependent. An experiment which sampled the energy range from $(E_b)_{\text{lower}}$ to $(E_b)_{\text{upper}} \lesssim (E_{b\,\max})_0=(m_a/2)(1-m_b^2/m_a^2)$ would measure values of the spectral parameters due to the subset of all the modes occurring in the $l_a^+\to\bar{\nu}_{l_a}l_b^+\nu_{l_b}$ decay which satisfied $(E_b)_{\max}(m(\nu_i),m(\nu_j),m_b)>(E_b)_{\text{lower}}$. Hence two experiments with different values of $(E_b)_{\text{lower}}$ would observe *different* values of the spectral parameters. In general, in the forthcoming high-precision μ-decay experiments[30-33] and the MARK III experiment on τ decay at SPEAR (Ref. 42) even if, after the necessary radiative corrections are extracted, a deviation from the $V-A$ values of one or more of the spectral parameters should be established, this deviation could, in a number of cases, be due *either* to a difference in the Lorentz structure of the weak couplings from the $V-A$ form *or* to neutrino masses and mixing, and consequently one could not *a priori* attribute it to either cause alone. Indeed, one of the purposes of the present analysis is to ascertain the distinctive features of the latter cause and to determine to what extent it can be distinguished from the former.

The experimental extraction of the spectral parameters is complicated by the fact that the value obtained for a given parameter depends on whether one assumes the $V-A$ values for certain other parameter(s). Specifically, for the isotropic spectrum, ρ and η are significantly correlated, and many experiments which measured the high-energy end of the e^+ spectrum to determine ρ assumed that $\eta=0$. (This was necessary since their spectrometer acceptance and resultant lower cut on E_e did not allow them to reach the small energy region where they could measure η.) In a later experiment Derenzo carried out a precise measurement of the low-energy part of the e^+ spectrum and then combined his own data with that from earlier experiments in a two-parameter

fit to ρ and η, thereby obtaining the values $\rho = 0.7518 \pm 0.0026$ and $\eta = -0.12 \pm 0.21$. These values of ρ and η are, respectively, essentially and exactly the values taken by the Particle Data Group.[43] Similarly, the parameters ξ and δ describing the size and momentum dependence of the term proportional to $|\vec{P}_\mu| \cos\theta$ in the decay distribution are extracted from a fit to the asymmetry, $a(E)$. In the analytic form used for this fit, one must make some choice as to the values of ρ and η to be used in the denominator unless one has independently determined these parameters in the same experiment. In practice, most previous experiments on ξ and δ in μ decay assumed the $V-A$ values of ρ and η.[43,44] In the work of Fryberger, however, it was noted that if one used the central values of ρ and η obtained in that experiment rather than the $V-A$ values, it would cause a negligible shift in δ (ξ was not measured).[28] For reference, the weighted means of the values of ξ and δ from all relevant experiments are $\xi = 0.972 \pm 0.013$ and $\delta = 0.7551 \pm 0.0085$.[43]

Let us state the form of the definition of the theoretical and observed spectral parameters in our general theory of weak processes. We shall follow the standard practice of extracting the radiative corrections to these parameters.[45] To begin, one must realize that the very terms "Lorentz structure of the weak couplings" have to be reinterpreted in the general theory. Recall that in the conventional theory one writes the effective local Hamiltonian for the decay $l_a \to \nu_{l_a} l_b \nu_{l_b}$ in the form[7,46]

$$\mathcal{H} = \frac{G_F}{\sqrt{2}} \sum_{k=S,P,V,A,T} [\bar{\psi}_{l_b} \Gamma_k \psi_{l_a}][\bar{\psi}_{\nu_{l_a}} \Gamma_k (g_k^{(a,b)} + g_k^{(a,b)\prime}\gamma_5)\psi_{\nu_{l_b}}] + \text{H.c.}, \tag{2.94}$$

where

$$\Gamma_S = 1, \quad \Gamma_P = \gamma_5, \quad \Gamma_V = \gamma_\rho, \quad \Gamma_A = \gamma_\rho\gamma_5, \quad \Gamma_T = \frac{\sigma_{\rho\tau}}{\sqrt{2}}, \tag{2.95}$$

and the dimensionless coupling constants $\{g_k^{(a,b)}\}$ and $\{g_k^{(a,b)\prime}\}$ are supposed to specify the Lorentz structure of the effective interaction completely. We include the superscript labels (a,b) to indicate that, although it was not stressed in the past literature, the Lorentz structure of the relevant weak couplings could differ for different sets (a,b) in the conventional theory as well as the general one. (Parenthetically, we note that the Hamiltonian is listed here in the charge-retention form; one can easily obtain the charge-changing form by the use of a Fierz transformation.) However, in the general theory it is *not* true that the Lorentz structure of the interaction is fully specified by these coupling constants. Rather, the true effective local Hamiltonian describing "the" decay $l_a \to \nu_{l_a} l_b \bar{\nu}_{l_b}$ is (again, in charge-retention form)

$$\mathcal{H} = \frac{G_0}{\sqrt{2}} \sum_{i,j} |U_{ai}^* U_{bj}|^2 \sum_{k=S,P,V,A,T} [\bar{\psi}_{l_b} \Gamma_k \psi_{l_a}][\bar{\psi}_{\nu_i} \Gamma_k (g_k^{(a,b;i,j)} + g_k^{(a,b;i,j)\prime}\gamma_5)\psi_{\nu_j}] + \text{H.c.} \tag{2.96}$$

In particular, the Lorentz structure of one mode $l_a \to \nu_i l_b \bar{\nu}_j$ would not necessarily be the same as that for another, $l_a \to \nu_r l_b \bar{\nu}_s$. This is analogous to the discussion given in paper I concerning the possible different Lorentz structures in different $M^+ \to l_a^+ \nu_i$ decays (see Sec. IIE and footnote 26 of Ref. 3 for elaboration and examples). It follows that in general there are *different* spectral parameters for each (i,j) decay mode. However, in contrast to the situation in M_{l2} decays where one might feasibly study each $M^+ \to l_a^+ \nu_i$ mode individually and determine the coefficients $c_Z^{(i)}$, $Z = S$, P, V, and A ($c_T^{(i)}$ does not contribute), the analogous study of individual (i,j) modes in $l_a \to \nu_{l_a} l_b \bar{\nu}_{l_b}$ decay is not feasible, as has been discussed above. Conventionally, the expression for the differential distribution in the case of arbitrary Lorentz structure can be written as

$$\frac{d^2\Gamma_{(\mathrm{GL})}^{(\mp)}}{dE_b\, d\cos\theta}(E_b, \theta; l_a^\pm \to \overset{(-)}{\nu}_{l_a} l_b^\pm \overset{(-)}{\nu}_{l_b}) = \frac{G_F^2 m_a^5}{192\pi^3}\left(\frac{A}{16}\right)[f_{1(\mathrm{GL})}(E_b; m_b; \rho^{(a,b)}, \eta^{(a,b)}) + \xi |\vec{P}_{l_a}| \cos\theta f_{s(\mathrm{GL})}(E_b; m_b; \xi^{(a,b)}, \delta^{(a,b)})], \tag{2.97}$$

where the subscript (GL) denotes "general Lorentz structure" and we have explicitly indicated the dependence of the spectral parameters on the type of decay. The functions $f_{1(\mathrm{GL})}$ and $f_{s(\mathrm{GL})}$ can be read off from standard treatments in the literature[40,7]; however, it will be useful to list them here in our notation since we will refer to details of their form later:

$$f_{1(\mathrm{GL})}(E_b; m_b; \rho^{(a,b)}, \eta^{(a,b)}) = 32(E_b^2 - b)^{1/2}\{3E_b[(E_{b\,\max})_0 - E_b] + 2\rho^{(a,b)}[\tfrac{4}{3}E_b^2 - (E_{b\,\max})_0 E_b - \tfrac{1}{3}b] + 3\eta^{(a,b)} b^{1/2}[(E_{b\,\max})_0 - E_b]\} \tag{2.98}$$

and

$$f_{s(\mathrm{GL})}(E_b; m_b; \xi^{(a,b)}, \delta^{(a,b)}) = 32\,\xi^{(a,b)}(E_b^{\,2} - b)\{[(E_{b\,\max})_0 - E_b] + 2\delta^{(a,b)}[\tfrac{4}{3}E_b - (E_{b\,\max})_0 - \tfrac{1}{3}b]\}, \tag{2.99}$$

where

$$(E_{b\,\max})_0 \equiv (E_b)_{\max}(0, 0, m_b) \tag{2.100}$$

in the notation of Eq. (2.1) and b, when used as an algebraic symbol, rather than a superscript or subscript, is given by m_b^2/m_a^2, as defined in Eq. (2.19). Observe that with our normalization

$$f_{1(\mathrm{GL})}(E_b; m_b; \rho^{(a,b)} = \tfrac{3}{4}, \eta^{(a,b)} = 0) = f_1(E_b; 0, 0, m_b) \tag{2.101}$$

and

$$f_{s(\mathrm{GL})}(E_b; m_b; \xi^{(a,b)} = 1, \delta^{(a,b)} = \tfrac{3}{4}) = f_s(E_b; 0, 0, m_b) \tag{2.102}$$

with the functions on the right-hand sides of Eqs. (2.101) and (2.102) being given in Eqs. (2.17) and (2.18). The constant A and the spectral parameters $\rho^{(a,b)}$, $\eta^{(a,b)}$, $\xi^{(a,b)}$, and $\delta^{(a,b)}$ are functions of the $\{g_k^{(a,b)}\}$ and $\{g_k^{(a,b)'}\}$; again, they are given in the literature[40,7] and will not be repeated here.

In the general theory the expression for the differential decay distribution in the case of arbitrary Lorentz structure is

$$\frac{d^2\Gamma^{(\mp)}_{(\mathrm{GL,GN})}}{dE_b\, d\cos\theta}(E_b, \theta; l_a^{\mp} \to \overset{(-)}{\nu}_{l_a} l_b^{\mp} \overset{(-)}{\nu}_{l_b})$$

$$= \Gamma_0(m_a) \sum_{i,j} |U_{ai}^* U_{bj}|^2 [f_{1(\mathrm{GL,GN})}(E_b; m(\nu_i), m(\nu_j), m_b; \{g_k^{(a,b;ij)}\}, \{g_k^{(a,b;i,j)'}\};$$

$$+ \xi |\vec{p}_{l_a}| \cos\theta f_{s(\mathrm{GL,GN})}(E_b; m(\nu_i), m(\nu_j), m_b; \{g_k^{(a,b;i,j)}\}, \{g_k^{(a,b;i,j)'}\})], \tag{2.103}$$

where the subscript (GN) denotes "general neutrino masses" and the functions $f_{1(\mathrm{GL,GN})}$ and $f_{s(\mathrm{GL,GN})}$ are the appropriate generalizations of Eqs. (2.98) and (2.99) for this case. However, since one cannot study each (i,j) mode individually, the spectral parameters for each mode are not directly useful objects to consider. Operationally, as noted before, in the general theory the effective spectral parameters that would be measured experimentally (after radiative corrections are extracted) depend on the interval $((E_b)_{\mathrm{lower}}, (E_b)_{\mathrm{upper}})$ used to perform the fit to the data. For the isotropic part of the spectrum they are given by the equation

$$f_{1(\mathrm{GL})}(E_b; m_b; \rho_{\mathrm{eff}}^{(a,b)}, \eta_{\mathrm{eff}}^{(a,b)}) = \lambda \sum_{i,j} |U_{ai}^* U_{bj}|^2 f_{1(\mathrm{GL,GN})}(E_b; m(\nu_i, m(\nu_j), m_b; \{g_k^{(a,b;ij)}\}, \{g_k^{(a,b;i,j)'}\}). \tag{2.104}$$

Here and elsewhere we recall that there are implicit Θ functions of the form $\Theta(m_a - m_b - m(\nu_i) - m(\nu_j))$ in f_1 and f_s. The normalization factor λ is given analytically by[47]

$$\lambda = \frac{\int_{(E_b)_{\mathrm{lower}}}^{(E_b)_{\mathrm{upper}}} dE_b f_{1(\mathrm{GL})}(E_b; m_b; \rho_{\mathrm{eff}}^{(a,b)}, \eta_{\mathrm{eff}}^{(a,b)})}{\sum_{i,j} |U_{ai}^* U_{bj}|^2 \int_{(E_b)_{\mathrm{lower}}}^{(E_b)_{\mathrm{upper}}} dE_b f_{1(\mathrm{GL,GN})}(E_b; m(\nu_i), m(\nu_j), m_b; \{g_k^{(a,b;i,j)}\}, \{g_k^{(a,b;i,j)'}\})}. \tag{2.105}$$

Similarly, the spectral parameters $\xi_{\mathrm{eff}}^{(a,b)}$ and $\delta_{\mathrm{eff}}^{(a,b)}$ would be determined via the equation

$$\frac{f_{s(\mathrm{GL})}(E_b; m_b; \xi_{\mathrm{eff}}^{(a,b)}, \delta_{\mathrm{eff}}^{(a,b)})}{f_{1(\mathrm{GL})}(E_b; m_b; \rho_{\mathrm{eff}}^{(a,b)}, \eta_{\mathrm{eff}}^{(a,b)})} = \frac{\sum_{i,j} |U_{ai}^* U_{bj}|^2 f_{s(\mathrm{GL,GN})}(E_b; m(\nu_i), m(\nu_j), m_b; \{g_k^{(a,b;i,j)}\}, \{g_k^{(a,b;i,j)'}\})}{\sum_{r,s} |U_{ar}^* U_{bs}|^2 f_{1(\mathrm{GL,GN})}(E_b; m(\nu_r), m(\nu_s), m_b; \{g_k^{(a,b;r,s)}\}, \{g_k^{(a,b;r,s)'}\})}, \tag{2.106}$$

where $\rho_{\mathrm{eff}}^{(a,b)}$ and $\eta_{\mathrm{eff}}^{(a,b)}$ would have been extracted from a fit to the isotropic part of the spectrum in a complete experiment, or, alternatively, taken from other work in an experiment devoted specifically to a study of the asymmetry. Equations (2.105) and (2.106) provide the foundation, in the general theory, for an analysis of the Lorentz structure of the relevant weak couplings in leptonic l_a decay based on a measurement of the spectral parameters.

In our study of the effects of neutrino masses and mixing on the spectral parameters, it is necessary to make some assumption concerning the Lorentz structure of the interaction. As before, in view of the fact that all measurements on μ and leptonic τ decay are consistent with the $V-A$ form (in the case of $\xi^{(\mu,e)}$, at the 2σ level), we shall assume this form. However, at appropriate points, we

shall comment on the effects of non-$(V-A)$ couplings. Let us begin with the isotropic part of the spectrum. Our treatment will be primarily oriented toward μ decay, since the most accurate measurements of the spectral parameters, and the only reported measurements of η, ξ, and δ, are available for this case. Accordingly, we shall make the notational convention that in the appropriate experimental context, unlabeled spectral parameters refer to μ decay. To reproduce the conditions of μ decay experiments, we have carried out two types of χ^2 fits. In the first, we set $\eta_{\rm eff}=0$ and $(E_b)_{\rm lower}=25$ MeV, and $(E_b)_{\rm upper}=53$ MeV, corresponding to the work of Refs. 26–28. In the second, we fit both ρ and η, and use the whole spectrum, corresponding to the combined fit by Derenzo.[29] For simplicity we assume that there is only one set of non-negligible heavy $\overset{(-)}{\nu}$ modes, viz., $l_a \to \nu_{{\rm HSC}\,i} l_b \bar{\nu}_{l_b}$, with U dependence

$$\sum_{j=1}^{n} |U_{ai}^* U_{bj}|^2 \Theta(m_{l_a} - m_{l_b} - m(\nu_i) - m(\nu_j)) \simeq |U_{ai}|^2 ,$$

and $l_a \to \nu_{l_a} l_b \bar{\nu}_{{\rm HSC}\,i}$ with U dependence

$$\sum_{i=1}^{n} |U_{ai}^* U_{bj}|^2 \Theta(m_{l_a} - m_{l_b} - m(\nu_i) - m(\nu_j)) \simeq |U_{bj}|^2 .$$

It is straightforward to extend our analysis to deal with the case of several different types of HSC modes. We label the heavy $\overset{(-)}{\nu}$ as $\overset{(-)}{\nu}_k$ and the relevant coupling coefficients as $|U_{rk}|^2$, $r=1$ or 2 and $k=i$ or j.

Before presenting our results, it is necessary to recall briefly what limits are placed on the $|U_{rk}|^2$ (HSC k) by our previous work.[2,3] In the case $r=1$, i.e., the $e\nu_k$ coupling, the R_π and R_K branching-ratio constraints, together with the bounds from the HSC peak search in K_{e} decay, imply that for the relevant range of $m(\nu_k)$, $|U_{1k}|^2$ is sufficiently small that it would probably not be possible to detect directly the effects of an HSC ν_k in the spectral parameters describing the μ decay distribution [see Eqs. (2.28) and (3.12) and Fig. 22 of Ref. 3]. Regarding an HSC ν_k coupled to e (or μ) in τ decay, the range of $m(\nu_k)$ extends far above that covered by the bounds discussed inRefs. 2 and 3, so that commensurately larger $|U_{rk}|^2$ are allowed. There are, of course, also constraints on the couplings of such a massive ν_k from data on possible neutrino oscillations. The positive effect reported recently by one experiment[48] would involve much lighter neutrinos than those which are significant here. Moreover, apart from possible decays of such heavy neutrinos,[49] they would have an approximately spatially uniform effect in an accelerator neutrino scattering experiment, a manifestation of the underlying *incoherence* in the original $M^\pm \to l_a^\pm \overset{(-)}{\nu}_i$ decays (where $M=\pi$ or K and $l_a=e$ or μ). Stated in other terms, the quasicoherent formalism which is conventionally used[50] to describe the propagation of massive neutrinos and gives rise to the label "neutrino oscillation" is, according to the general rules of quantum mechanics, applicable to neutrinos with sufficiently small (or nearly degenerate) masses but is not in general applicable to the heavy neutrinos of interest here. Furthermore, an obvious fact which is of relevance to τ decay is that if $m(\nu_i) > m_\pi$ or m_K, then the accelerator neutrino data provides much weaker constraints on the corresponding $|U_{rk}|^2$. Proceeding to the case $r=2$, i.e., the $\mu\nu_k$ coupling, the upper bounds on $R_{2k} \simeq |U_{2k}|^2$ resulting from the application of the spectral test proposed in Ref. 2 to existing π_{l2} and K_{l2} data were given in Ref. 3, in particular, Fig. 17 of that work. Subsequently, the peak search proposed in Ref. 2 was carried out in a preliminary new $\pi_{\mu 2}$ experiment by the Swiss Institute for Nuclear Research (SIN) group, which obtained the slightly better bounds $R_{2k} < 0.03$ for $m(\nu_k) \in$ (4 MeV, 9 MeV) and $R_{2k} < 0.02$ for $m(\nu_k) \in$ (6 MeV, 14 MeV).[51] The branching-ratio constraint analyzed in Ref. 3 does not yield a very strong bound on $|U_{2k}|^2$. Since the situation

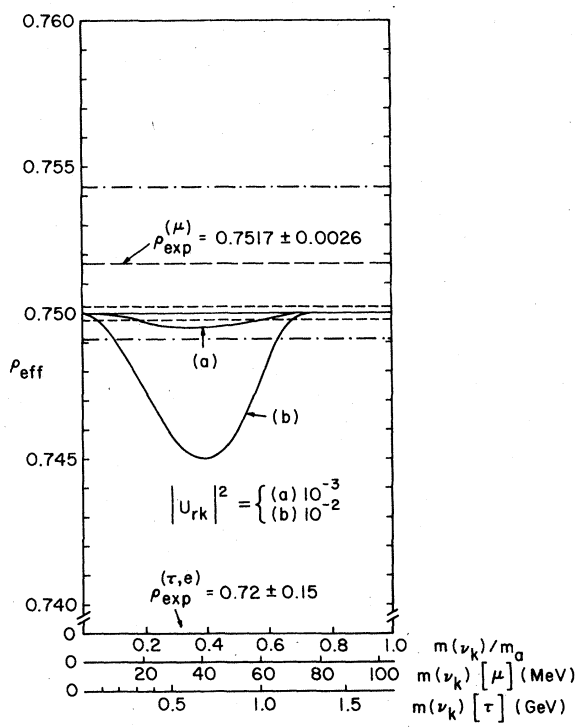

FIG. 22. Plot of $\rho_{\rm eff}$ determined from a two-parameter χ^2 fit to $d\Gamma/dE_b$ in terms of $\rho_{\rm eff}$ and $\eta_{\rm eff}$ for leptonic l_a decay involving one (anti)neutrino, denoted $(\overset{(-)}{\nu})_k$, of non-negligible mass. Results are shown for two values of the weak coupling coefficient $|U_{rk}|^2$. See text for further details.

concerning possible neutrino oscillations is unsettled at the present time, we shall only comment that the data is consistent with $|U_{2,\mathrm{HSC}\,k}|^2 \sim 10^{-2}$. Thus, the largest $|U_{2k}|^2$ values of relevance to μ decay are allowed for $m(\nu_k) \lesssim 14$ MeV and $m(\nu_k) \in$ (34 MeV, 82 MeV). As will be shown, for fixed $|U_{2k}|^2$, a mass $m(\nu_k)$ in the second interval would yield a greater effect on the spectral parameters in μ decay. Accordingly, given the above constraints on $|U_{2k}|^2$, the analysis of these spectral parameters (in particular, ρ) is probably most valuable as a probe of the effects of neutrino masses and mixing in the second region of $m(\nu_k)$.

In Fig. 22 we present curves of the effective ρ parameter, as a function of $m(\nu_k)$, as determined by the two-parameter fit to $d\Gamma/dE_b$, using the $V-A$ version of Eqs. (2.104) and (2.105) with $(E_b)_{\mathrm{lower}} = m_b \ll 1$ and $(E_b)_{\mathrm{upper}} = (E_{b\,\max})_0$. The corresponding values of η_{eff} are given in Fig. 25 and will be discussed later. The curves are plotted for two values of $|U_{2k}|^2$, viz., 10^{-2} and 10^{-3}. As should be clear from the preceding discussion concerning other constraints on $|U_{rk}|^2$ as a function of $m(\nu_k)$, we certainly do not mean to imply that values this large are allowed for all $m(\nu_k)$ in μ and τ decay. The reader is referred to Refs. 2 and 3 for an analysis of precisely how large $|U_{rk}|^2$ is allowed to be, as a function of $m(\nu_k)$, by other relevant constraints. The horizontal axis gives the dimensionless values of $m(\nu_k)/m_a$ together with the actual corresponding $m(\nu_k)$ values in μ and τ decay. (In the latter case the curve applies to the decay $\tau \to \nu_\tau e \bar{\nu}_e$, which was the mode studied in the DELCO experiment.[39]) Using Eqs. (2.94)–(2.96), one can generate the curves for the decay $\tau \to \nu_\tau \mu \bar{\nu}_\mu$ in an analogous manner; these are omitted for brevity. The central experimental value of $\rho_{\mathrm{eff}}^{(\mu,e)}$ is indicated by the horizontal dashed line, with the $\pm 1\sigma$ errors being represented by the accompanying dot-dashed lines. For any value of $m(\nu_k)$, the effect of the presence of a massive $\overset{(-)}{\nu}_k$ mode is to decrease the observed value of ρ_{eff} from its $V-A$ value of 0.75 where $m(\nu_i) = 0$ for all i. This general feature can be easily understood because as ρ_{eff} decreases below 0.75, the (area-normalized) function $f_{1(\mathrm{GL})}(E_b; m_b; \rho_{\mathrm{eff}}; \eta_{\mathrm{eff}})$ becomes larger for $E_b < \frac{3}{16}[1 + b + (1 + \frac{82}{9}b + b^2)^{1/2}] \simeq \frac{3}{8} + \frac{25}{24}b + O(b^2)$, and smaller for E_b above this value. Thus, a value of ρ_{eff} less than 0.75 yields a function $f_{1(\mathrm{GL})}$ which provides a better approximate fit to $d\Gamma/dE_b$ than would be the case if $\rho_{\mathrm{eff}} > 0.75$, since the function being fitted has the appearance indicated in Fig. 21. For fixed $|U_{rk}|^2$, and small $m(\nu_k)$, there is commensurately little change in ρ_{eff} since the kinematics is not very different than in the case of zero-mass neutrinos. For very large $m(\nu_k)$ there is again little change in ρ_{eff}, but for the different reason that the massive $\overset{(-)}{\nu}_k$ mode is kinematically very heavily suppressed. Thus, it could be anticipated before any calculation that the maximum decrease in ρ_{eff} would occur at an intermediate value of $m(\nu_k)$; our results show that this value is ~40 MeV. The deviation of ρ_{eff} from 0.75 is roughly proportional to $|U_{rk}|^2$ for the small values of this coupling coefficient of relevance here. The values of ρ_{eff} obtained in the one-parameter fit with η_{eff} assumed to be equal to zero are quite close to those obtained in the two-parameter fit.

Thus, for the ρ parameter our conclusion concerning the first application is that, indeed, given present constraints on HSC ν_k coupling coefficients, possible massive ν_k modes could significantly alter the observed value of ρ_{eff} and consequently, contrary to the conventional practice, one *cannot* use past data on ρ to constrain the Lorentz structure of the μ decay couplings in isolation. Rather, without further analysis (see below), one must consider these past measurements of ρ_{eff} to yield a *correlated bound* on deviations from $V-A$ weak couplings *and* the effects of massive neutrinos and lepton mixing. Note that this is true regardless of the bounds on the masses of the LDC (anti)neutrinos ν_1 and $\bar{\nu}_2$ in μ^+ decay. It also does not require that one assume that there are $n > 3$ generations of leptons, inasmuch as the current upper limit on $m(\nu_3)$ allows it to be anywhere in the range $(0, m_\mu)$. An analogous statement applies in principle to the use of the $\rho^{(\tau,l_b)}$ value measured in τ decay to constraint the $\tau\nu_\tau$ coupling, although the accuracy of the most sensitive determination, $\rho_{\mathrm{exp}}^{(\tau,e)} = 0.72 \pm 0.15$,[13] is not great enough for the effects of massive-neutrino modes to be important. As is well known, a deviation in the Lorentz structure of the relevant weak couplings from the $V-A$ form could cause ρ either to increase above 0.75 or decrease below this point. However, even if ρ_{eff} were measured to be greater than 0.75, one could still not *a priori* attribute the the effect entirely to non-$(V-A)$ couplings, since this increase might actually represent a larger increase due to a deviation in the Lorentz structure combined with a slight decrease due to massive-neutrino modes. Nevertheless, we have found a test which can reduce or eliminate this ambiguity. This test exploits the fact that the effects of massive-neutrino modes involve thresholds in E_b, whereas those due to deviations in the Lorentz structure of the weak couplings do not. It consists of using different ranges of E_b in the determination of the spectral parameters and then investigating whether or not the resulting values are significantly different. The underlying idea is illustrated in Fig. 23, for the measurement of

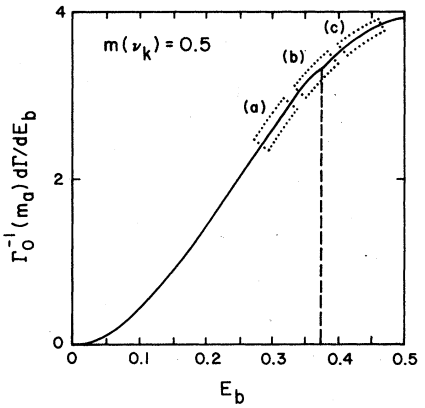

FIG. 23. Schematic illustration of the test using different energy intervals to distinguish the effects on the spectral parameters of possible non $V-A$ Lorentz structure and those due to possible neutrino masses and mixing. The graph shows $\Gamma_0^{-1}(m_a)d\Gamma/dE_b$ for a leptonic l_a decay involving one (anti)neutrino $(\overline{\nu})_k$ of non-negligible mass, taken here to be $m(\nu_k)=0.5$. In regions (a), (b), and (c) the single HSC $(\overline{\nu})_k$ modes would be fully present, partially present, and absent, respectively. One would compare the values of $\rho_{\rm eff}$, for example, obtained from fits over these three different regions. See text for further discussion.

$\rho_{\rm eff}$ in the case of one non-negligible set of HSC ν_k mode. For this example we take $m(\nu_k)=m_a/2$ so that the end point for the corresponding massive ν_k mode is $0.375m_a$. The size of this mode is exaggerated for visual clarity. In region (a) the ν_k mode is fully present, while in region (b) it is present in the lower end of the range but is phase-space forbidden in the upper range, and in region (c) it is absent entirely. Each of these three regions would thus clearly yield different values of $\rho_{\rm eff}$ [and only in region (c) would the measured value provide a direct probe of the Lorentz structure in the amplitude]. Thus, in principle, if (after appropriate radiative corrections are extracted), a spectral parameter such as $\rho_{\rm eff}$ is established to be different from its $V-A$ value and the test proposed above is performed, then (1) if the test yields the same non-$(V-A)$ value of the spectral parameter for all of the ranges of E_b that were used, then one can conclude that the effect is due to non-$(V-A)$ couplings and not to massive neutrinos, to the requisite level of accuracy; (2) if different ranges do yield different results, then one can conclude that at least part of the effect is due to massive neutrinos; and (3) if the deviation disappears as one used progressively higher ranges of E_b (given an appropriate definition of the area-normalized fitting function), then one can conclude that the effect is due to massive neutrinos rather than non-$(V-A)$ Lorentz structure, again to the requisite level of precision. We propose that this test be applied to past data on μ and leptonic τ decay, since even in the cases where spectral parameters obtained were consistent with $V-A$ couplings, the application of the test would yield new and valuable correlated bounds on neutrino masses and mixing. For the same reason we also strongly suggest that it be applied in the forthcoming high-precision μ and τ decay experiments.[30-34]

The second application of our study of the effects of neutrino masses and mixing on $\rho_{\rm eff}$ concerns the correlated bounds on these quantities that result from the measured values $\rho_{\rm exp}$. In view of our first conclusion, we must make some assumption regarding possible deviations of the Lorentz structure of the relevant weak couplings, and we make the natural and simplest assumption that such deviations are zero or negligibly small. The 1σ limit based on the measured value $\rho_{\rm exp}^{(\mu,e)}\equiv\rho_{\rm exp}^{(\mu)}$,

$$\left|\rho_{\rm eff}^{(\mu)}-\rho_{\rm exp}^{(\mu)}\right|<\sigma_\rho=0.0026\,, \qquad (2.107)$$

yields the upper bound shown in Fig. 24 on $|U_{rk}|^2$ as a function of $m(\nu_k)$. As was mentioned before, this bound is generally considerably weaker than the ones obtained in Refs. 2 and 3; however, in the case $r=2$ and the region $m(\nu_k)\in(\sim 38$ MeV, ~ 82 MeV) it is useful.

Finally, for the third application, we indicate the statistical accuracy in the measurement of $\rho_{\rm exp}$ expected in the future LAMPF experiment of Anderson, *et al.*,[30] viz. $\sigma_\rho^{(\rm stat)}=0.000\,23$, by the horizontal short-dashed lines in Fig. 22. For ρ and each of the other three spectral parameters,

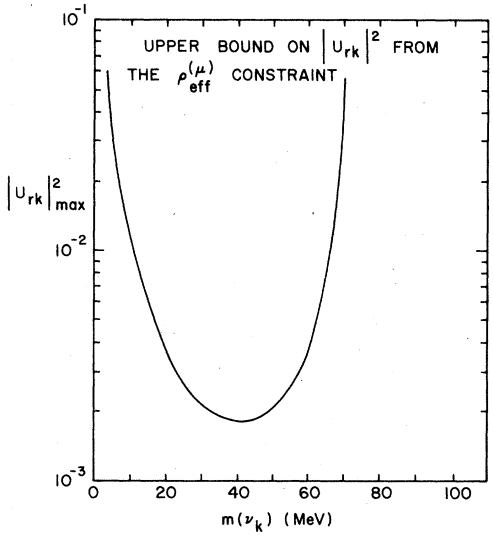

FIG. 24. Upper bound, at the 1σ level, on the coupling coefficient $|U_{rk}|^2$ from the $\rho_{\rm eff}^{(\mu)}$ constraint, for the case described in the caption to Fig. 22.

all of which are to be measured in this experiment, the systematic errors are expected to be comparable to, or perhaps somewhat less than, the statistical errors. Although we have chosen the canonical $V-A$, $m(\nu_i)=0$, $U\equiv 1$ value of $\rho_{\rm eff}$ around which to draw the $\pm 1\sigma^{\rm (stat)}$ errors, this obviously should not be taken to imply that the value of $\rho_{\rm exp}$ that will eventually be measured will be precisely 0.75. As is evident from Fig. 22, given the projected accuracy of the new LAMPF μ decay experiment, it will be sensitive to the effects of neutrino masses and mixing on the parameter $\rho_{\rm eff}$ for a reasonable range of intermediate values of $m(\nu_k)$, down to rather small $|U_{2k}|^2$. With this capability and the use of our proposed method of sampling different ranges of E_e, this experiment will be in a reasonable position to carry out a search for massive-neutrino effects.

In Fig. 25 we present our results for $\eta_{\rm eff}$ obtained from the two-parameter fit to $\rho_{\rm eff}$ and $\eta_{\rm eff}$ assuming $V-A$ weak couplings. We interpret the behavior of $\eta_{\rm eff}$ as follows. For relatively small $m(\nu_k)$, the net effect of the massive-neutrino mode is to decrease $d\Gamma/dE_e$, most markedly in the intermediate energy region, and hence yield a negative $\eta_{\rm eff}$. As $m(\nu_k)$ increases, however, the bump which appears in the total $d\Gamma/dE_e$ at the maximum of the HSC ν_k contribution moves down from high to intermediate E_e. The fitting curve thus favors positive $\eta_{\rm eff}$ since, as can be seen from Eq. (2.98), this increases the middle part of the $d\Gamma/dE_e$ while leaving the ends invariant. With our results as given in Fig. 25, we can address the three applications. First, it is clear that, in contrast to the situation with $\rho_{\rm eff}$, the errors in the present experimental measurement of η are sufficiently large that massive-neutrino effects are not important for the past use of $\eta_{\rm exp}$ to constrain the Lorentz structure of the weak couplings in μ decay. Of course, for the same reason, this constraint from $\eta_{\rm exp}$ was not very restrictive. Furthermore, one cannot use $\eta_{\rm exp}$ to obtain useful upper bounds on $|U_{rk}|^2$. More exciting is the third application. There are two future experiments which plan to measure η in μ decay: that of Anderson *et al.*, at LAMPF (ref. 30), and that of Crowe *et al.* at TRIUMF.[31] The expected total error in the latter experiment is ± 0.1, while the expected statistical error in the former is ± 0.006. The second error is shown as the short-dashed

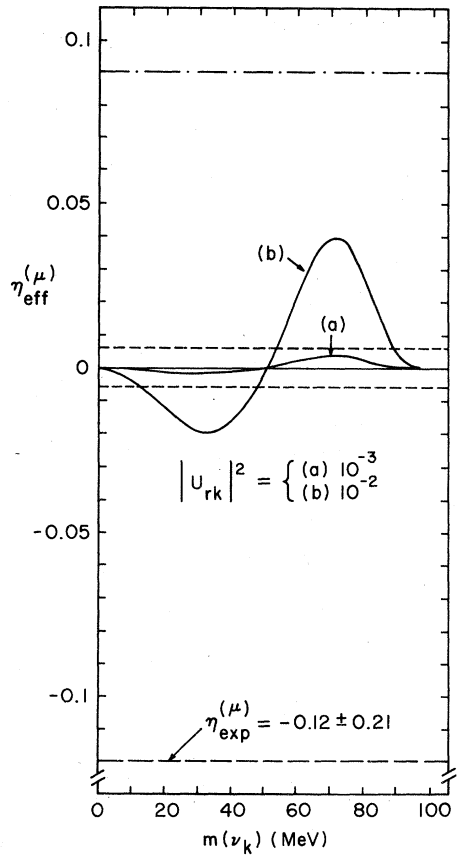

FIG. 25. Plot of $\eta_{\rm eff}$ determined from the two-parameter fit to $d\Gamma/dE_b$ in terms of $\rho_{\rm eff}$ and $\eta_{\rm eff}$ for μ decay, in the case described for Fig. 22. The results shown in Figs. 24–26 also apply to τ decay with an obvious scale change in the $m(\nu_k)$ axis.

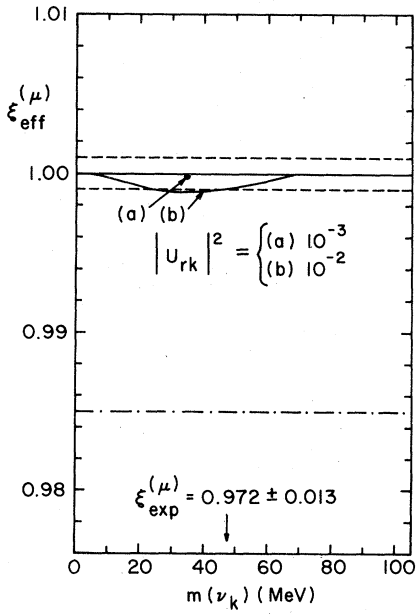

FIG. 26. Plot of $\xi_{\rm eff}$, determined from a one-parameter fit to the integrated asymmetry in μ decay, for the case described in the caption to Fig. 22. In this fit, to reproduce the procedure of past μ-decay experiments, the other spectral parameters $\rho_{\rm eff}$, $\eta_{\rm eff}$, and $\delta_{\rm eff}$ were taken to have their conventional $V-A$ values.

lines centered, according to the convention explained before, around the $V-A$, $m(\nu_k)=0$, $U\equiv 1$ value of $\eta_{\rm eff}$. The LAMPF experiment may have sufficient precision to detect possible massive neutrino effects in the parameter $\eta_{\rm eff}$.

Let us next proceed to analyze the effects of neutrino masses and mixing on the spectral parameters $\xi_{\rm eff}$ and $\delta_{\rm eff}$ which determine $f_{S(\rm GL)}$. In Fig. 26 we present curves of $\xi_{\rm eff}$ obtained from a fit to the integrated asymmetry, assuming $V-A$ couplings. This reproduces the conditions of the experiments of Ref. 44 (which dominate the present weighted world mean for $\xi_{\rm exp}$), since these experiments determined ξ from a fit to the function $N^{(+)}(\theta)=1+a^{(+)}\cos\theta$, i.e., from an integration over all energies, subject to standard cuts. Analytically, for a fit to the asymmetry integrated over the entire spectrum,

$$\xi_{\rm eff}^{(a,b)}\Big|_{\substack{\rm integrated\\ \rm fit}}=\frac{3\sum_{i,j}|U_{ai}^{*}U_{bj}|^{2}F_{s;0}(m(\nu_i),m(\nu_j),m_b)}{\sum_{r,s}|U_{ar}^{*}U_{bs}|^{2}F_{1;0}(m(\nu_r),m(\nu_s),m_b)}\,. \tag{2.108}$$

As with the $\eta_{\rm eff}$ and $\delta_{\rm eff}$ plots, one can obtain the behavior for the decay $\tau^{+}\to\bar{\nu}_\tau e^{+}\nu_e$ by an obvious scale change of the $m(\nu_k)$ axis; however, we are well aware of the difficulties inherent in trying to measure any of the three spectral parameters other than ρ in leptonic τ decay. As is evident from Fig. 26, the effect of the massive-neutrino mode is to reduce $\xi_{\rm eff}$ for all $m(\nu_k)$, the maximum reduction occurring in the region 30–40 MeV. This behavior can be understood directly from our earlier calculation of the integrated asymmetry $a^{(\mp)}$, or equivalently, $\langle\cos\theta\rangle^{(\mp)}$, presented, for l_a^{-} decay, in Fig. 13. It may be recalled from well-known formulas for the theoretical $\xi^{(a,b)}$ in terms of the $\{g^{(a,b)}\}$ and $\{g^{(a,b)'}\}$ in the conventional theory that a deviation in Lorentz structure from the $V-A$ form can cause this parameter to increase above, or decrease below, unity. Indeed, in the conventional theory, with zero neutrino masses for each of the four spectral parameters, denoted generically by $\mathfrak{p}_i$, the difference $\mathfrak{p}_i-\mathfrak{p}_i$ $(V-A)$ can be positive or negative. The curve shown in Fig. 26 is for $|U_{rk}|^{2}=10^{-2}$; a small dot indicates roughly the maximum decrease for $|U_{rk}|^{2}=10^{-3}$. With this integral method of extracting $\xi_{\rm eff}$, the massive-neutrino mode has little effect. The present experimental measurement of ξ is approximately 2σ below unity. We conclude that, given the constraints on $|U_{rk}|^{2}$, a massive-neutrino mode would have had a very small effect on past measurements of ξ in μ decay. There are two future experiments which will measure this parameter. The expected statistical accuracy for the measurement of ξ in the LAMPF experiment[30] is $\pm 0.000\,99$, while the expected total error in the TRIUMF experiment of Strovink *et al.*,[32] which is specifically devoted to a high-precision measurement of this parameter, is ± 0.001 (where in the latter experiment the fit is made assuming the conventional $V-A$ values $\rho=\frac{3}{4}$, $\eta=0$, and $\delta=\frac{3}{4}$). This error is depicted in Fig. 26 as the short-dashed lines around the conventional value of unity. Our conclusion is that if one chooses to extract $\xi_{\rm exp}$ by a fit to the integrated asymmetry alone, it may be difficult to detect any massive-neutrino effects. Furthermore, one would lose the capability of applying our suggested method of using different energy intervals to distinguish between deviations due to possible non-$(V-A)$ Lorentz structure and those due to massive neutrinos. Earlier in this work we proposed a different method of searching for the signatures of massive-neutrino modes in the angular distribution by exploiting the exact helicity zero of $d\Gamma^{(\mp)}/dE_b d\cos\theta$ for $\theta=0^\circ$ or 180°, in μ^{-} or μ^{+} decay, respectively, and $E_b=(E_{b\,\rm max})_0$, if $|\vec{P}_{l_a}|=1$ and neutrinos are massless. In contrast, a massive-neutrino mode would not have a zero at these respective values of θ, although it would, of course, vanish beyond its energy end point, (2.1). Our study indicated that the effect was small; however, we suggest that it would be worthwhile to try this search in the forthcoming μ decay experiments which will study the angular distribution.[30,32] The method will benefit from the ability of these experiments to achieve a $|\vec{P}_\mu|$ which is (a) extremely close to unity, and (b) known to very high precision, both of which features improve considerably upon past μ decay experiments. It is true that the behavior of $d^{2}\Gamma^{(+)}/dE_e d\cos\theta$ in the $\theta=180^\circ$, high-E_e region is sensitive to deviations from $V-A$ Lorentz structure as well as massive neutrinos. Indeed, this sensitivity has been stressed in Ref. 32, although no consideration was given there to the effects of massive neutrinos and lepton mixing. The method of different energy intervals can be applied to some extent here, but, as was discussed before, if one goes too far below $(E_{e\,\rm max})_0$ the helicity suppression of the LDC mode(s) largely disappears.

In addition to altering the magnitude of the effective asymmetry, massive-neutrino modes also change its momentum dependence. Figure 27 shows our results for $\delta_{\rm eff}$ as calculated in a two-parameter fit to $\xi_{\rm eff}$ and $\delta_{\rm eff}$ in μ decay, using Eq. (2.106) with $V-A$ couplings and, to reproduce typical experimental conditions (see, e.g., Ref. 28), assuming $\rho_{\rm eff}=\frac{3}{4}$ and $\eta_{\rm eff}=0$. The energy interval taken for this fit is the full range of E_e. One observes that for all values of $m(\nu_k)$, the effect of the massive-neutrino mode is to reduce $\delta_{\rm eff}$.

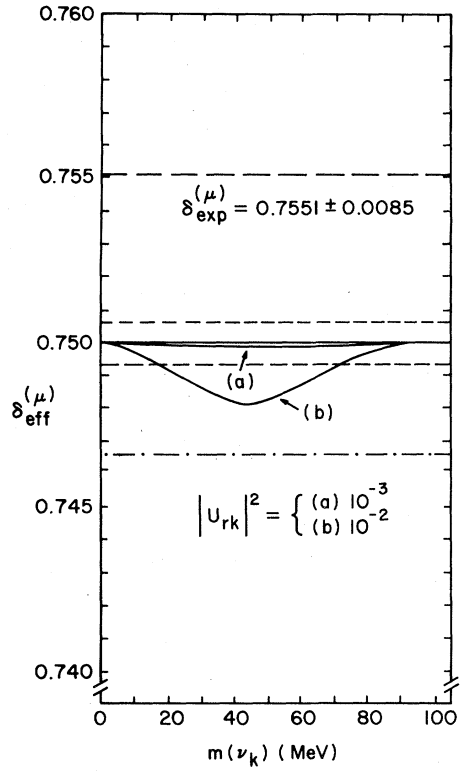

FIG. 27. Plot of $\delta_{\rm eff}$ determined from a two-parameter χ^2 fit to the asymmetry in terms of $\xi_{\rm eff}$ and $\delta_{\rm eff}$, for μ decay, in the case described for Fig. 22. In this fit, to reproduce the usual procedure of past μ-decay experiments, the other spectral parameters $\rho_{\rm eff}$ and $\eta_{\rm eff}$ were taken to have their conventional $V-A$ values.

Although the maximum decrease is small compared to the errors in the present experimental measurement, it is not completely negligible. The expected statistical error in the forthcoming measurement of δ by the LAMPF experiment[30] is $\pm 0.000\,64$, as indicated in Fig. 27. Again, it is clear that this experiment has the potential to detect the effect of massive neutrinos on the spectral parameter $\delta_{\rm eff}$. For brevity we shall not show the values of $\xi_{\rm eff}$ obtained via this two-parameter fit; we note, however, that they do differ somewhat from those computed from the one-parameter fit to the integrated asymmetry. This concludes our presentation of the general theory of the spectral parameters in leptonic l_a decay.

G. The l_b polarization

Up to this point we have analyzed the effects of neutrino masses and mixing on leptonic l_a decay assuming that one only measures E_b or $|\vec{p}_b|$ and θ. We now consider the effects on the l_b polarization $\vec{P}_{l_b} \equiv \vec{P}_b$. For this purpose, let us define an orthonormal coordinate system by $\hat{e}_L \equiv \hat{p}_b$, $\hat{e}_{\rm TIP} \equiv (\vec{P}_a - \vec{P}_a \cdot \vec{p}_b\vec{p}_b)/|\vec{P}_a - \vec{P}_a \cdot \vec{p}_b\vec{p}_b|$, and $\hat{e}_{\rm TOP} \equiv (\vec{P}_a \times \vec{p}_b)/|\vec{P}_a \times \vec{p}_b|$, where the subscripts L and T(I,O)P mean "longitudinal" and "transverse (in, out of) the $\vec{P}_a$, $\vec{p}_b$ plane". The components of the l_b polarization are then denoted by $(P_a)_c \equiv \vec{P}_a \cdot \hat{e}_c$, for $c = L$, TIP, and TOP. For a given decay mode $l_a \to \nu_i l_b \bar{\nu}_j$ or its charge conjugate we find, assuming $V-A$ couplings,

$$(P_b)_L^{(\mp)}(E_b, \theta; m(\nu_i), m(\nu_j), m_b) = \frac{h^{(\mp)}(E_b, \theta; m(\nu_i), m(\nu_j), m_b)}{(d^2\bar{\Gamma}^{(\mp)}/dE_b d\cos\theta)(E_b, \theta; m(\nu_i), m(\nu_j), m_b)}, \tag{2.109}$$

where the denominator was given in Eqs. (2.7)–(2.13) and

$$h^{(\mp)}(E_b, \theta; m(\nu_i), m(\nu_j), m_b) = \mp h_1(E_b; m(\nu_i), m(\nu_j), m_b) + |\vec{P}_a| \cos\theta h_s(E_b; m(\nu_i), m(\nu_j), m_b) \tag{2.110}$$

with

$$h_1(E_b; m(\nu_i), m(\nu_j), m_b) = 8(E_b^2 - b)[A_{ij}(1 - 2E_b + b) + B_{ij}(1 - E_b)] \tag{2.111}$$

and

$$h_s(E_b; m(\nu_i), m(\nu_j), m_b) = 8(E_b^2 - b)^{1/2}[-A_{ij}E_b \times (1 - 2E_b + b) + B_{ij}(E_b^2 - b)]. \tag{2.112}$$

For the actual experimental situation where one observes only the l_b, its longitudinal polarization is then

$$(P_b)_L^{(\mp)}(E_b, \theta) = \frac{\sum_{i,j} |U_{ai}^* U_{bj}|^2 h^{(\mp)}(E_b, \theta; m(\nu_i), m(\nu_j), m_b)}{\sum_{r,s} |U_{ar}^* U_{bs}|^2 (d^2\bar{\Gamma}^{(\mp)}/dE_b d\cos\theta)(E_b, \theta; m(\nu_r), m(\nu_s), m_b)}. \tag{2.113}$$

The expressions for the longitudinal polarization integrated over θ and over both θ and E_b are, respectively,

$$\langle (P_b)_L^{(\mp)} \rangle (E_b) = \frac{\mp \sum_{i,j} |U_{ai}^* U_{bj}|^2 h_1(E_b; m(\nu_i), m(\nu_j), m_b)}{\sum_{r,s} |U_{ar}^* U_{bs}|^2 f_1(E_b; m(\nu_r), m(\nu_s), m_b)} \tag{2.114}$$

and

$$\langle (P_b)_L^{(\mp)} \rangle = \frac{\mp \sum_{i,j} |U_{ai}^* U_{bj}|^2 H_{1;0}(m(\nu_i), m(\nu_j), m_b)}{\sum_{r,s} |U_{ar}^* U_{bs}|^2 F_{1;0}(m(\nu_r), m(\nu_s), m_b)}, \tag{2.115}$$

where, in analogy to Eq. (2.58),

$$H_{z;n}(m(\nu_i), m(\nu_j), m_b) \equiv \int_{m_b}^{(E_b)_{\max}(m(\nu_i), m(\nu_j), m_b)} dE_b E_b^n h_z(E_b; m(\nu_i), m(\nu_j), m_b), \quad z = 1 \text{ or } s. \tag{2.116}$$

In the conventional $V-A$ theory with $m(\nu_i) = 0$ for all i, the general expression (2.113) reduces to

$$(P_b)_{L,\text{conv.}}^{(\mp)}(E_b, \theta) = \frac{\mp \beta_b(3 - 4E_b + b) - |\vec{P}_a| \cos\theta [1 - 2(1+\beta_b^2)E_b - b]}{(3 - 4E_b + 3b - 2b/E_b) \pm \beta_b |\vec{P}_a| \cos\theta (1 - 4E_b + 3b)}$$

$$= \mp \left[1 + O\left(b; \frac{b}{E_b}\right)\right] \text{ for } b \ll 1. \tag{2.117}$$

For the integrated polarization one has

$$\langle (P_b)_L^{(\mp)} \rangle_{\text{conv}} = \frac{\mp(1 - \frac{40}{3}b + 32b^{3/2} - 30b^2 + \frac{32}{3}b^{5/2} - \frac{1}{3}b^4)}{\bar{\Gamma}(0,0,b^{1/2})} \simeq \mp(1 - \tfrac{16}{3}b) \text{ for } b \ll 1. \tag{2.118}$$

(Parenthetically, we note that the order-α radiative corrections to these conventional $V-A$ formulas have been calculated.[52]) Our results (2.7)–(2.13) and (2.111)–(2.113) show that, in fact, the same approximate equalities hold in the general $V-A$ theory with massive neutrinos and lepton mixing:

$$(P_b)_L^{(\mp)}(E_b, \theta) = \mp \left[1 + O\left(b; \frac{b}{E_b}\right)\right] \tag{2.119}$$

and

$$\langle (P_b)_L^{(\mp)} \rangle = \mp [1 + O(b)]. \tag{2.120}$$

For the other components we find that (assuming $V-A$ couplings) in the general theory with massive neutrinos and lepton mixing, just in the conventional $V-A$ theory with massless neutrinos,

$$(P_b)_{\text{TIP}}^{(\mp)}(E_b, \theta) = 0 \mp O\left(\frac{\beta_b}{\gamma_b}\right), \tag{2.121}$$

$$\langle (P_b)_{\text{TIP}}^{(\mp)} \rangle = 0 \mp O(b^{1/2}), \tag{2.122}$$

and

$$(P_b)_{\text{TOP}}^{(\mp)}(E_b, \theta) = 0. \tag{2.123}$$

It is worth commenting upon the latter result. In the conventional theory with massless neutrinos there is no CP violation in the lepton sector. A very important property of the general theory is that, for the case of $n \geq 3$ lepton generations, which is known to be the physically relevant one, the mixing matrix U contains complex phases which cannot be eliminated by redefinitions of the fields and which give rise to leptonic CP violation. The analog of this phenomenon in the quark sector was discussed by Kobayashi and Maskawa.[53] Nevertheless, basically because the $l_a \to \nu_i l_b \bar{\nu}_j$ decays are incoherent, this CP violation does not directly manifest itself in leptonic l_a decay. Experimentally, in μ decay several measurements have yielded the result that $(P_e^{(+)})_L = 1.00 \pm 0.13$.[54] A recent SIN experiment has measured $(P_e^{(+)})_{\text{TIP}}$ and $(P_e^{(+)})_{\text{TOP}}$ and found them both to be consistent with zero.[55] (These indicated average polarizations do involve cuts which are specified in Refs. 54 and 55.) At the present time there are, to our knowledge, no reported measurements of $\vec{P}_e$ or $\vec{P}_\mu$ in leptonic τ decay.

Thus, our analysis shows that the effects of neutrino masses and mixing on the l_b polarization are extremely small and, especially in view of the accuracy of existing and forseeable experiments, are not likely to provide useful signatures.

As the last part of this section we consider another manifestation of neutrino masses and mixing which appears in leptonic l_a decay for $a \geq 3$. This is generically similar to the effect on the observed ratio $R_M \equiv B(M^+ \to e^+\nu_e)/B(M^+ \to \mu^+\nu_\mu)$ (where $M = \pi$ or K) discussed in Ref. 3, in that it involves (a) integral quantities, and (b) a ratio of branching ratios, in contrast to the differential spectral effects in M_{l2} or leptonic l_a decay. The quantity of interest here is the ratio

$$R_{a\to b/a\to c} \equiv \frac{B(l_a \to \nu_{l_a} l_b \bar{\nu}_{l_b})}{B(l_a \to \nu_{l_a} l_c \bar{\nu}_{l_c})}, \quad a \geq 3. \tag{2.124}$$

In the conventional theory (with $m_a \equiv 1$) $(R_{a\to b/a\to c})_{\text{conv.}} = \bar{\Gamma}(0,0,m_b)/\bar{\Gamma}(0,0,m_c)$. Note that the order-$\alpha$ radiative corrections do not affect this equality, since they are mass independent.[16] For the one case of experimental interest, $(R_{\tau\to e/\tau\to\mu})_{\text{conv.}} = 1.0280$. However, in the general theory

TABLE II. The ratio $R_{\tau\to e/\tau\to\mu}$ as a function of $m(\nu_3)$ in the case in which the only significant massive-neutrino modes in τ decay are those involving ν_3.

$m(\nu_3)$ (MeV)	$R_{\tau\to e/\tau\to\mu}\equiv\frac{B(\tau\to\nu_\tau e\bar{\nu}_e)}{B(\tau\to\nu_\tau\mu\bar{\nu}_\mu)}$
0	1.0280
50	1.0281
100	1.0284
150	1.0290
200	1.0297
240	1.0304
experiment (Ref. 43)	0.95 ± 0.10

$$R_{a\to b/a\to c}=\frac{\sum_{i,j}|U_{ai}^*U_{bj}|^2\overline{\Gamma}(m(\nu_i),m(\nu_j),m_b)}{\sum_{r,s}|U_{ar}^*U_{cs}|^2\overline{\Gamma}(m(\nu_r),m(\nu_s),m_c)}, \tag{2.125}$$

which usually would differ from $(R_{a\to b/a\to c})_{\rm conv}$. A question which then arises is the following: as with the spectral parameters, given the present bounds on neutrino masses [in particular, $m(\nu_3)$] and lepton-mixing angles, how large could their effect on $R_{\tau\to e/\tau\to\mu}$ be? Furthermore, could one use the measured value of this ratio to obtain useful direct bounds on $m(\nu_3)$ or correlated bounds on the contributions of HSC (i,j) modes? Let us first consider the effects of DC modes on $R_{\tau\to e/\tau\to\mu}$. In this case, to a good approximation, one can neglect SC modes, so that $R_{\tau\to e/\tau\to\mu}\simeq\overline{\Gamma}(m(\nu_3)/m_\tau,0,m_e/m_\tau)/\overline{\Gamma}(m(\nu_3)/m_\tau,0,m_\mu/m_\tau)$. As $m(\nu_3)$ increases from zero to its currently allowed maximum[14] (at the 2σ level), 245 MeV, this ratio increases, but only slightly, as our results in Table II show. It is straightforward to calculate the changes in the ratio which would be caused by possible HSC modes; these are smaller than the HDC effect just analyzed. Thus, the questions posed above are answered; even with a substantial improvement in the accuracy of the measurements, the effects of neutrino masses and mixing on $R_{\tau\to e/\tau\to\mu}$ are unlikely to be detectable.

ACKNOWLEDGMENT

This research was supported in part by the National Science Foundation under Contract No. PHY-79-06376.

[1]R. E. Shrock, p. S63 in Particle Data Group, Rev. Mod. Phys. 52, S1 (1980).
[2]R. E. Shrock, Phys. Lett. 96B, 159 (1980).
[3]R. E. Shrock, Phys. Rev. D 24, 1232 (1981). Preliminary reports of the results in the present paper were given in seminars at Brookhaven, 1980 (unpublished) and TRIUMF, 1980 (unpublished) and in *Weak Interactions as Probes of Unification*, proceedings of the Workshop of the Virginia Polytechnic Institute, 1980, edited by G. B. Collins, L. N. Chang, and J. R. Ficenec (AIP, New York, 1981).
[4]S. Weinberg, Phys. Rev. Lett. 19, 1264 (1967); A. Salam, in *Elementary Particle Theory: Relativistic Groups and Analyticity (Nobel Symposium No. 8)*, edited by N. Svartholm (Almqvist and Wiksell, Stockholm, 1968), p. 367; S. Glashow, Nucl. Phys. B22, 579 (1961).
[5]See, for example, B. W. Lee and R. E. Shrock, Phys. Rev. D 16, 1444 (1977) and references therein for the case of Dirac neutrinos.
[6]The precise meaning of the words "in general" is stated in footnote 3 of Ref. 3.
[7]For a recent review of the conventional theory of μ decay see A. M. Sachs and A. Sirlin, in *Muon Physics*, edited by V. Hughes and C. S. Wu (Academic, New York, 1975), Vol. II, p. 49.
[8]For recent reviews of τ decay data, see M. Perl, in *Proceedings of the* 1977 *International Symposium on Lepton and Photon Interactions at High Energies, Hamburg*, edited by F. Gutbrod (DESY, Hamburg, 1977), p. 145; in *New Phenomena in Lepton Hadron Physics*, proceedings of the Summer Institute, Karlsruhe, 1978, edited by D. E. C. Fries and J. Weiss (Plenum, New York, 1979), p. 115; G. Feldman, in *Proceedings of the XIX International Conference on High Energy Physics, Tokyo, 1978*, edited by S. Homma, M. Kawaguchi, and H. Miyazawa (Physical Society of Japan, Tokyo, 1979), p. 777; G. Flügge, Z. Phys. C 1, 121 (1979); J. Kirkby, in *Proceedings of the 1979 International Symposium on Lepton and Photon Interactions at High Energies, Fermilab*, edited by T. B. W. Kirk and H. D. I. Abarbanel (Fermilab, Batavia, Illinois, 1980), p. 107.
[9]B. W. Lee and R. E. Shrock, Phys. Rev. D 17, 2410 (1978). See, in particular, Eqs. (4.39)–(4.45).
[10]Technically, given our definition of the demarcation point between the sets $\{\nu_{i_L}\}$ and $\{\nu_{i_H}\}$, the three types of l_a decay modes involving HDC (anti)neutrinos could also occur in μ decay. However, in this paper we shall often use the term "HDC ν_i" to denote a neutrino with a mass $m(\nu_i)$ which is not $\ll m_a$ (the mass of the parent lepton l_a), so that its kinematic effects might be detectable. In this context, we note that $m(\nu_2)_{\rm max}/m_\mu\simeq 4.9\times10^{-3}$, whereas $m(\nu_3)_{\rm max}/m_\tau\simeq 0.13$.
[11]M. Bardon *et al.*, Phys. Rev. Lett. 14, 449 (1965).
[12]M. Perl *et al.*, Phys. Rev. Lett. 70B, 487 (1977); R. Brandelik *et al.*, Phys. Lett. 73B, 109 (1978).
[13]W. Bacino *et al.*, Phys. Rev. Lett. 42, 749 (1979).
[14]C. A. Blocker, Ph.D. thesis, LBL Report No. LBL-10801, 1980 (unpublished).
[15]M. Daum *et al.*, Phys. Lett. 74B, 126 (1978); Phys. Rev. D 20, 2692 (1979).
[16]R. Behrends, R. Finkelstein, and A. Sirlin, Phys. Rev. 101, 866 (1956); T. Kinoshita and A. Sirlin, *ibid.* 107,

593 (1957); 107, 638 (1957); 113, 1652 (1952); S. M. Berman, *ibid.* 112, 267 (1958). See also S. Berman and A. Sirlin, Ann. Phys. (N.Y.) 20, 20 (1962); and A. Sirlin, Rev. Mod. Phys. 50, 573 (1978).

[17]T. Appelquist *et al.*, Phys. Rev. D 6, 2998 (1972); 7, 2998 (1973).

[18]M. Veltman, Phys. Lett. 91B, 95 (1980); M. Green and M. Veltman, Nucl. Phys. B169, 137 (1980); F. Antonelli *et al.*, Phys. Lett. 91B, 90 (1980).

[19]A. Sirlin, Phys. Rev. D 22, 971 (1980). See also W. Marciano, *ibid.* 20, 274 (1979).

[20]This fact can easily be deduced from an inspection of the structure of the Feynman integrands.

[21]L. Matsson, Nucl. Phys. B12, 647 (1969).

[22]It is interesting to note that, given the present lower bound on the mass of a possible fourth charged lepton, $m_{l_4} > 16$ GeV (95% C.L.) from PETRA, the relation $m_b^2 \ll m_a^2$ is already known to hold again for $a = 4$, as it does for $a = 2$ and 3. Quantitatively, $(m_{l_b}^2/m_{l_4}^2)_{\max} = (m_\tau^2/m_{l_4}^2) < 0.012$ (95% C.L.). For the bound on m_{l_4}, see B. Wilk, in *High Energy Physics—1980,* proceedings of the XXth International Conference, Madison, Wisconsin, edited by L. Durand and L. G. Pondrom (AIP, New York, 1980). (Mark J Collaboration), MIT Report No. 113, 1980 (unpublished).

[23]R. Plano, Phys. Rev. 119, 1400 (1960).

[24]For a discussion relevant to the old μ decay experiments, see R. Swanson, Phys. Rev. 112, 580 (1958). For very recent analyses relevant to forthcoming experiments, see Refs. 30 and 32.

[25]That is, the reconstructed $E_b = 0.49$; there would, of course, be some energy loss by the l_b in an actual experiment.

[26]J. Peoples, Ph.D. thesis, Nevis Report No. 147, 1966 (unpublished).

[27]B. Sherwood, Phys. Rev. 156, 1475 (1967).

[28]D. Fryberger, Phys. Rev. 166, 1379 (1968).

[29]S. Derenzo, Phys. Rev. 181, 1854 (1969).

[30]H. L. Anderson *et al.* (H. L. Anderson and J. D. Bowman, spokesmen)LAMPF Research Proposal, 1978 (unpublished); R. J. McKee, addendum to this proposal, 1979 (unpublished).

[31]K. M. Crowe *et al.* (K. M. Crowe, spokesman), TRIUMF Research Proposals No. 134 (for η) and 176 (for ξ) (unpublished).

[32]C. Oram *et al.* (M. Strovink, spokesman), TRIUMF Research Proposal, 1980 (unpublished).

[33]In addition to rare decays, ordinary μ decay may also be studied in H. L. Anderson *et al.* (D. A. Bryman and C. Hargrove, spokesmen), TRIUMF Research Proposal No. 104 (unpublished).

[34]R. Baltrusaitis *et al.* (Mark III Collaboration; D. Hitlin, spokesman), SLAC Proposal No. SP-31 (unpublished).

[35]R. E. Shrock, invited talk at the Caltech Workshop on High Energy Physics, 1979 (unpublished); R. E. Shrock, S. B. Treiman, and L.-L. Wang, Phys. Rev. Lett. 87B, 375 (1979); R. E. Shrock and M. B. Voloshin, Phys. Lett. 87B, 375 (1979). The finding that $|V_{13}V_{23}|^2 \equiv |V_{ub}/V_{cb}|^2 \ll 1$ has recently received experimental support from studies of B-meson production at CESR; see K. Berkelman in *High Energy Physics—1980,* proceedings of the XXth International Conference, Madison, Wisconsin, edited by L. Durand and L. G. Pondrom (AIP, New York, 1980), p. 1499; E. Thorndike, *ibid.*, p. 705. [Subsequent to the above Caltech Workshop report, the calculations given there were repeated by V. Barger, W. F. Long, and S. Pakvasa, Phys. Rev. Lett. 42, 1585 (1980). However, the basis for their analysis, in Eqs. (4) and (5) of this Letter, is incorrect. This fact has been noted independently by T. Inami and C. S. Lim, Prog. Theor. Phys. 65, 297 (1981)].

[36]M. Perl *et al.*, Phys. Lett. 63B, 466 (1976); 70B, 487 (1977).

[37]A. Barbaro-Galtieri *et al.*, Phys. Rev. Lett. 39, 1058 (1977).

[38]R. Brandelik *et al.*, Phys. Lett. 73B, 109 (1978).

[39]We have also examined e and μ momentum spectra in τ decay data from the Mark II SLAC-LBL experiment, reported in Blocker, Ref. 14 (Figs. 14, 15, 20, and 21) and K. G. Hayes, Ph.D. thesis, Stanford University, 1980 (unpublished) (Fig. 4.5). Some dips are again evident in this data, but a physics explanation of these should probably be withheld until more accurate data are available. See the further cautionary statements in the text. We thank M. Perl for sending us this unpublished data.

[40]C. Bouchiat and L. Michel, Phys. Rev. 106, 170 (1957); see also Ref. 7 and references therein.

[41]The quotation marks are included to emphasize that one does not directly observe the ν_e or ν_μ in a (π or K)$_{l2}$ experiment, and the e or μ events that are recorded do not necessarily correspond to all of the mass eigenstates in ν_e or ν_μ, respectively. See Ref. 2 and Sec. III of Ref. 3 for further discussion of this point.

[42]Baltrusaitis *et al.*, Ref. 34.

[43]Particle Data Group, Rev. Mod. Phys. 52, S1 (1980).

[44]M. Bardon, D. Berley, and L. Lederman, Phys. Rev. Lett. 2, 56 (1959); I. Gurevich *et al.*, Phys. Lett. 11, 195 (1964); I. A. E. 11, 1297 (1967).

[45]The possible importance of the order-α^2 radiative corrections for high-precision μ decay experiments has been stressed in particular by A. Sirlin (unpublished).

[46]We use the Bjorken-Drell metric and γ-matrix conventions.

[47]It might be noted that the term in $f_{1(GL)}$ proportional to ρ gives zero exactly when integrated over the full range of E_b.

[48]F. Reines, H. W. Sobel, and E. Pasierb, Phys. Rev. Lett. 45, 1307 (1980); see, however, R. P. Feynman and P. Vogel, Caltech report (unpublished).

[49]G. Kalbfleisch and R. Shrock (unpublished).

[50]Z. Maki, M. Nakagawa, and S. Sakata, Prog. Theor. Phys. 28, 870 (1962); V. Gribov and B. Pontecorvo, Phys. Lett. 28B, 495 (1969).

[51]R. Abela, M. Daum, G. Eaton, R. Frosch, B. Jost, P. Kettle, U. Rosengard, and E. Steiner, SIN Newsletter, No. 13, p. 11 (1980).

[52]W. Fischer and F. Scheck, Nucl. Phys. B83, 25 (1974); M. Mehr and F. Scheck, *ibid.* B149, 123 (1979).

[53]M. Kobayashi and T. Maskawa, Prog. Theor. Phys. 49, 652 (1973).

[54]A. Buhler *et al.*, Phys. Lett. 1, 368 (1963); B. Bloom *et al.*, *ibid.* 8, 87 (1964); J. Duclos *et al.*, *ibid.* 9, 62 (1964); D. Schwartz, Phys. Rev. 162, 1306 (1967).

[55]J. Egger, Nucl. Phys. A335, 87 (1980).